EXPLORING MODULATORS OF TAU SPREADING IN ALZHEIMER'S DISEASE THROUGH MULTI-MODAL NEUROIMAGING BIOMARKERS

Graduate School of
Systemic Neurosciences

LMU Munich

Dissertation at the

Graduate School of Systemic Neurosciences

Ludwig-Maximilians-Universität München

Anna Steward

May, 2024

First Supervisor and Reviewer: Dr. Nicolai Franzmeier
Institute for Stroke and Dementia, University Hospital of LMU Munich

Second Reviewer: Prof. Dr. Med. Peter zu Eulenburg
Institute for Neuroradiology & German Vertigo Center, University Hospital of LMU Munich

Date of Submission: 29/05/2024
Date of Defense: 19/09/2024

CONTENTS

1 SUMMARY

Alzheimer's disease (AD), the leading cause of dementia worldwide, is characterised by a cascade of pathological brain changes starting with the emergence of amyloid plaques decades before the eventual spreading of tau pathology which drives the development of dementia symptoms. There is significant heterogeneity within AD, leading to variations in how the condition manifests clinically and the trajectory in which it progresses. This clinical heterogeneity can be related to heterogeneity in the pathophysiological underpinnings of AD, specifically pertaining to tau pathology which has been identified as the main driver of neurodegeneration, giving rise to distinct clinical phenotypes depending on the deposition pattern and accumulation rate of tau pathology. Specifically, neuroimaging studies demonstrate individual variations in the spreading rate and spatial pattern of tau pathology which correspond to clinical manifestation and progression. However, our understanding of the mechanisms responsible for these variations in tau pathology progression in AD remains limited. Given that tau plays a pivotal role in neurodegeneration and cognitive decline, understanding its modulators is paramount for optimising therapeutic interventions against AD progression. The aim of this thesis was to uncover factors impacting tau spreading through multimodal neuroimaging and genetic markers, with the primary objective of advancing our comprehension of AD pathophysiological progression, and ultimately aiding the development of more precise therapeutic strategies against AD.

Recent translational research combining resting-state functional magnetic resonance imaging (rs-fMRI) and tau-positron emission tomography (PET) reveals that tau spreading is activity dependent. Originating from focal areas typically within the medial temporal lobe, tau progressively expands out across the cortex, traversing functionally connected brain regions. This observation demonstrates how tau progression takes distinct routes depending on brain network architecture. Building on this evidence, the first investigation of this dissertation tested whether the functional organisation of the brain i.e., the functional connectome, impacted the rate at which tau accumulation progresses through the cortex. Considering that the functional connectome is of a modular structure made up of communicative but distinct networks, longitudinal exploration was conducted to ascertain whether the baseline rs-fMRI defined functional segregation of networks was associated with the rate of annual tau-PET SUVR change. In a sample of 123 subjects either cognitively healthy or spanning the AD spectrum, it was demonstrated that higher network segregation is associated with an

attenuated rate of tau spreading. Moreover, we further demonstrated that the functional segregation of subject-specific tau epicentres i.e., the region where tau initially manifests, influences the subsequent trajectory of tau spreading whereby more segregated epicentres lead to lower tau accumulation rates in the most connected regions and slower future tau progression overall. Together, these results indicate that the spread of tau pathology is influenced by the brain's functional organisation. Specifically, a more diffuse brain network architecture facilitates inter-regional tau spreading, signifying that individual variations in tau-trajectories may be shaped by the brain's functional architecture.

In the light of new anti-amyloid therapies, the second investigation was conducted into modulators of tau progression in relation to amyloid. Given that amyloid initiates AD's pathological cascade, triggering tau propagation, it is crucial to identify factors that moderate this. This is essential for optimising therapeutic windows for anti-amyloid treatments to intercept tau before it drives clinical disease progression. The Apolipoprotein E ε4 (ApoE4) allele is the strongest known genetic risk-factor for sporadic AD, whereby carriers have increased amyloidosis and faster AD progression, however, how ApoE4 influences amyloid-related tau spreading is unclear. Therefore, we explored connectivity mapped individualised tau spreading trajectories corresponding to amyloid levels using PET data from 367 ApoE genotyped subjects spanning two independent samples to determine the influence of ApoE4 carriage on amyloid's potential to trigger tau spreading. Results demonstrated that ApoE4 carriers had increased tau accumulation mediated by stronger amyloid deposition in early spreading stages and an accelerated tau spreading trajectory starting at lower amyloid levels. These findings indicate an indirect effect of ApoE4 carriage on tau spreading by driving increased amyloidosis, but also a direct effect whereby tau spreading was triggered earlier and faster relative to amyloid levels in ApoE4 carriers. This implies a need to intervene with anti-amyloid therapies in ApoE4 carriers earlier, to intercept tau progression promptly.

In summary, this thesis introduces novel evidence concerning modulators of tau progression in vivo, by employing a multi-modal neuroimaging approach to reflect the connectivity mediated spreading of tau pathology throughout the AD spectrum. Utilising longitudinal Tau-PET, individualised patterns of tau spreading were tracked and mapped to brain connectivity dynamics derived from rs-fMRI data, revealing that the onset and pace of tau spreading across interconnected brain regions are influenced by the brain's connectome and a specific genetic risk factor for AD, i.e., ApoE4. Overall, these findings enrich our understanding of

tau's progression within the cortex and carries implications for individualised approaches in determining the timing and target of therapeutic interventions.

2 ABBREVIATIONS OF INTRODUCTION AND DISCUSSION

Aβ	amyloid-beta
AD	Alzheimer's disease
ApoE4	apolipoprotein E ε4
CN	cognitively normal
CSF	cerebrospinal fluid
DWI	diffusion weighted magnetic resonance imaging
FDG-PET	fluorodeoxyglucose positron emission tomography
fMRI	functional magnetic resonance imaging
GWAS	genome wide association studies
MRI	magnetic resonance imaging
MCI	mild cognitive impairment
NfL	neurofilament light
PET	positron emission tomography
P-tau	phosphorylated tau
Q1 – 4	connectivity stage 1– 4
ROI	region of interest
Rs-fMRI	resting state functional magnetic resonance imaging
SUVR	standardized uptake value ratio

3 INTRODUCTION

3.1 The impact of Alzheimer's disease on the societal and patient level

Alzheimer's disease (AD) is the leading cause of age-related dementia, responsible for 60 to 80% of dementia cases (Dumurgier & Sabia, 2021), which impacts an estimated 55 million individuals globally. Standing as one of the most cost-intensive disorders worldwide, the challenges associated with AD are expected to exacerbate with the aging population, imposing an unprecedented strain on healthcare systems (Winblad et al., 2016). Owing to the nature of AD progression, it not only incurs treatment related costs but notable indirect costs for both the health-system and caregivers; The worsening of functional, behavioural and cognitive ability result in an ultimate loss of autonomy necessitating social care or residential care. Addressing this escalating burden of Alzheimer's disease demands an urgent focus on developing and implementing effective strategies to alleviate its societal, economic, and healthcare impacts. AD initiates a gradual decline in cognitive function, often marked by loss of episodic memory, language function and/or visuospatial function (Porsteinsson et al., 2021). However, preceding this, many subtle alterations occur in psychiatric, behavioural and functional domains (Bature et al., 2017) before treatment is sought. One of the significant challenges posed by AD is its accurate early detection, which is complicated owing to the subtle and heterogenous clinical signs in the very early stages of the disease. Identifying AD well before the onset dementia symptoms is crucial not only for lifestyle preparation for the patient (Brooker et al., 2014) but for optimising treatment. However, the duration from the onset of initial cognitive symptoms to the onset of dementia exhibits considerable variability among individuals making prognosis difficult (Duara & Barker, 2023; Ye et al., 2018). In the current era of disease-modifying antibody therapies for AD, such as Lecanemab (Van Dyck et al., 2022), early diagnosis and accurate prognosis is even more critical for successful treatment and additionally, to facilitate the enrolment of suitable early-stage AD patients in future therapeutic trials.

3.2 The amyloid cascade reflected through biomarkers

The early diagnosis of AD in clinical practice poses a challenge reliant on recognising the initial subtle and heterogenous clinical effects of the disease (Albert et al., 2013). However, continual advancements in the field of AD biomarkers have enabled the detection of underlying brain changes even before symptom onset (Frisoni et al., 2017). This progress is instrumental in

achieving early and accurate diagnoses of AD. Therefore, the quest for reliable and accessible biomarkers is increasingly important for our understanding of early disease manifestations and better insight into disease progression.

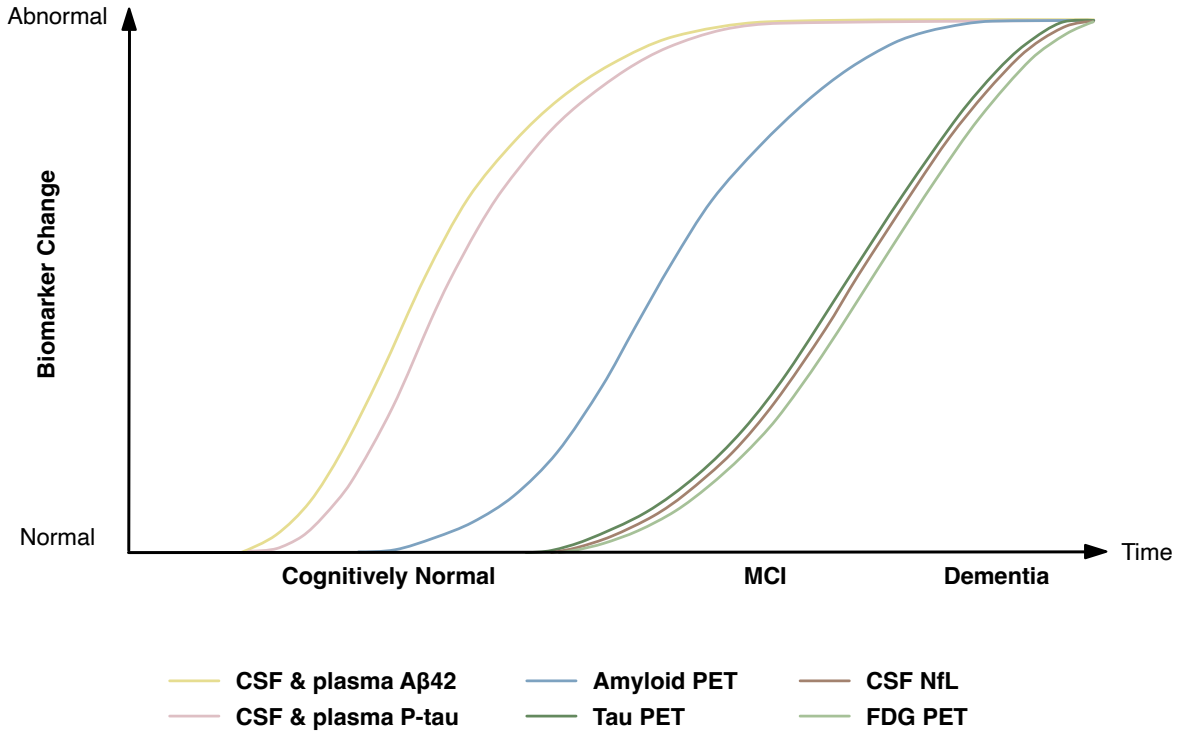

Figure 1. A model depicting the temporal dynamics and order in which biomarker abnormalities progress through clinical progression, starting with cognitively normal moving to mild cognitive impairment (MCI) and finally Dementia. Figure adapted from Zetterberg and Bendlin (2021) with permission from Springer Nature Limited.

AD is defined by cascade of pathological events which can be recapitulated in vivo by a combination of fluid and neuroimaging biomarkers. The first known abnormal brain change that occurs in AD is the development of extracellular beta-amyloid (Aβ) plaques, which precede the first cognitive symptoms by up to 20 years (Jack et al., 2013; Jansen et al., 2015). The formation of Aβ plaques occur from the aggregation of Aβ, a protein cleaved from the cell surface and released into the extracellular space. Abnormality in Aβ metabolism is the earliest detectable pathological process of AD, reflected by a reduction of soluble $A\beta_{1\text{-}42}$ peptides in cerebrospinal fluid (CSF) and plasma (see CSF & plasma Aβ42 in figure 1)

potentially resulting from their recruitment into Aβ plaques (Molinuevo et al., 2018). Insoluble Aβ plaque pathology become detectable with Aβ sensitive positron emission tomography (PET; see amyloid PET in figure 1) after Aβ peptides are detected (Palmqvist et al., 2019) with high specificity (Teipel et al., 2015). Post-mortem and Aβ PET research indicates that Aβ plaques accumulate in a relatively diffuse dispersed pattern found exclusively through the neocortex before emerging in the allocortical regions and then the rest of the brain (Braak & Braak, 1991; Grothe et al., 2017; Thal et al., 2002).

The onset of Aβ aggregation triggers the next major phase of the cascade: pathological tau accumulation. This is initiated by the hyperphosphorylation of tau, a microtubule stabilising protein principally expressed in neurons, which is prone to aggregation and eventually forms insoluble neurofibrillary tau tangles (Medeiros et al., 2011). The hyperphosphorylation of tau is the earliest detectable sign of tau pathology, which is reflected by the rise of soluble phosphorylated tau in CSF and blood plasma (see CSF & plasma P-tau in figure 1) which precedes the aggregation and fibrilisation of tau (Molinuevo et al., 2018). The detection of phosphorylated tau typically occurs soon after abnormalities are detectable in fluid Aβ biomarker levels and well before the onset of clinical symptoms and the emergence of insoluble neurofibrillary tau pathology (Palmqvist et al., 2019; Zetterberg et al., 2021).

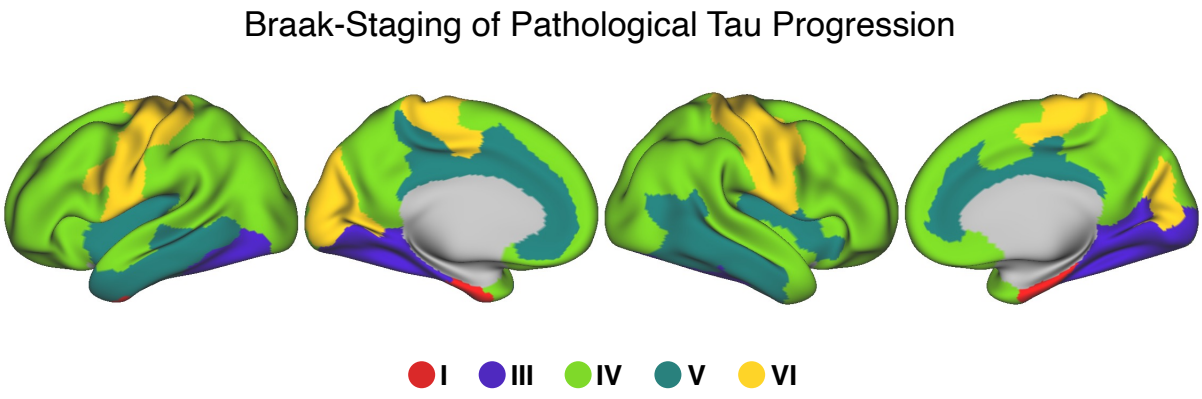

Figure 2. Braak Staging displayed on surface rendering. Braak stages rendered to cortical surface excluding the non-surface region Braak stage II i.e. limbic structures.

The eventual formation of insoluble neurofibrillary tau tangles progress in a specific manner throughout the cortex, typically – but not always – emerging from the medial temporal lobe and spreading gradually out towards the allocortex (see figure 2). The extensive progression

of tau is seemingly reliant on the presence of Aβ pathology, as tau is seldom found beyond the temporal lobe in absence of Aβ (Crary et al., 2014). The distinct hierarchical pattern of Aβ-related tau accumulation in AD has been summarized into a disease staging model i.e. Braak staging, derived from post-mortem assessments (Braak & Braak, 1997) which owing to the recent advent of tau-specific PET ligands (Leuzy et al., 2019), has been confirmed in-vivo (Wang et al., 2016). The formation of neurofibrillary tau tangle pathology is closely linked to cognitive decline, and research integrating tau-PET and cognitive testing shows that tau burden is predictive of future cognitive decline (Bejanin et al., 2017; Biel et al., 2021; Ossenkoppele et al., 2021; Pontecorvo et al., 2019).

Closely following the path of tau pathology is neurodegeneration marking the culmination of the amyloid cascade. The earliest signs of neurodegeneration are expressed in CSF and plasma as neurofilament light (NfL; see CSF NfL in figure 1), signifying general axonal degeneration (Khalil et al., 2018) which are detectable directly after neurofibrillary tau tangle pathology. Tau is the main driver of neurodegeneration and research combining, tau PET and fluorodeoxyglucose (FDG) PET (glucose hypometabolism) reveal that tau's spatial deposition aligns with patterns of neurodegeneration and clinical manifestation (La Joie et al., 2020; Ossenkoppele et al., 2016). This robust body of evidence reinforces the amyloid cascade hypothesis, elucidating tau's central role in the cascade of events bridging Aβ to neurodegeneration, resulting in eventual cognitive impairment and dementia.

3.3 Preclinical evidence for trans-neuronal tau propagation

The specific hierarchical pattern of tau accumulation (Braak et al., 1997) implies the influence of a specific mechanism determining tau's evolution through the cortex. Preclinical advancements have contributed to unveiling the biological mechanism driving the distinct pattern of tau accumulation across the brain. Early evidence for tau spreading was demonstrated by injecting brain extract from mice with mutant tau into mice with wild-type human tau, resulting in the formation of filaments and the spread of wild-type human tau to proximal brain regions (Clavaguera et al., 2009). Subsequent mouse-model studies expand on this research and reveal tau's specificity in spreading to downstream connected neurons, indicating its propagation through neuronal systems (Ahmed et al., 2014; De Calignon et al., 2012). Expanding on this, in vitro research exploring tau propagation in artificial neuronal

circuits revealed that synaptic contact significantly facilitated tau spreading which occurred through trans-synaptic propagation (Calafate et al., 2015). Collectively, this research provides evidence that tau spreads through the cortex trans-synaptically according to connectivity. This emphasizes the crucial importance of understanding brain connectivity in predicting the route of tau pathology, it is therefore essential to focus on investigating neuronal connections and brain activity to better predict tau's advancement in AD.

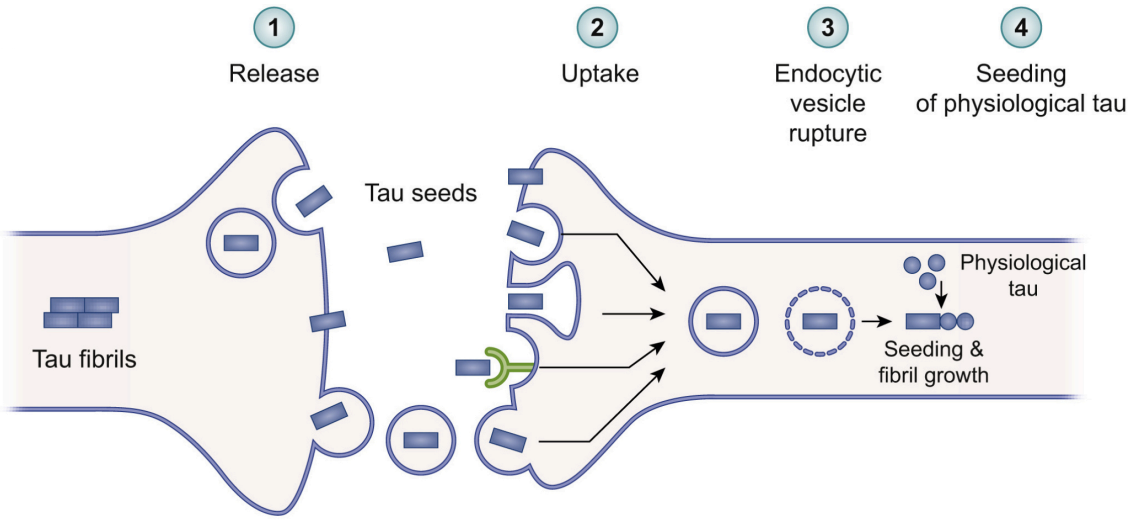

Figure 3. Propagation of phosphorylated tau seed pathology across the synaptic cleft via different release and uptake mechanisms including extracellular and synaptic vesicles as well as translocation. Tau seeds are taken up by the post-synaptic membrane and lead to the seeding of physiological tau. Figure taken from Vogels et al. (2020). For rights and permissions licensing information please see https://creativecommons.org/licenses/by-nc-nd/4.0/

3.4 Functional MRI

A way to non-invasively explore brain activity in vivo is through functional magnetic resonance imaging (fMRI). Neural activation requires local cerebral blood-flow to provide glucose and oxygen to support the increased metabolic demands of active neurons during cognitive processes and brain function. This close relationship between neural activity and blood-flow i.e. neurovascular coupling, is harnessed by fMRI which takes advantage of the magnetic differences between oxygenated and deoxygenated blood, causing alterations in the magnetic field of an MRI scanner. Oxygenated haemoglobin is diamagnetic, exhibiting weak repulsion when exposed to a magnetic field. However, when oxygen levels decrease, haemoglobin becomes deoxygenated resulting in a sudden shift to paramagnetism. This

alteration triggers variations in the blood-oxygen-level-dependent (BOLD) signal detected by fMRI. When oxygenated blood floods the area, it elevates the BOLD signal captured by

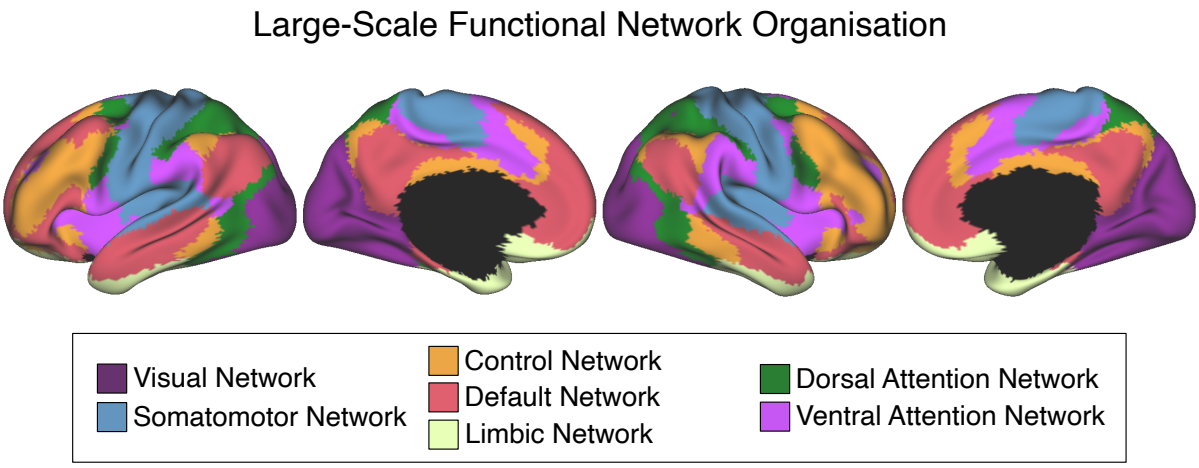

fMRI, serving as an indicator of underlying neuronal activity (Gauthier & Fan, 2019).

Figure 4. 7 major cortical large-scale networks estimated with a clustering approach derived from the rs-fMRI data of 1000 subjects separated into discovery and replication samples. Cortical brain rendering made with regions defined by Yeo et al. (2011)

Major discoveries with fMRI have revolved around the mapping of functions to regional activations, which was previously restricted to specific autopsy cases. This has been pivotal to expanding our previously limited knowledge of brain function localisation. Beyond mapping regions to function, fMRI has also allowed us to understand more about the brain's functional architecture and interactions between distributed regions. Resting-state (rs) fMRI, which monitors brain activity during wakeful rest i.e., in the absence of a specific cognitive task, reveals consistent inter-regional co-fluctuations in fMRI BOLD signal. The collective activation of specific brain regions reflects the intrinsic connectivity crucial for effective communication and coordination between regions, which is constrained by the underlying anatomical connections (Honey et al., 2009). The in-depth analysis of large-scale rs-fMRI has delineated the inter-regional synchronization into specialised networks (see figure 4) according to a number of different methods, which organise the brain's spontaneous activity into a range of systems supporting primary functions such as visual and motor, to complex multimodal functions such as control (Damoiseaux et al., 2006; Power et al., 2011; Yeo et al., 2011).

3.5 Neuroimaging evidence for connectivity-driven trans-neuronal tau spreading

Connectivity driven trans-neuronal tau propagation has now been observed in living AD patients through neuroimaging techniques. The combination of rs-fMRI and tau-PET allows the mapping of tau deposition patterns to connectivity patterns. Cross-sectional research employing this multi-modal approach reveals a notable relationship between tau accumulation and connectivity, demonstrating that tau accumulates preferentially in highly connected regions, i.e. “hub” regions (Cope et al., 2018) and that interregional connectivity predicts the similarity in tau SUVR levels, whereby connectivity strength between regions correlates with tau covariance (Adams et al., 2019; Franzmeier et al., 2019; Ossenkoppele et al., 2019). Furthermore, research combining tau-PET and a simulated diffusion model based on anatomical and functional connections corroborate the concept of connectivity driven trans-neuronal tau spreading by simulating tau spreading through the cortex. The simulated results were highly comparable to tau-PET assessed cross-sectional tau deposition patterns in AD patients affirming the concept of focal tau initiation and subsequent spread across neural connections (Vogel et al., 2020).

Subsequent longitudinal tau-PET investigations have strengthened the understanding of tau's progressive connectivity driven propagation by allowing within-subject tracking of tau progression through time. Research combining functional connectivity analysis with longitudinal tau-PET from AD spectrum subjects indicates that tau spreading starts from a focal region, typically within the medial temporal lobe, spreading to the next most connected regions and ultimately reaching the least connected regions (Franzmeier et al., 2020a). This connectivity spreading pattern is supported by further research using a graph theory driven tau spreading model to predict tau spreading acceleration patterns based on the connectivity of a medial temporal lobe seed (i.e., entorhinal cortex). Connectivity predicted tau acceleration regions aligned with longitudinal tau-PET dynamics in AD individuals who exhibited faster tau accumulation in these given regions (Lee et al., 2022) demonstrating the acceleration effects of highly connected regions on overall tau spreading rates.

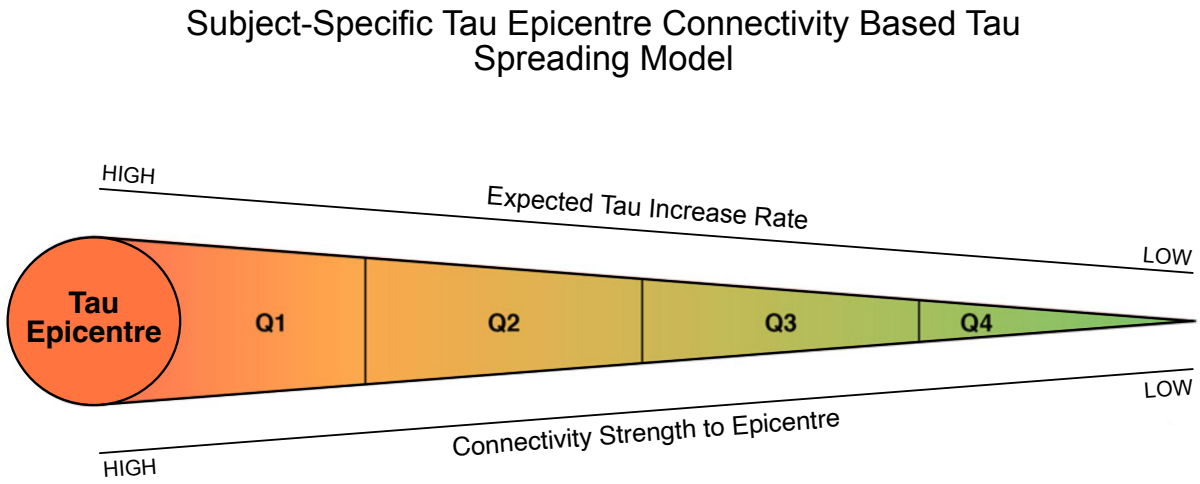

Figure 5. Model of tau epicentre connectivity predicted tau accumulation in connectivity strength defined regions, q1 being the most functionally connected region to the epicentre with the highest expected tau accumulation rate and q4 the least functionally connected region to the epicentre with the lowest expected tau accumulation rate. Figure adapted from Franzmeier et al. (2020a). For rights and permissions licensing information please see https://creativecommons.org/licenses/by-nc/4.0/

Importantly, functional findings are supported by longitudinal anatomical evidence examining major white matter tracts with diffusion weighted MRI. This research reveals that the extent of tau deposition in downstream brain regions to those harbouring tau is seemingly impacted by the diffusivity of connecting structural tracts. Observed results indicated that increased diffusivity of the connecting tract corresponded to heightened tau presence in the downstream region. These findings align with fMRI evidence, providing structurally backed support for the mechanism of tau propagation across neural connections (Jacobs et al., 2018).

Overall, in vivo evidence elucidates the importance of the functional connectome for trans-neuronal tau spreading and contributes greatly to our understanding of the temporal and spatial trajectory of tau spreading.

3.6 Variability in Alzheimer's disease progression

3.6.1 Progression rate variability

Sporadic AD has highly variable clinical trajectories, whereby individuals exhibit different onset ages and rates of cognitive decline. A reason for heterogenous clinical progression is variation in neuropathological progression. Subtypes of AD have emerged from tau-PET evidence delineating the different routes and rates which tau takes through the cortex, resulting in deficiencies in different cognitive domains and varying rates of clinical

progression (Ossenkoppele et al., 2016; Risacher et al., 2017; Vogel et al., 2021). This body of research reveals a strong link between faster more aggressive cognitive decline and a fronto-parietal focused tau deposition route compared to a slower route through medial-temporal limbic regions, which typically starts at a later age.

Nevertheless, the factors influencing the diverse routes and speed of tau spreading remain unclear. A recent study utilising fMRI-derived connectivity offers the functional characteristics of the tau epicentre as a potential explanation for the variability observed in tau progression. Findings reveal that individuals with stronger tau load in hub regions had faster subsequent tau spreading suggesting that the global connectivity of initial tau harbouring regions predicts the speed of subsequent tau accumulation (Frontzkowski et al., 2022). Consistent with earlier investigations, this study reveals an association between younger age of onset and a heightened tau load particularly in fronto-parietal regions, known to be rich in crucial globally connected hubs that are crucial for cognitive function (Van den Heuvel & Sporns, 2013). This suggests that the connectivity of high tau-burden regions drives the rate of tau spreading and thus cognitive decline. These findings strongly support the concept that not only does functional architecture determine the spatial route of trans-neuronal tau spreading but also the temporal dynamics.

3.6.2 Known tau modulators

There is a growing body of literature identifying specific tau modulating factors. Firstly, sex differences have been suggested to influence pathophysiological progression of AD whereby women with abnormal Aβ deposition have been identified at higher risk for early tau deposition in the entorhinal cortex and outside of the temporal lobe compared to men (Buckley et al., 2019; Buckley et al., 2022). Sex differences in AD are speculated to be due to hormonal changes related to the menopause (Buckley et al., 2022) however, the mechanisms are elusive. Furthermore, vascular risk has also been linked to increased tau pathology in Aβ positive individuals in which patients with an elevated risk of developing coronary heart disease, estimated with a sex-specific algorithm, had more tau-PET uptake in the temporal lobe (Rabin et al., 2019). Moreover, research examining self-reported levels of physical activity and tau-PET found that individuals that exercised frequently had lower levels of neocortical tau burden compared to individuals that exercised infrequently, which was

independent of cardiovascular health (Brown et al., 2018). Together, this research provides compelling evidence that tau dynamics are susceptible to specific factors, emphasizing the importance of recognising and understanding modulating factors to mitigate the risk of accelerated tau progression.

3.6.3 Genetic landscape and ApoE4

Sporadic AD has been estimated to have substantial heritability, with comprehensive European population-based twin studies attributing roughly 60-80% of the variance for developing AD to genetic factors (Gatz et al., 2006; Karlsson et al., 2022). Genome wide association studies (GWAS) have enabled a broader exploration of the genetic AD landscape; however, genome research has not come close to identifying all contributable variants implied by twin studies. As GWAS are progressively becoming larger, more and more previously unidentified gene loci are being uncovered (Bellenguez et al., 2022; Wightman et al., 2021). Many common genetic variants have been linked to AD risk, most having an individually small impact on AD vulnerability however, the complexity lies in the cumulative effect of these common genetic variants. It is predicted that there could be as many as 10,000 different variants responsible for sporadic AD, with intricate polygenic interactions (Holland et al., 2021). Analysis of identified AD risk variants points towards a predominant involvement in amyloid and tau pathways (Bellenguez et al., 2022), but the direct association of genes to AD pathophysiological processes remains an evolving field. Nevertheless, it is evident that implicated genes extend beyond direct involvement in tau and amyloid pathways and contribute to a number of different processes.

In the past few decades several standout genetic variants with a substantial individual effect on AD risk have been identified, including Myc box-dependent-interacting protein 1 (BIN1), implicated in endocytic processes (Prokic et al., 2014), triggering receptor expressed on myeloid cells 2 (TREM2), expressed by microglia and implicated in neuroinflammation (Gratuze et al., 2018) and sortilin related receptor 1 (SORL1) implicated in the metabolism of amyloid precursor protein (Rogaeva et al., 2007). Most notably is the ε4 allele on the apolipoprotein E (ApoE4) which is responsible for controlling cholesterol and lipid transport (Mahley, 2016). ApoE4 is the most significant risk factor across populations (Reitz et al., 2013) contributing to 9% of total AD risk (Karlsson et al., 2022). ApoE4 carriers typically

exhibit an earlier age of disease onset (van der Flier et al., 2011) with homozygotic carriers succeeding non-carriers up to 10 years (Blacker et al., 1997). Research has demonstrated that ApoE4 is robustly linked to increased and earlier amyloidosis (Liu et al., 2017) and emerging research is increasingly linking ApoE4 to elevated tau accumulation, both dependently and independently of Aβ (Benson et al., 2022; Therriault et al., 2020; Young et al., 2023). Nevertheless, the precise mechanisms through which ApoE4 accelerates Aβ and tau progression remain unclear, yet highly pertinent owing to the prevalence AD patients who carry an ApoE4 allele (Ward et al., 2012).

3.7 Thesis aims

Overall, uncovering more about the functional and genetic architecture of AD is pertinent to understanding the major processes of AD pathophysiology therefore, the major aims of this thesis are 1) to explore differences in functional connectivity and its impact on tau progression and 2) to understand how certain genes, in particular ApoE4, link to the onset and progression rate of tau. These investigations would enable the identification of functional and genetic risk factors with the potential to guide more effective treatment targets capable of intercepting tau progression in a timelier manner.

4 STUDIES

4.1 Functional network segregation is associated with attenuated tau spreading in Alzheimer's disease

The following section presents the original research article "Functional network segregation is associated with attenuated tau spreading in Alzheimer's disease" which was published in Alzheimer's & Dementia (Steward et al., 2022)

Received: 28 March 2022 | Revised: 1 September 2022 | Accepted: 5 October 2022

DOI: 10.1002/alz.12867

Alzheimer's & Dementia®
THE JOURNAL OF THE ALZHEIMER'S ASSOCIATION

RESEARCH ARTICLE

Functional network segregation is associated with attenuated tau spreading in Alzheimer's disease

Anna Steward[1] | Davina Biel[1] | Matthias Brendel[2,3,4] | Anna Dewenter[1] | Sebastian Roemer[1,5] | Anna Rubinski[1] | Ying Luan[1] | Martin Dichgans[1,3,4] | Michael Ewers[1,3] | Nicolai Franzmeier[1,4] | for the Alzheimer's Disease Neuroimaging Initiative (ADNI)

[1]Institute for Stroke and Dementia Research (ISD), University Hospital, LMU, Munich, Germany

[2]Department of Nuclear Medicine, University Hospital, LMU Munich, Munich, Germany

[3]German Center for Neurodegenerative Diseases (DZNE), Munich, Germany

[4]Munich Cluster for Systems Neurology (SyNergy), Munich, Germany

[5]Department of Neurology, University Hospital, LMU Munich, Munich, Germany

Correspondence
Dr. Nicolai Franzmeier, Institute for Stroke and Dementia Research (ISD), University Hospital, LMU Munich, 81377 Munich, Germany.
E-mail: Nicolai.Franzmeier@med.uni-muenchen.de

Data used in preparation of this article were obtained from the Alzheimer's Disease Neuroimaging Initiative (ADNI) database (adni.loni.usc.edu). As such, the investigators within the ADNI contributed to the design and implementation of ADNI and/or provided data but did not participate in analysis or writing of this report. A complete listing of ADNI investigators can be found at: http://adni.loni.usc.edu/wp-content/uploads/how_to_apply/ADNI_Acknowledgement_List.pdf

Abstract

Introduction: Lower network segregation is associated with accelerated cognitive decline in Alzheimer's disease (AD), yet it is unclear whether less segregated brain networks facilitate connectivity-mediated tau spreading.

Methods: We combined resting state functional magnetic resonance imaging (fMRI) with longitudinal tau positron emission tomography (PET) in 42 betamyloid-negative controls and 81 amyloid beta positive individuals across the AD spectrum. Network segregation was determined using resting-state fMRI–assessed connectivity among 400 cortical regions belonging to seven networks.

Results: AD subjects with higher network segregation exhibited slower brain-wide tau accumulation relative to their baseline entorhinal tau PET burden (typical onset site of tau pathology). Second, by identifying patient-specific tau epicenters with highest baseline tau PET we found that stronger epicenter segregation was associated with a slower rate of tau accumulation in the rest of the brain in relation to baseline epicenter tau burden.

Discussion: Our results indicate that tau spreading is facilitated by a more diffusely organized connectome, suggesting that brain network topology modulates tau spreading in AD.

KEYWORDS
Alzheimer's disease, functional magnetic resonance imaging, network segregation, tau spreading, tau positron emission tomography

Highlights

- Higher brain network segregation is associated with attenuated tau pathology accumulation in Alzheimer's disease (AD).
- A patient-tailored approach allows for the more precise localization of tau epicenters.
- The functional segregation of subject-specific tau epicenters predicts the rate of future tau accumulation.

1 | INTRODUCTION

Alzheimer's disease (AD) is characterized by cerebral amyloid beta (Aβ) plaques and tau tangles. Aβ accumulates decades before symptom manifestation whereas tau pathology develops closely before symptom onset.[1,2] The severity of tau pathology, assessed via tau positron emission tomography (PET) and fluid biomarkers, has been shown to predict subsequent cognitive decline[3–5] suggesting that tau is a key driver of clinical disease progression; hence, it is clinically important to understand the mechanisms that drive the development of tau pathology.

Tau pathology spreads in a characteristic pattern from the medial temporal lobe toward the neocortex,[6] closely followed by neurodegeneration.[7] Preclinical studies have shown that tau spreads via synapses in an activity-dependent manner via anatomical connections rather than seeping into proximal brain regions.[8–10] These findings have recently been translated to biomarker data from AD patients by combining resting state functional magnetic resonance imaging (rs-fMRI) for assessing functional brain connectivity and tau PET imaging for mapping tau pathology spread. Specifically, we and others found that (1) tau pathology distributes preferentially across functionally connected brain regions,[11–13] (2) connected brain regions show correlated tau accumulation rates, and (3) tau pathology emerges in circumscribed epicenters, from where it spreads across functionally connected brain regions.[14–16] Together, these findings provide evidence that the brain's connectome plays an important role in routing tau spread in AD, thereby determining disease progression.

Numerous rs-fMRI studies have revealed that the functional connectome is modular and comprised of functionally specialized networks integral to cognitive functioning.[17,18] Previous studies found that modularity of brain networks diffuses with age resulting in desegregated networks with stronger inter-network connections[19–22] and a general deterioration of functional ability.[23,24] We have shown recently that reduced rs-fMRI–assessed network segregation is linked to stronger cognitive deficits relative to the level of AD pathology in sporadic and inherited AD.[25] Furthermore, modulating effects of network segregation on cognition are supported by longitudinal work, suggesting decreased segregation to be a risk factor for increased severity of dementia symptoms.[26] These studies propose that brain network segregation modulates AD symptom severity by offering resilience toward primary AD pathology, whereby individuals with higher network segregation maintain better cognition despite higher disease burden. However, it is unclear whether higher network segregation only provides resilience against the impact of AD pathology on cognition, or whether higher segregation also attenuates the progression of primary AD pathology, therefore providing resistance against AD pathology. Because tau pathology spreads across connected brain regions,[14–16] it is possible that stronger network segregation restricts inter-regional tau spreading thereby attenuating cognitive decline. Thus, our major aim was to investigate whether stronger network segregation is associated with reduced tau progression and whether a more diffuse network topology is linked to faster tau expansion.

RESEARCH IN CONTEXT

1. **Systematic Review**: Heterogeneity in Alzheimer's disease (AD) progression is problematic for clinical prognosis; therefore, understanding its modulators is highly important. The brain's functional connectome, identified as a critical route for the spreading of connectivity-mediated tau pathology, could be crucial in understanding AD progression.
2. **Interpretation**: Analysis of tau positron emission tomography and resting state functional magnetic resonance imaging data revealed that higher network segregation and higher segregation of patient-specific tau epicenters (onset site of tau pathology) were associated with a slower rate of pathological tau accumulation in the rest of the brain. Findings suggest that a more diffuse network topology facilitates connectivity-mediated inter-regional tau spreading indicating that inter-individual differences in global and tau epicenter connectivity impact the speed of pathological tau progression in AD.
3. **Future Directions**: Using the patient-tailored approach to understand more about the functional heterogeneity of tau epicenters and their specific impact on tau dynamics.

To investigate this, we assessed rs-fMRI and longitudinal flortaucipir tau PET in 81 biomarker-defined AD and 42 control subjects from the Alzheimer's Disease Neuroimaging Initiative (ADNI) database. Our major aim was to assess whether higher network segregation is associated with attenuated tau spreading from brain regions in which tau emerges first (i.e., tau epicenters) to the rest of the brain. Therefore, adhering to the Braak-like stereotypical pattern of tau spreading, we explored first if higher network segregation attenuated the relationship between baseline entorhinal tau burden (i.e., Braak I, the typical site of tau onset), and the rate of tau accumulation in the rest of the brain. Second, we adopted a patient-tailored approach, in which subject-specific tau epicenters were identified as sites with the highest baseline tau PET standardized uptake value ratio (SUVR). We then assessed whether higher segregation of subject-specific tau epicenters was associated with attenuated tau accumulation in the rest of the brain.

2 | METHODS

2.1 | Participants

We included 123 participants from the ADNI database based on availability of longitudinal ^{18}F-flortaucipir tau PET (>1 visit), 3T rs-fMRI and ^{18}F-florbetapir/florbetaben amyloid PET obtained within 6 months of the initial tau PET scan. All subjects were classified as Aβ positive or

negative (Aβ+/−) based on established global 18F-florbetapir (global SUVR > 1.11) and global ^{18}F-florbetaben amyloid PET thresholds (global SUVR > 1.08)[27] applied to amyloid PET SUVR data provided by the ADNI PET core. ADNI investigators diagnosed subjects as either cognitively normal (CN; Mini-Mental State Examination [MMSE] ≥ 24, Clinical Dementia Rating [CDR] = 0, non-depressed), mildly cognitively impaired (MCI; MMSE ≥ 24, CDR = 0.5, objective memory impairment on education-adjusted Wechsler Memory Scale II, preserved activities of daily living) or demented (MMSE = 20–26, CDR > 0.5, National Institute of Neurological and Communicative Disorders and Stroke/Alzheimer's Disease and Related Disorders Association criteria for probable AD). The sample included 42 Aβ− CN subjects and 81 Aβ+ covering the AD spectrum: (CN/MCI/dementia n = 38/25/18); Aβ− subjects with a diagnosis other than CN were excluded owing to suspected non-AD pathology. Ethical approval was obtained by ADNI sites and written informed consent was collected from all participants.

2.2 | MRI and PET acquisition

Structural and functional MRI were acquired using 3T Siemens (SIEMENS Healthineers) and 3T GE scanners. T1-weighted structural scans were collected using a magnetization-prepared rapid gradient echo sequence (repetition time [TR] = 2300 ms; voxel size = 1 × 1 × 1 mm; for parameter details see: https://adni.loni.usc.edu/wp-content/uploads/2017/07/ADNI3-MRI-protocols.pdf). rs-fMRI was obtained using a 3D echo-planar imaging (EPI) sequence with 200 fMRI volumes per subject (TR/echo time [TE] = 3000/30 ms; flip angle = 90°; voxel size = 3.4 × 3.4 × 3.4 mm).

PET data were assessed post–intravenous injection of ^{18}F-labeled tracers (flortaucipir: 6 × 5 minute time frames, 75–105 minutes post-injection; florbetapir: 4 × 5 minute time frames, 50–70 minutes post-injection; florbetaben: 4 × 5 minute time frames, 90–110 minutes post-injection; for more information see http://adni.loni.usc.edu/methods/pet-analysis-method/pet-analysis/).

2.3 | MRI and PET preprocessing

All images were screened for artifacts before preprocessing. T1 scans were skull stripped, bias corrected, segmented, and non-linearly normalized to Montreal Neurological Institute (MNI) space using the advanced normalization tools (ANTs) software package. EPI images were slice-time and motion corrected and co-registered to the native T1-weighted images. Using rigid-transformation parameters, T1-derived gray matter, white matter, and cerebrospinal fluid (CSF) segments were transformed to EPI space. To denoise EPI images, we regressed out nuisance covariates (i.e., white matter and CSF time series plus six motion parameters and their derivatives) and applied detrending and band-pass filtering (0.01–0.08 Hz) in EPI native space. To further reduce movement artifacts that may compromise connectivity assessment[28] we performed motion scrubbing, in which volumes exceeding a 0.5 mm frame-wise displacement threshold were removed, as well as one prior and two subsequent volumes. Subjects for which >30% of volumes had to be removed were not included in the study.[29] Spatial smoothing was not performed to avoid artificially enhancing functional connectivity caused by signal spilling between adjacent brain regions. Preprocessed rs-fMRI images were subsequently normalized to MNI space via T1-derived spatial normalization parameters. To assess the effect of different rs-fMRI processing protocols on our findings, we repeated all analyses further including global signal regression and applying a more restrictive frame-wise displacement threshold of 0.3 mm.

Dynamically acquired tau PET images were realigned and averaged to obtain single flortaucipir images. Using brain-extracted T1-weighted images and ANTs-derived non-linear spatial normalization parameters,[30] tau PET images were affine registered to T1-weighted images, spatially normalized to MNI space, and subsequently intensity normalized using an inferior cerebellar gray reference.[31] Spatially normalized tau PET images were parceled into 400 cortical regions of interest (ROIs) of the Schaefer atlas by averaging ROI-specific voxels (Figure 1A).[32] The atlas was additionally masked using a group-specific gray matter mask binarized at 0.3 probability.

2.4 | Functional connectivity assessment

Functional connectivity was assessed among the 400 ROIs[32] which are grouped into seven major functional networks (Figure 1A), including the default mode network (DMN); ventral attention network (VAN); dorsal attention network (DAN); frontoparietal control network (FPCN); as well as visual, limbic, and motor networks.[33] This atlas was chosen for its suitability for the combination of tau PET and fMRI, owing to the atlas' exclusion of areas outside of the neocortex, which are susceptible to off-target binding of the flortaucipir tracer.[34,35] Fisher z–transformed Pearson-moment correlations of preprocessed ROI-specific rs-fMRI time series were assessed between all possible ROI pairs, and negative values and autocorrelations were set to 0, following our pre-established approach.[25]

2.5 | Network segregation

For the first major analysis, network segregation was calculated according to each ROIs connectivity and its respective network affiliation[33] using a pre-established system segregation (SyS) equation (Equation 1)[19]:

$$SyS = \frac{\overline{zw} - \overline{zb}}{\overline{zw}} \quad (1)$$

whereby zw is the mean within network connectivity and zb is the mean between network connectivity.[19] To ensure that our measure of SyS was not associated with in-scanner motion, we tested the association between SyS and mean framewise displacement during the rs-fMRI scan. Here, no association was found (P = 0.735) using linear regression.

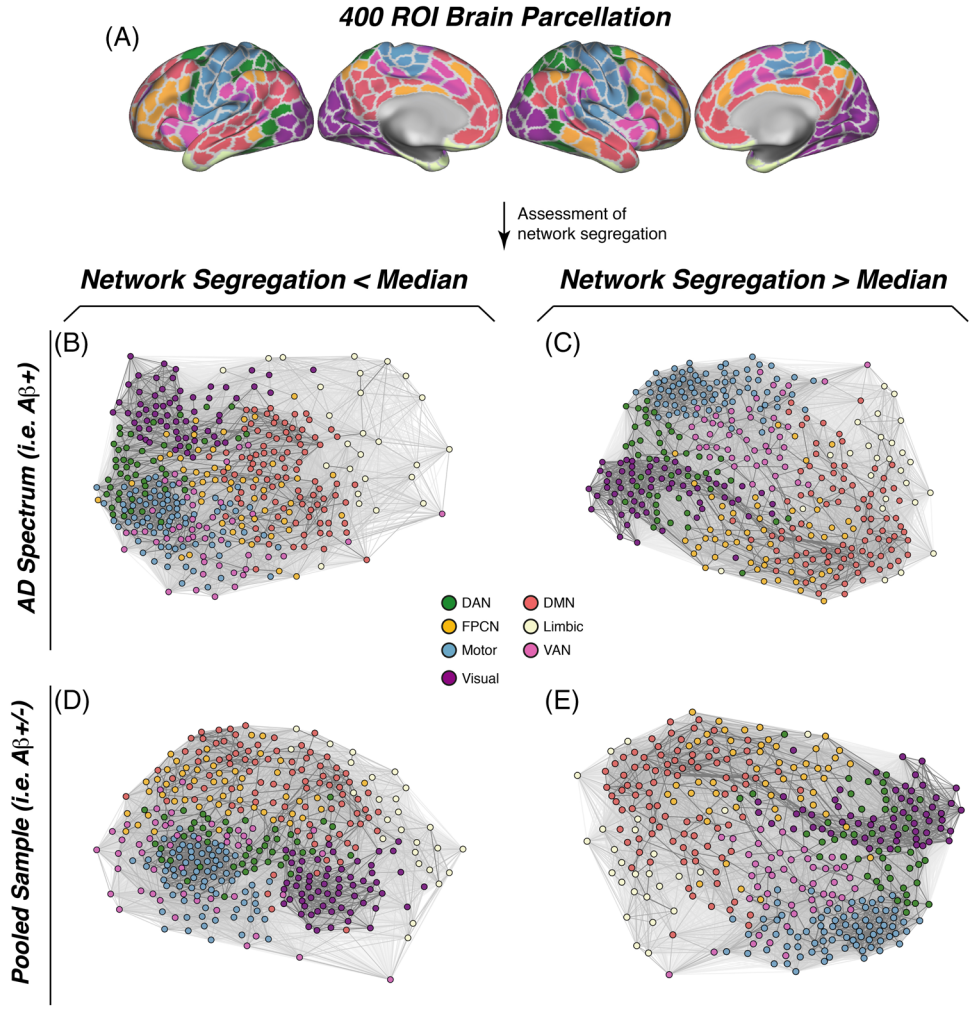

FIGURE 1 The Schaefer 400 region of interest (ROI) brain parcellation grouped into seven major networks was used to determine functional connectivity and network segregation between brain networks (A). Force-directed plots illustrating brain network topology, stratified by amyloid beta positivity (Aβ+: B,C; pooled: D,E) and network segregation level (median split), whereby shorter node distance is representative of higher connectivity strength. Plots were generated using the Fruchtermann–Reingold algorithm applied to group-average functional connectivity data. DAN, dorsal attention network; DMN, default mode network; FPN, frontoparietal control network; VAN, ventral attention network

2.6 | Definition of tau epicenters and epicenter segregation

To assess whether higher segregation of those epicenter regions in which tau is assumed to develop first attenuates the subsequent spreading of tau to the rest of the brain, we determined both the location of tau epicenters as well as the segregation of epicenters for each patient. Epicenters, that is, the potential sites of tau onset in a given individual, were determined for each Aβ+ subject by systematically applying pre-defined tau PET SUVR thresholds to the Schaefer atlas (baseline tau PET SUVRs of 1.3, 1.2, and 1.1).[12,14,16] Subsequently, ROI-wise segregation was defined for each subject, whereby *zw* is the connectivity of a given ROI to all ROIs in its own network and *zb* is the given ROI's connectivity to all other network ROIs as shown in Equation (1). Epicenter segregation was subsequently estimated by averaging the segregation scores of all ROIs belonging to a subject-specific epicenter. Further, we obtained an alternative global measure of network segregation by averaging segregation measures across all 400 ROIs to compare the ROI-wise segregation approach to the whole-brain method used to determine global segregation.[19] Both SyS scores were highly correlated ($r = 0.95$, $R2 = 0.90$, $P < 0.001$) indicating high consistency between the two methods.

2.7 | Statistical analysis

Differences in demographic, cognitive, and PET measures between diagnostic groups were tested using analyses of variance (ANOVAs) for continuous variables and chi-squared (χ^2) tests for categorical variables (Table 1). Annual tau PET change rates were calculated for each ROI by fitting linear mixed models with tau PET SUVR as the dependent variable and time from baseline in years as the independent variable, including random slope and intercept.[36]

To test the main hypothesis of whether higher network segregation attenuates tau spreading, we investigated the interaction effect

TABLE 1 Demographics and sample characteristics

	CN Aβ− (*n* = 42)	CN Aβ+ (*n* = 38)	MCI Aβ+ (*n* = 25)	Dementia Aβ+ (*n* = 18)	*P*-value
Sex (F/M)	26/16	22/16	11/14	6/12	0.151
Age	71.7 (7.24)	74.1 (5.72)	73.4 (6.60)	76.0 (8.26)	0.149
Years of education	16.5 (2.50)	16.5 (2.36)	16.5 (2.76)	15.5 (2.50)	0.511
ADAS13	7.67 (5.01)[c,d]	9.70 (5.43)[d]	15.4 (5.06)[a,d]	26.8 (10.8)[a,b,c]	<0.001
Global tau PET SUVR	1.07 (0.090)[c,d]	1.12 (0.092)[d]	1.22 (0.246)[a,d]	1.40 (0.375)[a,b,c]	<0.001
Annual change in global tau PET SUVR	0.00271 (0.00755)[c,d]	0.00927 (0.0103)[c,d]	0.0183 (0.0163)[a,b]	0.0196 (0.0219)[a,b]	<0.001
Tau PET follow-up in years	1.84 (0.955)	1.84 (0.723)	1.45 (0.499)	1.52 (0.521)	0.098
Centiloid	−4.57 (12.7)[b,c,d]	71.5 (32.9)[a]	82.2 (30.1)[a]	92.0 (37.0)[a]	<0.001
Amyloid PET tracer (florbetapir/florbetaben)	34/8	24/14	15/10	10/8	0.133
SyS	0.507 (0.100)	0.523 (0.083)	0.540 (0.064)	0.514 (0.072)	0.458
rs-fMRI—mean framewise displacement	0.11 (0.06)	0.12 (0.06)	0.08 (0.05)[d]	0.14 (0.06)[c]	0.023

Note: *P*-values were derived from ANOVA for continuous measures and from chi-squared tests for categorical measures. Mean values significantly ($P < 0.05$, Tukey post hoc tests) different from—
[a]CN Aβ−.
[b]CN Aβ+.
[c]MCI Aβ+.
[d]Dementia Aβ+.

between baseline entorhinal tau (i.e., Braak I, the stereotypical site of tau onset of the Braak staging scheme) and global segregation on the rate of longitudinal tau accumulation outside of the entorhinal cortex. To this end, linear models were fit with each subject's baseline entorhinal tau PET SUVR and their global segregation value as well as their interaction as independent variables, and the rate of longitudinal tau change outside of the entorhinal cortex as the dependent variable controlling for age, sex, diagnosis, scanner manufacturer, and mean framewise displacement during the rs-fMRI scan. All interaction effects were computed using continuous measures of tau PET in Braak I and SyS. To understand the influence of network segregation on distinct stages of tau expansion, further exploratory linear models using the same covariates as described above were fitted to isolate the effect of higher network segregation and entorhinal tau (i.e., Braak I) on tau change rates in earlier affected areas, Braak stages III and IV, and in the last affected areas, Braak stages V and VI. To assess the robustness of the interaction effects and to ensure that our results were not biased by influential cases, we recomputed all above-described models using 1000 bootstrapped samples (i.e., a random sample with replacement is drawn from the overall sample for each bootstrapping iteration) and determined 95% confidence intervals of the interaction effect beta values.

Our second aim was to explore whether higher segregation of patient-specific tau epicenters, not necessarily confined to the entorhinal cortex, limited the rate of tau accumulation outside of the epicenter, using baseline tau PET SUVRs of individualized tau epicenters at different thresholds and average annual tau PET accumulation across ROIs outside of the epicenter. To define epicenters, we selected brain regions that surpassed a pathological threshold of a tau PET SUVR > 1.3 at baseline, to ensure that epicenters are confined to regions with actual tau pathology. We further repeated this analysis using more liberal epicenter thresholds (i.e., SUVRs > 1.2 or 1.1), to assess whether the interaction effect becomes weaker if also regions with less tau pathology are included, which should be less influential for tau accumulation in the rest of the brain. A linear model was fitted taking each subject's epicenter tau PET SUVR value, epicenter segregation value, and their interaction as the independent variables and the rate of longitudinal tau change outside of the epicenter as the dependent variable controlling for age, sex, diagnosis, scanner manufacturer, and mean framewise displacement during the rs-fMRI scan. To further explore the effect of epicenter size on the interaction between epicenter segregation and tau PET SUVR on the rate of tau spreading, linear models with the same variables were repeated at different epicenter thresholds systematically varied between tau PET SUVRs of 1.0 to 1.3 in steps of 0.01. The standardized beta value of the interaction effect (epicenter segregation x epicenter tau PET SUVR) was extracted from each linear model and correlated with epicenter SUVR threshold to assess whether interaction effects weakened at more liberal epicenter definitions. All statistical analyses were conducted in R. All analyses were repeated across different rs-fMRI preprocessing protocols, including or excluding global signal regression and applying different framewise displacement thresholds of 0.5 mm and 0.3 mm.

2.8 | Data availability

ADNI data are publicly available (adni.loni.usc.edu) upon registration and compliance with the data use agreement. The data that support the findings of this study are available on reasonable request from the

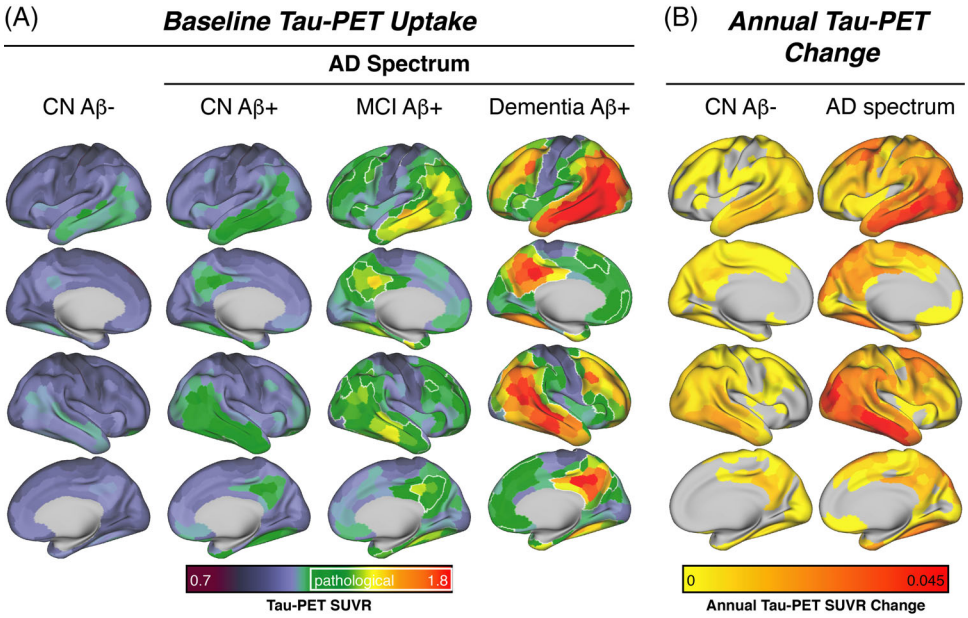

FIGURE 2 Group-average tau PET SUVRs at baseline stratified by amyloid status and diagnostic group. Tau PET SUVRs are shown as continuous values, white outlines define areas which surpass a pre-established pathological tau SUVR threshold of 1.3[58] (A). Group average tau SUVR annual change rates defined by linear mixed models, stratified by amyloid positivity (B). AD, Alzheimer's disease; CN, cognitively normal; MCI, mild cognitive impairment; PET, positron emission tomography; SUVR, standardized uptake volume ratio

corresponding author. The analysis R code can be found in the supporting information.

3 | RESULTS

3.1 | Sample characteristics

A total of 123 subjects were included in the study, of which 81 were classified as Aβ+ and diagnosed within the AD spectrum, versus 42 Aβ− CN controls. ANOVAs and χ^2 tests revealed no significant differences in baseline demographics (i.e., age, sex, education) or tau- PET follow-up times, but the expected group differences in baseline tau PET SUVRs ($F[3,119] = 13.64$, $P < 0.001$), annual tau PET change rates ($F[3,119] = 10.78$, $P < 0.001$), amyloid PET levels ($F[3,119] = 86.69$, $P < 0.001$), and global cognition (i.e., Alzheimer's Disease Assessment Scale 13-item cognitive subscale, $F[3,119] = 11.71$, $P < 0.001$). All group characteristics and the directionality of group differences are summarized in Table 1. When mapping the spatial pattern of tau PET uptake and annual tau PET change rates across groups, increasing AD severity was associated with stronger temporoparietal and frontal tau deposition (Figure 2A) and AD groups showed faster temporoparietal tau accumulation than controls (Figure 2B). No significant difference was found for global network segregation (i.e., SyS) across groups ($F[3,119] = 0.871$, $P = 0.458$). Force-directed plots for illustrating brain network topologies in the pooled and AD spectrum sample are shown in Figure 1B,E.

3.2 | Higher network segregation attenuates the association between entorhinal tau PET and tau accumulation in the rest of the brain

To test our main hypothesis of whether a more segregated brain network topology is associated with attenuated tau spreading from Braak I (i.e., entorhinal cortex) to Braak III to VI regions (Figure 3A), we tested whether higher global network segregation (i.e., SyS) attenuated the rate of tau spreading from the entorhinal cortex to the rest of the brain in Aβ+. Supporting this, results revealed an interaction between SyS and baseline entorhinal tau PET SUVRs on the subsequent tau accumulation rate in Braak III through VI regions in Aβ+ ($\beta = -2.11$, $P = 0.023$; Figure 3B). Specifically, at a given level of entorhinal tau PET, subjects with higher network segregation had slower rates of tau accumulation in Braak III through VI regions. Congruent effects were found when exploratorily investigating this association in separate Braak-stage ROIs. Specifically, we found significant interaction effects between SyS and entorhinal tau PET SUVRs on the rate of tau accumulation in Braak III and IV ($\beta = -2.17$ $P = 0.027$; Figure 3C) and Braak V and VI ROIs ($\beta = -2.01$, $P = 0.024$; Figure 3D). All findings were consistent but less pronounced when the same analysis was repeated in the pooled Aβ− and Aβ+ sample in Braak III through VI ($\beta = -1.44$, $P = 0.033$; Figure 3E), Braak III and IV ($\beta = -1.33$, $p = .056$; Figure 3F) and Braak V and VI ROIs ($\beta = -1.44$, $P = 0.028$; Figure 3G). All results were non-parametrically confirmed by bootstrapping. Detailed statistics including bootstrapped confidence intervals and R^2 values are summarized in Table 2. Further, all results remained consistent when repeated across

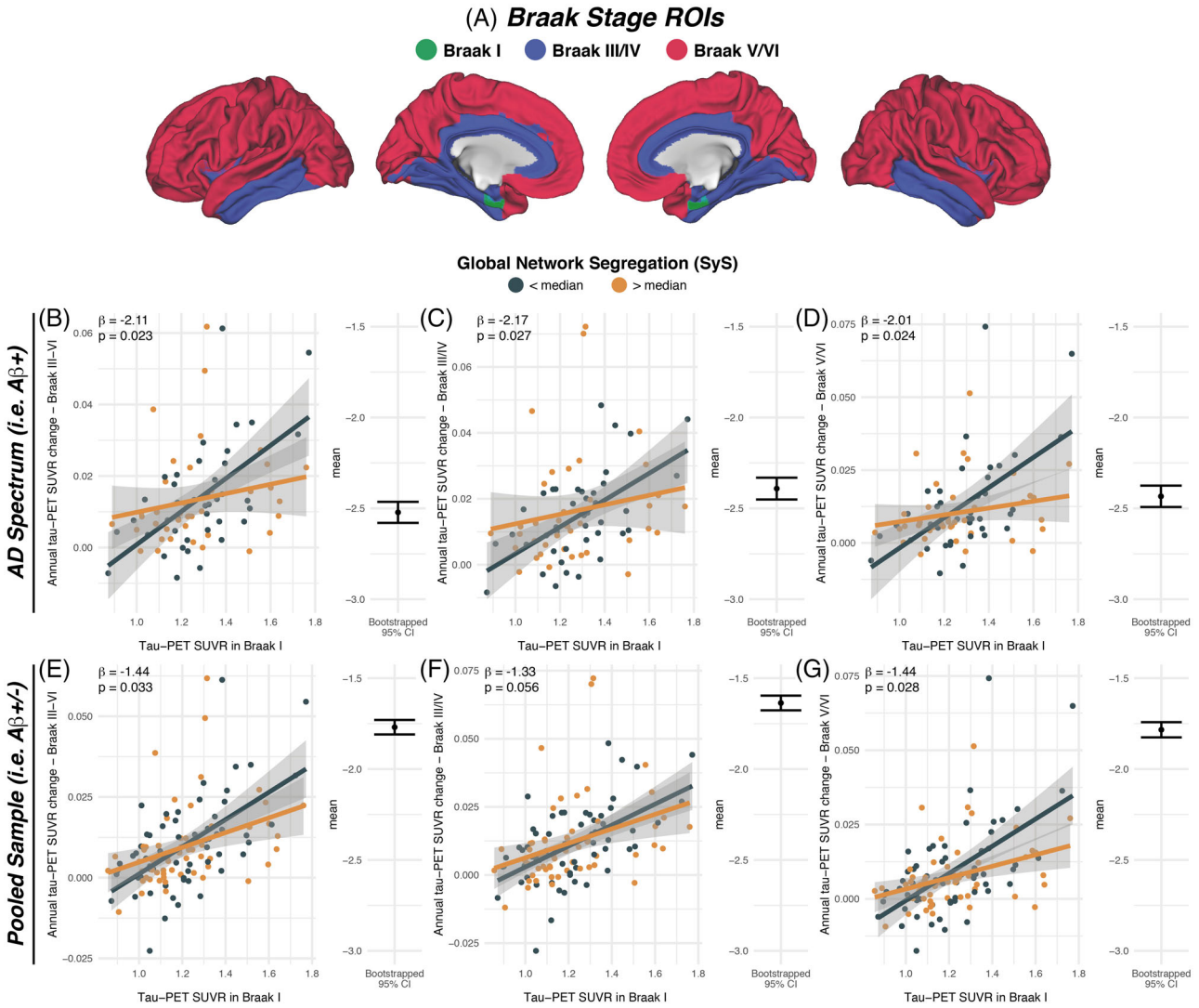

FIGURE 3 Surface rendering of the Braak-staging regions of interest (ROIs) that were applied to tau positron emission tomography (PET) data to determine baseline tau PET levels and longitudinal tau PET changes (A). Scatterplots illustrating the interaction effect between global network segregation (SyS) and entorhinal tau PET levels at baseline on tau PET increase in the remaining brain for amyloid beta positivity (Aβ+), showing that higher network segregation is associated with an attenuated association between entorhinal tau PET and tau accumulation in the rest of the brain (B). Exploratory analyses were performed in Aβ+ subjects, testing the same regression models for earlier Braak regions III/IV (C) and late Braak regions V/VI (D). Analyses were repeated also including the Aβ− control group (E–G). All statistical tests were fitted with continuous data, the use of median split to divide subjects is solely for visual purposes. 95% confidence intervals of interaction effects determined on 1000 bootstrapped iterations are displayed next to each scatterplot. SUVR, standardized uptake value ratio

different rs-fMRI preprocessing protocols (Table S1 in supporting information).

3.3 | Epicenter segregation attenuates tau spreading in AD

Next, we investigated whether the segregation of patient-specific tau epicenters affects subsequent tau accumulation in the rest of the brain in AD. This aim was motivated by evidence for heterogeneous tau spatial distribution patterns that deviate from the stereotypical Braak staging pattern.[14,37,38] To illustrate heterogeneity in tau epicenters, we rendered tau epicenter probabilities across different epicenter thresholds (i.e., tau PET SUVRs > 1.3/1.2/1.1; Figure 4A,C,E) in Aβ+. Linear models for epicenters across varying epicenter thresholds revealed that the interaction of epicenter segregation and the level of baseline epicenter tau SUVR significantly predicted the rate of tau accumulation outside of the epicenter. Specifically, Aβ+ subjects with higher epicenter segregation had slower annual tau accumulation rates in non-epicenter regions at an epicenter tau PET SUVR threshold > 1.3 ($\beta = -4.283$, $P = 0.003$, Figure 4B); however, the effects became statistically weaker at more liberal epicenter thresholds (tau PET SUVR > 1.2: $\beta = -2.754$, $P = 0.014$, Figure 4D; tau PET SUVR > 1.1: $\beta = -2.460$, $P = 0.024$, Figure 4F). Detailed statistics including bootstrapped

TABLE 2 Interaction effects of baseline tau PET in Braak I times SyS on tau PET rate of change in downstream Braak ROIs (i.e., Braak III-VI)

Group	Tau PET ROC in	*β*-value	*t*-value	*P*-value	Partial *R*2	Bootstrapped beta (mean [95% CI])
A*β*+	Braak III–VI	−2.11	−2.330	0.023	0.070	−2.434 [−2.493; −2.375]
	Braak III–IV	−2.17	−2.267	0.027	0.067	−2.391 [−2.451; −2.331]
	Braak V–VI	−2.01	−2.311	0.024	0.069	−2.433 [−2.493; −2.375]
A*β*+/A*β*− pooled	Braak III–VI	−1.44	−2.164	0.033	0.039	−1.769 [−1.809; −1.729]
	Braak III–IV	−1.33	−1.927	0.056	0.032	−1.636 [−1.677; −1.596]
	Braak V–VI	−1.44	−2.225	0.028	0.042	−1.783 [−1.825; −1.742]

Note: All statistics are based on linear models that were controlled for age, sex, diagnosis, scanner manufacturer, and mean framewise displacement during the resting-state fMRI scan. Regression weights are displayed as standardized beta values. Interaction effects have been computed using continuous measures of SyS and tau PET SUVRs in Braak I. Bootstrapping of interaction effects was performed using 1000 iterations to determine 95% confidence intervals. Confidence intervals not including zero provide non-parametric evidence for the significance of effects.
Abbreviations: A*β*, amyloid beta; CI, confidence interval; PET, positive emission tomography; fMRI, functional magnetic resonance imaging; ROC, receiver operating characteristic; ROIs, regions of interest; SUVR, standardized uptake value ratio; SyS, system segregation.

confidence intervals and R^2 values are summarized in Table 3. Further, all analyses remained consistent across different fMRI preprocessing protocols (Table S2 in supporting information). In addition, we performed null-model analyses, to test the specificity of epicenter tau PET and segregation as a predictor of tau PET change in remaining brain regions. To this end, we assessed the interaction between baseline tau PET in the non-epicenter and segregation of the non-epicenter on subsequent tau PET change rates in the tau epicenter. As expected, we did not find significant interaction effects across different thresholds (tau PET SUVR 1.3/1.2/1.1, $P = 0.23/0.47/0.63$), supporting the view that specifically epicenter regions with high tau pathology at baseline are informative for tau accumulation in remaining brain regions with low tau, and that higher segregation of the epicenter attenuates this association. To systematically investigate whether the effect of epicenter thresholds on the interaction effect between epicenter tau PET and epicenter segregation on tau accumulation in the rest of the brain weakened if epicenters were defined more liberally, we repeated this analysis while systematically reducing epicenter thresholds from tau PET SUVRs of 1.3 to 1.0 in steps of 0.01. In line with the previous analyses, interaction effects became weaker at more liberal epicenter definitions; that is, moving from higher to lower epicenter tau PET thresholds (Figure 5). This result pattern was mirrored in a negative association between epicenter thresholds and the strength of the interaction effect (i.e., beta value) between epicenter segregation and epicenter tau PET on the tau PET rate of change outside of the epicenter ($\beta = -0.81$, $P < 0.001$). Again, this result was consistent across different fMRI preprocessing protocols (Table S3 in supporting information).

4 | DISCUSSION

Our major finding was that higher segregation of functional brain networks is associated with attenuated tau accumulation in AD. Using rs-fMRI, we determined network segregation among seven major brain networks and found that individuals with higher network segregation exhibited a weaker association between baseline tau PET in the entorhinal cortex and the rate of tau accumulation in the rest of the brain. This finding, in line with the concept of connectivity-mediated tau spreading, conveys that inter-regional tau spreading is restricted by the sparser inter-network connections associated with stronger network segregation. Second, by identifying individualized tau epicenters as sites of patient-specific tau onset, we demonstrated that epicenter segregation similarly impacts heterogeneous tau spreading patterns, whereby individuals with higher epicenter segregation exhibited attenuated tau accumulation in the rest of the brain.

Our major finding that higher global network segregation is associated with an attenuated rate of pathological tau spreading in AD further reinforces preclinical evidence and extends translational research by supporting activity-dependent trans-neuronal tau spreading. Translational research revealed that the more connected a brain region is, the more vulnerable it is to tau pathology[11,12,38] and regions functionally connected to areas harboring tau are more likely to also harbor tau, regardless of spatial proximity.[14] We substantiate the concept of functional connectivity-related tau vulnerability introduced by these previous studies by demonstrating that the abundance and dispersion of functional connections are related to the ease of tau spreading.

Second, we demonstrate that tau accumulation can be determined by the segregation of subject-specific tau epicenters. In accordance with our first finding, we show that higher epicenter segregation is similarly related to curbed tau vulnerability, whereby high epicenter segregation may act as a barrier keeping tau more restricted to the epicenter. Additionally, we identify that defining an epicenter as a region with an abnormally high baseline tau load (i.e., SUVR > 1.3) holds the most predictive power about an individual's impending AD progression by illustrating a deterioration of the epicenter's predictive power as it is defined more liberally. These findings illustrate how regions that harbor less tau at baseline explain little about future tau progression, thereby emphasizing the importance of defining epicenters precisely as regions harboring significant tau pathology to maximize the model's strength for predicting patient-level future tau accumulation. Further, it is clear from previous studies that regional variability in tau deposition exists in AD;[14,37] therefore, assuming stereotypical tau deposition

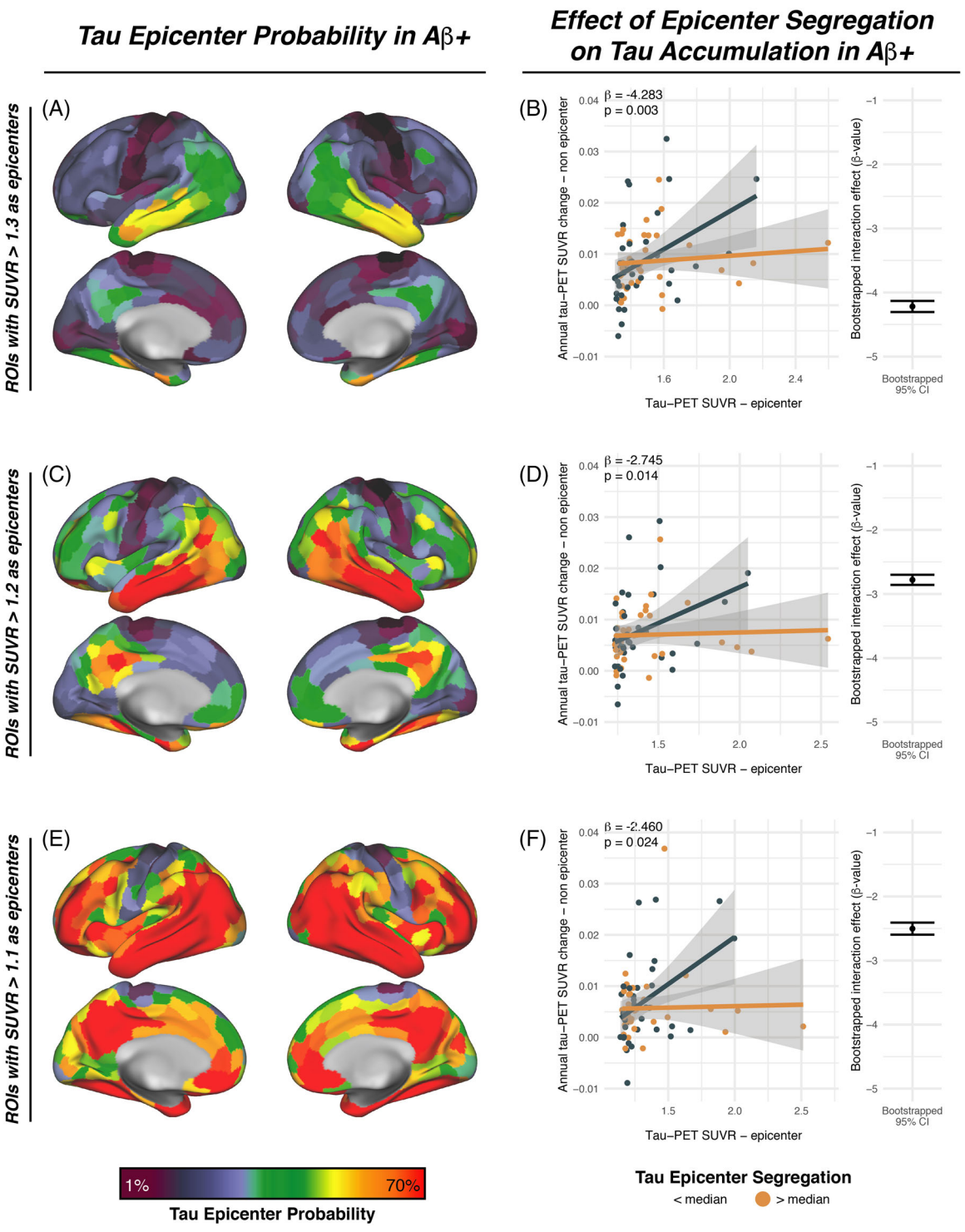

FIGURE 4 Illustration of the association between baseline tau positron emission tomography (PET) in patient-specific tau epicenters and resting state functional magnetic resonance imaging–assessed epicenter segregation on the longitudinal tau PET increase in the remaining non-epicenter regions of interest (ROIs) in amyloid beta positive (Aβ+) subjects. When retaining ROIs above 1.3 tau PET standardized uptake value ratios (SUVRs) as tau epicenters (i.e., 10 ROIs), the highest epicenter probability is found in the inferior temporal lobe, as illustrated by the epicenter probability mapping (A). Regression analyses revealed that higher segregation of the epicenter was associated with slower longitudinal tau PET increase outside of the tau epicenter (B). Analyses were repeated for epicenter tau PET SUVR thresholds of 1.2 (C,D) and 1.1 (E,F), showing that the effect of epicenter segregation decreases statistically if tau epicenters are defined more liberally. All statistical tests were fitted with continuous data, the use of median split to divide subjects is solely for visual purposes. 95% confidence intervals of interaction effects determined on 1000 bootstrapped iterations are displayed next to each scatterplot

TABLE 3 Interaction effects of baseline tau PET in the tau epicenter on tau PET rate of change in non-epicenter ROIs across different epicenter thresholds in Aβ+ subjects

		B	*t*-value	*P*-value	Partial R^2	Bootstrapped beta (mean [95% CI])
Tau PET ROC in epicenter defined as ROIs above a tau-PET SUVR threshold of	SUVR > 1.3	−4.283	−3.041	0.003	0.126	−4.218 [−4.305; −4.131]
	SUVR > 1.2	−2.745	−2.532	0.014	0.091	−2.779 [−2.858; −2.7]
	SUVR > 1.1	−2.460	−2.313	0.024	0.077	−2.502 [−2.597; −2.408]

Note: All statistics are based on linear models that were controlled for age, sex, diagnosis, scanner manufacturer, and mean framewise displacement during the resting-state fMRI scan. Regression weights are displayed as standardized beta values. Interaction effects have been computed using continuous measures of epicenter segregation and epicenter tau PET SUVRs. Bootstrapping of interaction effects was performed using 1000 iterations to determine 95% confidence intervals. Confidence intervals not including zero provide non-parametric evidence for the significance of effects.

Abbreviations: CI, confidence interval; PET, positive emission tomography; fMRI, functional magnetic resonance imaging; ROIs, regions of interest; SUVR, standardized uptake value ratio.

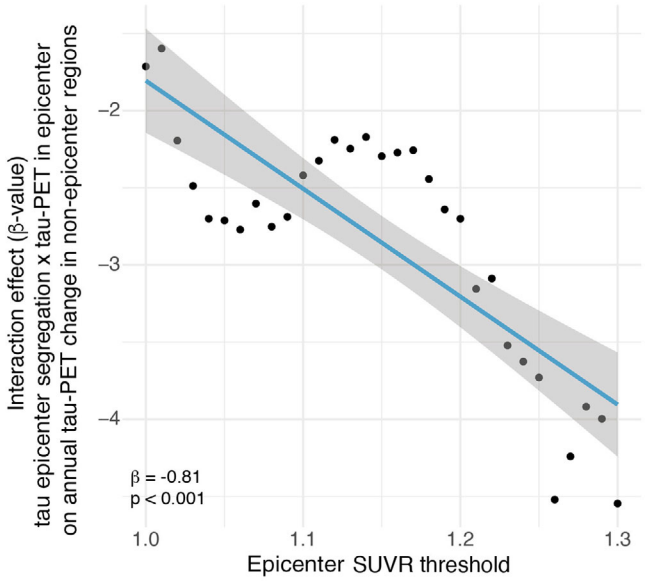

FIGURE 5 Standardized beta values reflecting the interaction between epicenter tau positron emission tomography (PET) standardized uptake value ratios (SUVRs) and resting state functional magnetic resonance imaging–assessed epicenter segregation on the rate of tau accumulation in non-epicenter regions of interest (ROIs) were extracted from linear models fitted with epicenter SUVR thresholds ranging between 1.0 to 1.3 in steps of 0.01. The scatterplot maps out the interaction effect strengths according to epicenter threshold to illustrate the weakening interaction effect as epicenters are defined more liberally, that is, epicenter segregation better predicts tau accumulation when the epicenter is defined more restrictively. All beta values were determined using linear regression

patterns may bias predictions about impending tau progression for individuals with heterogeneous onset sites. Based on our findings, we reason that an individualized approach could be essential in paving the way toward patient-tailored models for predicting tau progression in AD.

Empirical work preceding ours provides support for an association between network segregation and cognitive functioning in AD.[25,26] Specifically, these studies suggest that network segregation provides resilience against the impact of AD primary pathology on cognition whereby individuals are able to maintain higher functional and cognitive ability regardless of pathological burden. Our findings, on the other hand, demonstrate that network segregation also provides resistance against AD pathology by impeding tau spreading.[39] In line with evidence that tau is the key driver of cognitive decline in AD,[3–5] our findings provide a mechanistic intermediary process by which network segregation could modulate prospective tau spreading and thus cognitive outcomes in AD. It is important to mention that our results do not mitigate the protective role of network segregation against cognitive decline in terms of cognitive resilience; indeed, we believe there are inarguable protective effects of network segregation that are determined long before the onset of tau pathology (e.g., Chan et al.[26]) which offer alternative clinical utility for attenuating AD progression and attractive motivation for future research. A key open question for future research will be to assess whether inter-individual differences in brain network segregation persist throughout the lifespan and which factors may have caused such differences. Here, previous studies have related higher education to higher segregation in older adults[40] while stronger vascular brain changes have been linked to lower brain network segregation,[41] which may explain why patients with vascular co-pathology are more prone to tau accumulation in AD.[42] Here, life span studies will be needed to address potential genetic,[43] lifestyle,[40,44] and age-specific factors[45] that influence segregation, which will be important to assess whether brain network segregation can in fact be modulated to potentially attenuate tau accumulation and spreading in AD.

Various caveats should be taken into account when interpreting our results. First, unspecific flortaucipir off-target binding is common place[46] and we have therefore compensated for it by excluding particularly problematic regions such as the hippocampus and basal ganglia. Although the exclusion of known off-target binding sites may reduce confound considerably, off-target binding can still occur elsewhere in the brain and it is therefore impossible to completely eliminate its confound from our analyses. In addition, owing to the exclusion of certain brain regions we cannot confirm that critical stages of tau spreading were not missed; a particular ROI, the hippocampus, an early site of tau pathology,[47,48] unfortunately cannot be explored with first-generation tau PET tracers. Second, functional connectivity reflects direct but also indirect neuronal connections, whereby multiple intermediary neu-

rons are involved.[49,50] The assumptions made in this study rely on the accurate mapping of tau PET to functional connectivity, which unfortunately cannot be fully backed by structural data owing to present-day methodological drawbacks.[51] Therefore, any complex multi-synaptic connections captured by our functional connectivity analysis anticipates confirmation from modern structural techniques that are able to pick up distanced cortico-cortical connections.

Third, our longitudinal AV1451 tau PET analysis was carried out without partial volume correction (PVC) owing to insufficient temporally corresponding MR images. Previous research demonstrates that longitudinal changes in AV1451 tau PET can be accurately measured without PVC;[52,53] therefore, we believe that our longitudinal findings accurately reflect tau accumulation patterns. Finally, although our results follow on from previous preclinical and translational research, we of course recommend validation using another sample from the AD population before generalization, once sufficient data become publicly available.

Together, the current study revealed that higher network segregation is associated with attenuated tau spreading and demonstrates the impact of inter-individual differences in the tau epicenter's and the functional connectome's organization on AD progression. These findings add to the growing literature on factors that may modulate tau spreading, including sex, physical activity, and genetic factors.[42,54–57] Here, it will be important for future studies to systematically assess the individual and potentially synergistic effects of modulators of tau pathology to develop patient-tailored approaches to attenuate the development of tau pathology on the individual level, which may hold promise for attenuating neurodegeneration and cognitive decline in AD. In addition, our findings hold value for clinical research as they promote the brain's complex network topology as a therapeutic target and bring the functional properties of the tau epicenter into focus for future investigations, and not exclusively in AD, but potentially in other tauopathies.

ACKNOWLEDGMENTS

Data collection and sharing for this project was funded by the Alzheimer's Disease Neuroimaging Initiative (ADNI; National Institutes of Health Grant U01 AG024904) and DOD ADNI (Department of Defense award number W81XWH-12-2-0012). ADNI is funded by the National Institute on Aging, the National Institute of Biomedical Imaging and Bioengineering, and through generous contributions from the following: AbbVie; Alzheimer's Association; Alzheimer's Drug Discovery Foundation; Araclon Biotech; BioClinica, Inc.; Biogen; Bristol-Myers Squibb Company; CereSpir, Inc.; Cogstate; Eisai Inc.; Elan Pharmaceuticals, Inc.; Eli Lilly and Company; EuroImmun; F. Hoffmann-La Roche Ltd and its affiliated company Genentech, Inc.; Fujirebio; GE Healthcare; IXICO Ltd.; Janssen Alzheimer Immunotherapy Research & Development, LLC; Johnson & Johnson Pharmaceutical Research & Development LLC; Lumosity; Lundbeck; Merck & Co., Inc.; Meso Scale Diagnostics, LLC; NeuroRx Research; Neurotrack Technologies; Novartis Pharmaceuticals Corporation; Pfizer Inc.; Piramal Imaging; Servier; Takeda Pharmaceutical Company; and Transition Therapeutics. The Canadian Institutes of Health Research is providing funds to support ADNI clinical sites in Canada. Private sector contributions are facilitated by the Foundation for the National Institutes of Health (www.fnih.org). The grantee organization is the Northern California Institute for Research and Education, and the study is coordinated by the Alzheimer's Therapeutic Research Institute at the University of Southern California. ADNI data are disseminated by the Laboratory for Neuro Imaging at the University of Southern California. The study was funded by grants from the LMU (FöFoLe, 1032, awarded to NF, FöFoLe, 1119 awarded to DB), the Hertie foundation for clinical neurosciences (awarded to NF), the SyNergy excellence cluster (EXC 2145/ID 390857198) and the German Research Foundation (DFG, INST 409/193-1 FUGG).

Open access funding enabled and organized by Projekt DEAL.

CONFLICTS OF INTEREST

The authors report no competing interests. Author disclosures are available in the supporting information.

REFERENCES

1. Scholl M, Lockhart SN, Schonhaut DR, et al. PET imaging of tau deposition in the aging human brain. *Neuron*. 2016;89:971-82.
2. Jack CR, Jr., Knopman DS, Jagust WJ, et al. Hypothetical model of dynamic biomarkers of the Alzheimer's pathological cascade. *Lancet Neurol*. 2010;9:119-28.
3. Cullen NC, Leuzy A, Janelidze S, et al. Plasma biomarkers of Alzheimer's disease improve prediction of cognitive decline in cognitively unimpaired elderly populations. *Nat Commun*. 2021;12:3555.
4. Ossenkoppele R, Smith R, Mattsson-Carlgren N, et al. Accuracy of tau positron emission tomography as a prognostic marker in preclinical and prodromal Alzheimer disease: a head-to-head comparison against amyloid positron emission tomography and magnetic resonance imaging. *JAMA Neurol*. 2021;78:961-71.
5. Biel D, Brendel M, Rubinski A, et al. Tau-PET and in vivo Braak-staging as prognostic markers of future cognitive decline in cognitively normal to demented individuals. *Alzheimers Res Ther*. 2021;13:137.
6. Braak H, Braak E. Neuropathological stageing of Alzheimer-related changes. *Acta Neuropathol*. 1991;82:239-59.
7. La Joie R, Visani AV, Baker SL, et al. Prospective longitudinal atrophy in Alzheimer's disease correlates with the intensity and topography of baseline tau-PET. *Sci Transl Med*. 2020;12.
8. Calafate S, Buist A, Miskiewicz K, et al. Synaptic contacts enhance cell-to-cell tau pathology propagation. *Cell Report*. 2015;11:1176-83.
9. De Calignon A, Polydoro M, Suárez-Calvet M, et al. Propagation of tau pathology in a model of early Alzheimer's disease. *Neuron*. 2012;73:685-97.
10. Ahmed Z, Cooper J, Murray TK, et al. A novel in vivo model of tau propagation with rapid and progressive neurofibrillary tangle pathology: the pattern of spread is determined by connectivity, not proximity. *Acta Neuropathologica*. 2014;127:667-83.
11. Cope TE, Rittman T, Borchert RJ, et al. Tau burden and the functional connectome in Alzheimer's disease and progressive supranuclear palsy. *Brain*. 2018;141:550-67.
12. Franzmeier N, Rubinski A, Neitzel J, et al. Functional connectivity associated with tau levels in ageing, Alzheimer's, and small vessel disease. *Brain*. 2019;142:1093-107.
13. Vogel JW, Iturria-Medina Y, Strandberg OT, et al. Spread of pathological tau proteins through communicating neurons in human Alzheimer's disease. *Nat Commun*. 2020;11:2612.
14. Franzmeier N, Dewenter A, Frontzkowski L, et al. Patient-centered connectivity-based prediction of tau pathology spread in Alzheimer's disease. *Sci Adv*. 2020;6.

15. Adams JN, Maass A, Harrison TM, Baker SL, Jagust WJ. Cortical tau deposition follows patterns of entorhinal functional connectivity in aging. *Elife*. 2019;8.
16. Franzmeier N, Neitzel J, Rubinski A, et al. Functional brain architecture is associated with the rate of tau accumulation in Alzheimer's disease. *Nat Commun*. 2020;11:347.
17. Sporns O, Betzel RF. Modular brain networks. *Annu Rev Psychol*. 2016;67:613-40.
18. Wig GS. Segregated systems of human brain networks. *Trends Cogn Sci*. 2017;21:981-96.
19. Chan MY, Park DC, Savalia NK, Petersen SE, Wig GS. Decreased segregation of brain systems across the healthy adult lifespan. *Proc Natl Acad Sci U S A*. 2014;111:E4997-5006.
20. Betzel RF, Byrge L, He Y, Goñi J, Zuo X-N, Sporns O. Changes in structural and functional connectivity among resting-state networks across the human lifespan. *Neuroimage*. 2014;102:345-57.
21. Chong JSX, Ng KK, Tandi J, et al. Longitudinal changes in the cerebral cortex functional organization of healthy elderly. *J Neurosci*. 2019;39:5534-50.
22. Meunier D, Achard S, Morcom A, Bullmore E. Age-related changes in modular organization of human brain functional networks. *Neuroimage*. 2009;44:715-23.
23. Chan MY, Alhazmi FH, Park DC, Savalia NK, Wig GS. Resting-state network topology differentiates task signals across the adult life span. *J Neurosci*. 2017;37:2734-45.
24. Han L, Savalia NK, Chan MY, Agres PF, Nair AS, Wig GS. Functional parcellation of the cerebral cortex across the human adult lifespan. *Cerebral Cortex*. 2018;28:4403-23.
25. Ewers M, Luan Y, Frontzkowski L, et al. Segregation of functional networks is associated with cognitive resilience in Alzheimer's disease. *Brain*. 2021;144:2176-85.
26. Chan MY, Han L, Carreno CA, et al. Long-term prognosis and educational determinants of brain network decline in older adult individuals. *Nature Aging*. 2021;1(11):1053-1067.
27. Landau SM, Mintun MA, Joshi AD, et al. Amyloid deposition, hypometabolism, and longitudinal cognitive decline. *Ann Neurol*. 2012;72:578-86.
28. Power JD, Mitra A, Laumann TO, Snyder AZ, Schlaggar BL, Petersen SE. Methods to detect, characterize, and remove motion artifact in resting state fMRI. *Neuroimage*. 2014;84:320-41.
29. Franzmeier N, Düzel E, Jessen F, et al. Left frontal hub connectivity delays cognitive impairment in autosomal-dominant and sporadic Alzheimer's disease. *Brain*. 2018;141:1186-200.
30. Avants BB, Tustison NJ, Song G, Cook PA, Klein A, Gee JC. A reproducible evaluation of ANTs similarity metric performance in brain image registration. *Neuroimage*. 2011;54:2033-44.
31. Baker SL, Maass A, Jagust WJ. Considerations and code for partial volume correcting [(18)F]-AV-1451 tau PET data. *Data Brief*. 2017;15:648-57.
32. Schaefer A, Kong R, Gordon EM, et al. Local-global parcellation of the human cerebral cortex from intrinsic functional connectivity MRI. *Cereb Cortex*. 2018;28:3095-114.
33. Yeo B, Krienen FM, Sepulcre J, et al. The organization of the human cerebral cortex estimated by intrinsic functional connectivity. *J Neurophysiol*. 2011;106:1125-65.
34. Marquié M, Normandin MD, Vanderburg CR, et al. Validating novel tau positron emission tomography tracer [F-18]-AV-1451 (T807) on postmortem brain tissue. *Ann Neurol*. 2015;78:787-800.
35. Leuzy A, Chiotis K, Lemoine L, et al. Tau PET imaging in neurodegenerative tauopathies-still a challenge. *Mol Psychiatry*. 2019;24:1112-34.
36. Preische O, Schultz SA, Apel A, et al. Serum neurofilament dynamics predicts neurodegeneration and clinical progression in presymptomatic Alzheimer's disease. *Nat Med*. 2019;25:277-83.
37. Ossenkoppele R, Schonhaut DR, Schöll M, et al. Tau PET patterns mirror clinical and neuroanatomical variability in Alzheimer's disease. *Brain*. 2016;139:1551-67.
38. Vogel JW, Young AL, Oxtoby NP, et al. Four distinct trajectories of tau deposition identified in Alzheimer's disease. *Nat Med*. 2021;27:871-81.
39. Stern Y. Cognitive reserve in ageing and Alzheimer's disease. *Lancet Neurol*. 2012;11:1006-12.
40. Chan MY, Han L, Carreno CA, et al. Long-term prognosis and educational determinants of brain network decline in older adult individuals. *Nat Aging*. 2021;1:1053-67.
41. Kong TS, Gratton C, Low KA, et al. Age-related differences in functional brain network segregation are consistent with a cascade of cerebrovascular, structural, and cognitive effects. *Netw Neurosci*. 2020;4:89-114.
42. Rabin JS, Yang HS, Schultz AP, et al. Vascular risk and beta-amyloid are synergistically associated with cortical tau. *Ann Neurol*. 2019;85:272-9.
43. Dumitrescu L, Mahoney ER, Mukherjee S, et al. Genetic variants and functional pathways associated with resilience to Alzheimer's disease. *Brain*. 2020;143:2561-75.
44. Livingston G, Huntley J, Sommerlad A, et al. Dementia prevention, intervention, and care: 2020 report of the Lancet Commission. *Lancet*. 2020;396:413-46.
45. Chan D, Shafto M, Kievit R, et al. Lifestyle activities in mid-life contribute to cognitive reserve in late-life, independent of education, occupation, and late-life activities. *Neurobiol Aging*. 2018;70:180-3.
46. Lemoine L, Leuzy A, Chiotis K, Rodriguez-Vieitez E, Nordberg A. Tau positron emission tomography imaging in tauopathies: the added hurdle of off-target binding. *Alzheimers Dement (Amst)*. 2018;10:232-6.
47. Lace G, Savva G, Forster G, et al. Hippocampal tau pathology is related to neuroanatomical connections: an ageing population-based study. *Brain*. 2009;132:1324-34.
48. Mu Y, Gage FH. Adult hippocampal neurogenesis and its role in Alzheimer's disease. *Mol Neurodegener*. 2011;6:1-9.
49. Honey CJ, Sporns O, Cammoun L, et al. Predicting human resting-state functional connectivity from structural connectivity. *Proc Natl Acad Sci*. 2009;106:2035-40.
50. Grandjean J, Zerbi V, Balsters JH, Wenderoth N, Rudin M. Structural basis of large-scale functional connectivity in the mouse. *J Neurosci*. 2017;37:8092-101.
51. Abhinav K, Yeh F-C, Pathak S, et al. Advanced diffusion MRI fiber tracking in neurosurgical and neurodegenerative disorders and neuroanatomical studies: a review. *Biochim Biophys Acta*. 2014;1842:2286-97.
52. Harrison TM, La Joie R, Maass A, et al. Longitudinal tau accumulation and atrophy in aging and Alzheimer disease. *Ann Neurol*. 2019;85:229-40.
53. Jack Jr., CR, Wiste HJ, Schwarz CG, et al. Longitudinal tau PET in ageing and Alzheimer's disease. *Brain*. 2018;141:1517-28.
54. Brown BM, Rainey-Smith SR, Dore V, et al. Self-reported physical activity is associated with tau burden measured by positron emission tomography. *J Alzheimers Dis*. 2018;63:1299-305.
55. Buckley RF, O'Donnell A, McGrath ER, et al. Menopause status moderates sex differences in tau burden: a Framingham PET study. *Ann Neurol*. 2022;92:11-22.
56. Franzmeier N, Ossenkoppele R, Brendel M, et al. The BIN1 rs744373 Alzheimer's disease risk SNP is associated with faster Abeta-associated tau accumulation and cognitive decline. *Alzheimers Dement*. 2021;18(1):103-115.
57. Franzmeier N, Rubinski A, Neitzel J, Ewers M, Alzheimer's Disease Neuroimaging I. The BIN1 rs744373 SNP is associated with increased tau-PET levels and impaired memory. *Nat Commun*. 2019;10:1766.

58. Maass A, Landau S, Baker SL, et al. Comparison of multiple tau-PET measures as biomarkers in aging and Alzheimer's disease. *Neuroimage*. 2017;157:448-63.

SUPPORTING INFORMATION

Additional supporting information can be found online in the Supporting Information section at the end of this article.

How to cite this article: Steward A, Biel D, Brendel M, et al. Functional network segregation is associated with attenuated tau spreading in Alzheimer's disease. *Alzheimer's Dement*. 2023;19:2034–2046. https://doi.org/10.1002/alz.12867

vSupplementary table 1:
Interaction effects of baseline tau-PET in Braak I times SyS on tau-PET rate of change in downstream Braak ROIs (i.e. Braak III-VI) across different resting-state fMRI preprocessing strategies

Group	Tau-PET ROC in	B	t-value	p-value	Partial R^2	Bootstrapped beta (mean [95%CI])
Preprocessing pipeline: 24HMP8Phys, 0.5mm FD threshold						
Aβ+	Braak III-VI	-2.11	-2.330	0.023	0.070	-2.434 [-2.493;-2.375]
	Braak III-IV	-2.17	-2.267	0.027	0.067	-2.391 [-2.451;-2.331]
	Braak V-VI	-2.01	-2.311	0.024	0.069	-2.433 [-2.493;-2.375]
Aβ+/Aβ- pooled	Braak III-VI	-1.44	-2.164	0.033	0.039	-1.769 [-1.809;-1.729]
	Braak III-IV	-1.33	-1.927	0.056	0.032	-1.636 [-1.677;-1.596]
	Braak V-VI	-1.44	-2.225	0.028	0.042	-1.783 [-1.825;-1.742]
Preprocessing pipeline: 24HMP8Phys, 0.3mm FD threshold						
Group	Tau-PET ROC in	B	t-value	p-value	Partial R^2	Bootstrapped beta (mean [95%CI])
Aβ+	Braak III-VI	-1.992	-2.09	0.040	0.058	-2.413 [-2.468;-2.358]
	Braak III-IV	-1.962	-1.97	0.053	0.052	-2.297 [-2.354;-2.239]
	Braak V-VI	-1.827	-2.006	0.049	0.054	-2.319 [-2.376;-2.263]
Aβ+/Aβ- pooled	Braak III-VI	-1.347	-1.967	0.052	0.033	-1.712 [-1.753;-1.671]
	Braak III-IV	-1.274	-1.795	0.075	0.028	-1.584 [-1.625;-1.543]
	Braak V-VI	-1.318	-1.976	0.051	0.033	-1.725 [-1.768;-1.682]
Preprocessing pipeline: 24HMP8Phys + GSR, 0.5mm FD threshold						
Group	Tau-PET ROC in	B	t-value	p-value	Partial R^2	Bootstrapped beta (mean [95%CI])
Aβ+	Braak III-VI	-3.887	-2.261	0.027	0.067	-4.019 [-4.128;-3.91]
	Braak III-IV	-3.163	-1.736	0.087	0.041	-3.251 [-3.365;-3.137]
	Braak V-VI	-4.265	-2.642	0.010	0.089	-4.449 [-4.55;-4.348]
Aβ+/Aβ- pooled	Braak III-VI	-2.627	-2.132	0.035	0.039	-2.898 [-2.992;-2.804]
	Braak III-IV	-1.80	-1.396	0.165	0.017	-2.076 [-2.171;-1.982]
	Braak V-VI	-3.323	-2.808	0.006	0.065	-3.568 [-3.66;-3.477]
Preprocessing pipeline: 24HMP8Phys + GSR, 0.3mm FD threshold						
Group	Tau-PET ROC in	B	t-value	p-value	Partial R^2	Bootstrapped beta (mean [95%CI])
Aβ+	Braak III-VI	-3.487	-2.018	0.047	0.054	-3.618 [-3.729;-3.508]
	Braak III-IV	-2.779	-1.522	0.132	0.032	-2.872 [-2.987;-2.757]
	Braak V-VI	-3.888	-2.392	0.019	0.075	-4.064 [-4.168;-3.96]
Aβ+/Aβ- pooled	Braak III-VI	-2.320	-1.88	0.063	0.03	-2.561 [-2.654;-2.469]
	Braak III-IV	-1.528	-1.187	0.238	0.012	-1.77 [-1.862;-1.677]
	Braak V-VI	-3.001	-2.528	0.013	0.054	-3.226 [-3.318;-3.133]

All statistics are based on linear models that were controlled for age, sex, diagnosis, scanner manufacturer and mean framewise displacement during the resting-state fMRI scan. Bootstrapping was performed using 1000 iterations.

Supplementary table 2:
Interaction effects of baseline tau-PET in the tau epicentre on tau-PET rate of change in non epicentre ROIs across different epicenter thresholds and resting-state fMRI preprocessing strategies. The analysis was restricted to Aβ+ subjects

Preprocessing pipeline: 24HMP8Phys, 0.5mm FD threshold						
	Threshold	B	t-value	p-value	Partial R^2	Bootstrapped beta (mean [95%CI])
Tau-PET ROC in epicentre defined as ROIs above a tau-PET SUVR threshold of	SUVR > 1.3	-4.283	-3.041	0.003	0.126	-4.218 [-4.305;-4.131]
	SUVR > 1.2	-2.745	-2.532	0.014	0.091	-2.779 [-2.858;-2.7]
	SUVR > 1.1	-2.460	-2.313	0.024	0.077	-2.502 [-2.597;-2.408]
Preprocessing pipeline: 24HMP8Phys, 0.3mm FD threshold						
	Threshold	B	t-value	p-value	Partial R^2	Bootstrapped beta (mean [95%CI])
Tau-PET ROC in epicentre defined as ROIs above a tau-PET SUVR threshold of	SUVR > 1.3	-4.189	-3.036	0.003	0.126	-4.151 [-4.238;-4.064]
	SUVR > 1.2	-2.813	-2.646	0.01	0.099	-2.902 [-2.983;-2.82]
	SUVR > 1.1	-2.582	-2.469	0.016	0.087	-2.693 [-2.792;-2.594]
Preprocessing pipeline: 24HMP8Phys + GSR, 0.5mm FD threshold						
	Threshold	B	t-value	p-value	Partial R^2	Bootstrapped beta (mean [95%CI])
Tau-PET ROC in epicentre defined as ROIs above a tau-PET SUVR threshold of	SUVR > 1.3	-3.804	-2.982	0.004	0.122	-3.857 [-3.949;-3.765]
	SUVR > 1.2	-2.675	-2.592	0.012	0.095	-2.816 [-2.906;-2.726]
	SUVR > 1.1	-2.646	-2.659	0.01	0.1	-2.9 [-3.005;-2.796]
Preprocessing pipeline: 24HMP8Phys + GSR, 0.5mm FD threshold						
	Threshold	B	t-value	p-value	Partial R^2	Bootstrapped beta (mean [95%CI])
Tau-PET ROC in epicentre defined as ROIs above a tau-PET SUVR threshold of	SUVR > 1.3	-3.597	-2.886	0.005	0.115	-3.659 [-3.75;-3.569]
	SUVR > 1.2	-2.627	-2.63	0.011	0.098	-2.792 [-2.88;-2.704]
	SUVR > 1.1	-2.646	-2.731	0.008	0.104	-2.927 [-3.035;-2.82]

All statistics are based on linear models that were controlled for age, sex, diagnosis, scanner manufacturer and mean framewise displacement during the resting-state fMRI scan. Bootstrapping was performed using 1000 iterations.

Supplementary table 3:
Association between tau epicentre thresholds and the strength of the interaction effect (i.e. beta-value) epicentre segregation and baseline tau-PET SUVRs in the epicentre on tau-PET rate of change outside of the epicentre. The analysis was restricted to Aβ+ subjects

Preprocessing pipeline: 24HMP8Phys, 0.5mm FD threshold		
B	p-value	R^2
-0.81	<0.001	0.65
Preprocessing pipeline: 24HMP8Phys, 0.3mm FD threshold		
B	p-value	R^2
-0.74	<0.001	0.55
Preprocessing pipeline: 24HMP8Phys + GSR, 0.5mm FD threshold		
B	p-value	R^2
-0.60	<0.001	0.36
Preprocessing pipeline: 24HMP8Phys + GSR, 0.5mm FD threshold		
B	p-value	R^2
-0.52	0.002	0.27

4.2 ApoE4 and connectivity-mediated spreading of tau pathology at lower amyloid levels

The following section presents the original research article “Apoe4 and Connectivity-Mediated Spreading of Tau Pathology at Lower Amyloid Levels” which was published in Jama Neurology (Steward et al., 2023)

JAMA Neurology | Original Investigation

ApoE4 and Connectivity-Mediated Spreading of Tau Pathology at Lower Amyloid Levels

Anna Steward, MSc; Davina Biel, PhD; Anna Dewenter, PhD; Sebastian Roemer, MD; Fabian Wagner, MD; Amir Dehsarvi, PhD; Saima Rathore, PhD; Diana Otero Svaldi, PhD; Ixavier Higgins, PhD; Matthias Brendel, MD; Martin Dichgans, MD; Sergey Shcherbinin, PhD; Michael Ewers, PhD; Nicolai Franzmeier, PhD

IMPORTANCE For the Alzheimer disease (AD) therapies to effectively attenuate clinical progression, it may be critical to intervene before the onset of amyloid-associated tau spreading, which drives neurodegeneration and cognitive decline. Time points at which amyloid-associated tau spreading accelerates may depend on individual risk factors, such as apolipoprotein E ε4 (ApoE4) carriership, which is linked to faster disease progression; however, the association of ApoE4 with amyloid-related tau spreading is unclear.

OBJECTIVE To assess if ApoE4 carriers show accelerated amyloid-related tau spreading and propose amyloid positron emission tomography (PET) thresholds at which tau spreading accelerates in ApoE4 carriers vs noncarriers.

DESIGN, SETTING, AND PARTICIPANTS This cohort study including combined ApoE genotyping, amyloid PET, and longitudinal tau PET from 2 independent samples: the Alzheimer's Disease Neuroimaging Initiative (ADNI; n = 237; collected from April 2015 to August 2022) and Avid-A05 (n = 130; collected from December 2013 to July 2017) with a mean (SD) tau PET follow-up time of 1.9 (0.96) years in ADNI and 1.4 (0.23) years in Avid-A05. ADNI is an observational multicenter Alzheimer disease neuroimaging initiative and Avid-A05 an observational clinical trial. Participants classified as cognitively normal (152 in ADNI and 77 in Avid-A05) or mildly cognitively impaired (107 in ADNI and 53 in Avid-A05) were selected based on ApoE genotyping, amyloid-PET, and longitudinal tau PET data availability. Participants with ApoE ε2/ε4 genotype or classified as having dementia were excluded. Resting-state functional magnetic resonance imaging connectivity templates were based on 42 healthy participants in ADNI.

MAIN OUTCOMES AND MEASURES Mediation of amyloid PET on the association between ApoE4 status and subsequent tau PET increase through Braak stage regions and interaction between ApoE4 status and amyloid PET with annual tau PET increase through Braak stage regions and connectivity-based spreading stages (tau epicenter connectivity ranked regions).

RESULTS The mean (SD) age was 73.9 (7.35) years among the 237 ADNI participants and 70.2 (9.7) years among the 130 Avid-A05 participants. A total of 107 individuals in ADNI (45.1%) and 45 in Avid-A05 (34.6%) were ApoE4 carriers. Across both samples, we found that higher amyloid PET–mediated ApoE4-related tau PET increased globally (ADNI *b*, 0.15; 95% CI, 0.05-0.28; *P* = .001 and Avid-A05 *b*, 0.33; 95% CI, 0.14-0.54; *P* < .001) and in earlier Braak regions. Further, we found a significant association between ApoE4 status by amyloid PET interaction and annual tau PET increases consistently through early Braak- and connectivity-based stages where amyloid-related tau accumulation was accelerated in ApoE4carriers vs noncarriers at lower centiloid thresholds, corrected for age and sex.

CONCLUSIONS AND RELEVANCE The findings in this study indicate that amyloid-related tau accumulation was accelerated in ApoE4 carriers at lower amyloid levels, suggesting that ApoE4 may facilitate earlier amyloid-driven tau spreading across connected brain regions. Possible therapeutic implications might be further investigated to determine when best to prevent tau spreading and thus cognitive decline depending on ApoE4 status.

Editorial

Supplemental content

Author Affiliations: Author affiliations are listed at the end of this article.

Corresponding Author: Nicolai Franzmeier, PhD, Institute for Stroke and Dementia Research, University Hospital, Ludwig Maximilian University of Munich, Feodor Lynen Str 17, Munich 81377, Germany (nicolai.franzmeier@med.uni-muenchen.de).

JAMA Neurol. doi:10.1001/jamaneurol.2023.4038
Published online November 6, 2023.

In Alzheimer disease (AD), amyloid-β (Aβ) is thought to initiate the spreading of neurofibrillary tau pathology[1] from temporal-lobe epicenters to connected cortical regions,[2-6] driving neurodegeneration and cognitive decline.[7-10] Accordingly, Aβ-targeting therapies should ideally be applied at low tau levels to efficiently attenuate the AD cascade and slow tau-related neurodegeneration[11] and clinical progression.[9,12] It is therefore crucial to determine Aβ thresholds at which tau spreading is triggered to potentially inform treatment decisions.[9]

However, tau spreading from the medial temporal lobe to the cortex is modulated by patient-specific factors, including sex,[13,14] vascular comorbidities,[15] brain network architecture,[16] and genetic predispositions. Aβ thresholds marking tau spreading may vary individually.[17-19] Carriage of the apolipoprotein E ε4 (ApoE4) allele,[20] the strongest known risk factor for sporadic AD, has been linked to abnormal Aβ-independent tau biomarker levels[19,21,22] and cortical tau spreading patterns that closely align with cerebral APOE messenger RNA expression.[23] Yet, ApoE4 carriage is neither linked to higher risk of developing primary tauopathies nor to spreading of age-related medial temporal lobe tau to the cortex in the absence of Aβ[24,25]; therefore, tau spreading in ApoE4 carriers is seemingly associated with Aβ. However, it is unclear whether ApoE4 carriage lowers the Aβ threshold for tau spreading, leading to earlier symptom onset and faster clinical progression.[19,26] Given that clinical AD progression is thought to be largely driven by tau rather than Aβ,[9,10] anti-Aβ interventions may require earlier intervention within disease progression in ApoE4 carriers to effectively intercept tau spreading and consequent cognitive deterioration.[27] Addressing this is critical since 40% to 60% of patients with sporadic AD carry at least 1 ApoE4 allele[28] and will likely seek antiamyloid treatment at some point.

The major goal of this study was to investigate whether ApoE4 carriage is associated with earlier and faster Aβ-related tau spreading throughout the cortex. We assessed ApoE4 status, baseline [^{18}F]florbetaben/florbetapir amyloid-positron emission tomography (PET), and longitudinal [^{18}F]flortaucipir tau PET in individuals without dementia across the spectrum of aging and AD, including patients at the earliest stages of amyloidosis—a potentially promising target group for anti-Aβ treatments owing to less progressed pathology than that typically found in patients with dementia in which tau accumulation is more likely driven by local replication rather than Aβ-related transneuronal spread.[29-31] Samples were taken from the Alzheimer's Disease Neuroimaging Initiative (ADNI; n = 237) and Avid-A05 (n = 130) to independently validate findings. To capture AD-related tau aggregation and spread via tau PET, we used Braak stage–specific readouts, temporal-lobe tau meta regions of interest (ROIs),[32] and individualized connectivity-based tau stages (Q1-Q4), which specifically capture the gradual spread of tau across connected brain regions.[3,29] Using these data, we first assessed whether faster tau accumulation in ApoE4 carriers was associated with higher Aβ and second, whether tau accumulation was accelerated at lower Aβ levels in ApoE4 carriers vs noncarriers. Based on this analysis, we determined PET-based Aβ cut points at which tau accumulation rates diverged between ApoE4 carriers vs noncarriers. Third, we ran simulated trials to determine whether therapeutic effects on tau accumulation can be detected at lower Aβ levels in ApoE4 carriers vs noncarriers.

Key Points

Question Do apolipoprotein E ε4 (ApoE4) carriers show accelerated amyloid-related tau spreading?

Findings In this cohort study of 2 longitudinal tau positron emission tomography samples (N = 367), ApoE4 carriers showed an acceleration of amyloid-mediated tau spreading at a lower amyloid threshold compared to ApoE4 noncarriers, controlling for age and sex.

Meaning ApoE4 carriage was associated with earlier amyloid-induced tau spreading, indicating that the timing of therapeutic windows in antiamyloid therapies may need special consideration in ApoE4 carriers compared to noncarriers to successfully attenuate tau spreading.

Methods

ADNI Participants

We included 237 ADNI participants without dementia with at least 2 [^{18}F]flortaucipir tau PET scans and baseline [^{18}F]florbetapir (n = 175) or [^{18}F]florbetaben (n = 62) amyloid PET within 6 months of the baseline tau PET. Centiloids were estimated from global [^{18}F]florbetapir and [^{18}F]florbetaben standardized uptake value ratios (SUVRs) according to ADNI guidelines.[68] ADNI investigators diagnosed patients as cognitively normal (Mini-Mental State Examination [MMSE] score ≥24, Clinical Dementia Rating [CDR] score of 0, and not depressed), mild cognitive impairment (MMSE score ≥24, CDR score of 0.5, objective memory impairment on education-adjusted Wechsler Memory Scale II, and preserved activities of daily living). Participants with the ApoE ε2/ε4 genotype were excluded to avoid confounding effects of the potentially protective ε2 allele.[33] ADNI investigators obtained ethical approval from their respective local institutional ethical review board; all participants provided written informed consent. Supplementary analyses included an additional 34 patients diagnosed with dementia (MMSE score of 20-26, CDR score ≥0.5, National Institute of Neurological and Communicative Diseases and Stroke/Alzheimer's Disease and Related Disorders Association criteria for probable AD) fulfilling the same PET data availability criteria (21 with [^{18}F]florbetapir and 13 with [^{18}F]florbetaben).

Avid-A05 Participants

A total of 130 patients without dementia were selected from the Avid-1451-A05 phase 2/3 trial,[69,70] with at least 2 [^{18}F]flortaucipir tau PET scans and 1 [^{18}F]florbetapir amyloid PET scan within 30 days of the initial tau PET scan. All tau PET follow-up scans were taken at fixed intervals (9 and 18 months). Centiloid values were estimated from global [^{18}F]florbetapir SUVRs according to Avid guidelines.[34] Participants were classified as cognitively normal (MMSE score ≥29, no history of cognitive impairment) or mildly cognitively impaired (MMSE score

24 to less than 29, showing mild cognitive impairment according to the National Institute on Aging and the Alzheimer's Association working group's diagnostic guidelines[35]). Individuals with the ApoE ε2/ε4 genotype were excluded. The study was approved by each clinical investigator's local institutional review board; all participants provided written informed consent. Supplementary analyses included an additional 35 patients diagnosed with dementia (MMSE score 10-24, showing possible or probable AD based on the National Institute on Aging and the Alzheimer's Association working group's diagnostic guidelines) fulfilling the same PET data availability criteria. For transparency and generalizability, we have reported self-reported racial and ethnic distributions using predefined categories to depict the demographic composition of both groups.

Connectivity Assessment

Functional connectivity of 42 cognitively normal participants who were Aβ negative from the same ADNI sample was assessed using the 200 ROI Schaefer atlas[36] as Fisher *z*-transformed Pearson moment correlations between ROI pairs. Participant-specific connectivity matrices were averaged to determine a connectivity template, and negative values and autocorrelations were set to 0, following our preestablished approach.[37] All neuroimaging acquisition and processing is described in the eAppendix in Supplement 1. Participant-specific tau-spreading ROIs were generated by grouping 95% of regions into quartiles according to their template-based connectivity to 5% of brain regions with highest baseline tau PET (ie, the participant-specific tau epicenter, where Q1 indicates the strongest connectivity to the epicenter and Q4 indicates the weakest connectivity to the epicenter).[3,16,29]

Statistical Analysis

Group demographic characteristics were compared using analyses of variance for continuous and χ^2 tests for categorical variables. ROI-specific annual tau PET change rates were estimated using linear mixed models with longitudinal tau PET SUVR values as the dependent variable and time from baseline as the independent variable, including random slope and intercept.[3,16,29]

To confirm previous evidence that ApoE4 carriers have elevated Aβ and faster tau accumulation, we assessed differences in baseline centiloids and global tau PET change rates between ApoE4 carriers and noncarriers using analyses of covariance controlling for age and sex.[19]

To test our main hypothesis that ApoE4 carriers show accelerated Aβ-related tau accumulation and spread, we first investigated whether faster ApoE4-related tau accumulation was associated with higher Aβ. Bootstrapped mediation models with 1000 iterations conducted in R version 4.2.2 (R Foundation) were fitted for both samples separately with ApoE4 status as the independent variable, centiloids as the mediator, and the annual rate of global tau PET change as the dependent variable (ie, the average tau PET change across all 200 cortical Schaefer ROIs). These models were additionally stratified by Braak stage to determine whether ApoE4 associations with tau accumulation were most present in early tau-susceptible regions. All mediation models were controlled for age and sex, and a significance threshold was set at $P \leq .05$.

To further assess whether ApoE4 was associated with an acceleration of tau spreading at lower Aβ levels, we tested the centiloids by ApoE4 interaction on annual tau PET SUVR change rates through Braak and connectivity stage ROIs (Q1-Q4). In line with evidence for nonlinear progression of tau according to amyloid,[38] quadratic interaction models fit the data better than linear interactions (according to Akaike information criterion and analyses of variance); therefore, we report quadratic regression models controlled for age and sex (eTable 2 in Supplement 1). Centiloid thresholds in which ApoE4 carrier and noncarrier tau accumulation trajectories diverged were defined in all regression models according to a nonparametric resampling technique, which involved identifying where 95% CIs of the regression lines diverged or reconverged on the y-axis averaged across 1000 bootstrapped regressions to ensure thresholds were robust and not influenced by specific observations. To explore whether ApoE4 was associated with an acceleration of tau spreading at lower Aβ levels across an extended Aβ spectrum, linear models with CI thresholds were repeated with additional participants diagnosed with dementia. All analyses were carried out in both ADNI and Avid-A05 participants.

Lastly, we tested in the larger ADNI sample with good coverage of patients with early-stage and preclinical AD whether the sensitivity for detecting potential treatment effects on tau accumulation was higher among ApoE4 carriers at lower Aβ levels. To this end, simulated interventions with attenuated tau PET change rates of 30% (ie, simulated effect of interest) were carried out for global tau PET increase or tau PET change rates in the temporal meta[32] or Q1 ROI.[3,29] Simulated interventions were performed using 2 approaches, by defining a 70-centiloid–wide window with an upper and lower boundary that was shifted from −20 centiloids to 140 centiloids using a sliding window approach vs defining a lower centiloid boundary for defining the sample of interest, which was systematically increased from −20 centiloids to 70 centiloids in increments of 10. The required sample sizes were estimated using the R package pwr (settings: 2-sample *t* test, comparing actual vs attenuated cognitive changes; 2-tailed α = .05, power = 0.8). Statistical analyses were computed using R statistical software version 4.0.2 (R Foundation). Our primary hypothesis-driven analyses were not controlled for multiple comparisons due to our independent validation approach across 2 samples, yet false discovery rate-corrected *P* values are also reported in **Tables 1** and **2**.[39] The study followed the Strengthening the Reporting of Observational Studies in Epidemiology (STROBE) reporting guideline.

Results

Sample Characteristics

A total of 237 ADNI participants (mean [SD] age, 73.9 [7.35] years; 1 American Indian [0.4%], 1 Asian [0.4%], 13 Black [5.4%], 5 of more than 1 race or ethnicity [2.1%], and 217

Table 1. Mediation Results[a]

	b (95% CI)[b]	*P* value
ADNI		
Global	0.15 (0.05 to 0.28)	.01[c]
Braak I	0.03 (−0.09 to 0.14)	.68
Braak III	0.19 (0.07 to 0.32)	<.001[c]
Braak IV	0.17 (0.06 to 0.30)	.01[c]
Braak V	0.12 (0.01 to 0.24)	.03[c]
Braak VI	0.09 (−0.02 to 0.21)	.11[c]
Avid-A05		
Global	0.33 (0.14 to 0.54)	<.001[c]
Braak I	−0.02 (−0.17 to 0.13)	.78
Braak III	0.33 (0.14 to 0.54)	<.001[c]
Braak IV	0.28 (0.11 to 0.48)	<.001[c]
Braak V	0.34 (0.15 to 0.55)	<.001[c]
Braak VI	0.27 (0.10 to 0.46)	<.001[c]

Abbreviation: ADNI, Alzheimer's Disease Neuroimaging Initiative.

[a] The mediation models are controlled for age and sex. Additional mediation models correcting for diagnosis are shown in eTable 3 in Supplement 1.

[b] Values are average causal mediation effect values derived from mediation analyses with apolipoprotein E ε4 risk as predictor, centiloid as mediator, and the annual tau standardized uptake value ratio rate of change in the respective Braak stage as the dependent variable.

[c] Significant at false discovery rate–corrected $P < .05$.

White [91.6%]), including 107 ApoE4 carriers, were included. Analysis of variance and χ^2 tests revealed no significant differences between sex, clinical status (cognitively normal vs mildly cognitively impaired), or years of education, but ApoE4 carriers had significantly lower MMSE scores, were significantly younger with a higher proportion meeting amyloid PET positivity thresholds,[40,41] and had shorter tau PET follow-up. Of the 130 Avid-A05 participants (mean [SD] age, 70.2 [9.7] years; 2 Asian [1.5%], 12 Black [9.2%], 114 White [87.7%], and 2 other [unspecified] [1.5%]), 45 ApoE4 carriers were included. Sample characteristics were congruent with ADNI except for clinical status; there were significantly fewer cognitively normal ApoE4 carriers than cognitively normal noncarriers or moderately cognitively impaired ApoE4 carriers. Results are summarized in eTable 1 in Supplement 1. As expected, ApoE4 carriers had significantly higher centiloids (ADNI $F_{1,232} = 45.12$; $P < .001$; Avid-A05 $F_{1,125} = 20.73$; $P < .001$) and a faster annual rate of global tau PET SUVR accumulation (ADNI $F_{1,232} = 15.47$; $P < .001$; Avid-A05 $F_{1,125} = 11.38$; $P < .001$), controlling for age and sex. The demographic and clinical characteristics of additional participants with dementia added to supplementary analyses are displayed in eTable 5 in Supplement 1. Tau PET uptake and accumulation rates stratified by diagnostic group and ApoE4 status are shown in **Figure 1** (for further stratification by Aβ-status, see eFigure 1 in Supplement 1).

Faster Tau Accumulation in ApoE4 Carriers Mediated by Higher Aβ

We first assessed whether higher ApoE4-conferred Aβ burden was associated with faster tau accumulation. Supporting this, bootstrapped mediation analyses revealed that the association between ApoE4 status and faster annual rate of tau PET SUVR accumulation was mediated by higher centiloids (ADNI average causal mediation effect: *b*, 0.15; 95% CI, 0.05-0.28; $P = .001$ and Avid-A05 ACME average causal mediation effect: *b*, 0.33; 95% CI, 0.14-0.54; $P < .001$) (**Figure 2**).

When repeating the mediation analysis stratified by Braak ROIs, we found no mediation of amyloid on ApoE4 risk on tau accumulation in Braak I, but found a mediation in Braak III followed by a weakening in subsequent Braak ROIs in both samples (Figure 2; Table 1). This suggests that ApoE4 carriage was not associated with an acceleration in the initial emergence of tau pathology in the earliest tau-vulnerable region, Braak I, but may propel amyloid-related tau accumulation particularly in cortical regions.[1,9] For exploratory purposes, we also found no main effect of ApoE4 on tau accumulation in Braak I (ADNI: $F = 2.95$; $P = .09$; Avid-A05: $F = 2.31$; $P = .13$), suggesting the initial dynamics of tau are not driven by Aβ or ApoE. Sensitivity analyses also controlling for clinical diagnosis are shown in eTable 3 in Supplement 1.

ApoE4 Carriage Associated With a Lower Threshold for Amyloid-Related Tau Spreading

Second, we tested whether ApoE4 not only accelerates tau accumulation via increased amyloid (ie, mediation effect), but whether ApoE4 and amyloid have synergistic effects on accelerating tau accumulation as suggested by previous cross-sectional studies.[42,43] Supporting this, we found significant centiloid-by-ApoE4 status interactions on annual tau accumulation rates for Braak ROIs III-V in ADNI and for Braak III and V in Avid-A05 (**Figure 3**). On average, tau trajectories diverged at approximately 15 centiloids for ADNI and at approximately 12 centiloids for Avid-A05, as determined by nonparametric resampling. This result pattern was consistent for connectivity-based tau stages, which better capture individualized tau spread. Here, significant ApoE4-by-centiloids interactions were found for Q1 AND Q2 in ADNI and avid-A05 (Figure 3), where ApoE4-related tau accumulation accelerated at approximately 13 centiloids for ADNI and approximately 12 centiloids for Avid-A05. The strength of the interaction effect became weaker across Q1 throughQ4, suggesting that ApoE4 carriage was specifically associated with accelerated tau spreading from patient-specific epicenters to closely connected regions (Table 2). Sensitivity analyses also controlling for clinical diagnosis are shown in eTable 4 in Supplement 1. Exploratory analyses also including participants with dementia (271 in ADNI and 165 in Avid-A05) yielded consistent results (eFigure 3 and eTable 6 in Supplement 1). Together, these results suggest that ApoE4 carriage facilitates tau spreading at lower amyloid thresholds. Linear regression models revealed further that higher annual rate of tau SUVR accumulation was associated with faster MMSE decline in ADNI (*b*, −0.32; $P < .001$) and Avid-A05 (*b*, −0.28; $P = .002$) (eTable 7 in Supplement 1). This suggests that earlier ApoE4-related tau accumulation in the presence of Aβ may translate into faster cognitive decline.

ApoE4 Associated With Higher Sensitivity to Detect Treatment-Related Tau Attenuation at Lower Amyloid Levels

Lastly, we assessed whether the sensitivity to detect therapeutic effects on tau accumulation at lower Aβ levels was higher

Table 2. Interaction Effects Estimated by Linear Regression[a]

	b	t value	P value[b]	Partial R^2	Mean (95% CI)	
					Lower cut point	Upper cut point
Braak stage						
ADNI						
Braak III	−0.34	−3.35	<.001[a]	0.05	16.10 (15.43 to 16.76)	75.90 (75.05 to 76.75)
Braak IV	−0.36	−3.51	<.001[a]	0.05	12.44 (11.74 to 13.15)	74.20 (73.33 to 75.06)
Braak V	−0.28	−2.64	.009[a]	0.03	12.43 (11.43 to 13.42)	79.80 (78.76 to 80.84)
Braak VI	−0.18	−1.63	.104	0.01	NA	NA
A05						
Braak III	−0.27	−2.19	.030	0.04	15.42 (14.14 to 16.70)	60.47 (58.32 to 62.61)
Braak IV	−0.16	−1.28	.204	0.02	NA	NA
Braak V	−0.26	−2.23	.028	0.05	11.03 (9.89 to 12.17)	63.96 (61.82 to 66.10)
Braak VI	−0.09	−0.71	.480	0.03	NA	NA
Connectivity stage						
ADNI						
Q1	−0.39	−3.78	<.001[a]	0.06	11.20 (10.61 to 11.80)	83.60 (82.74 to 84.45)
Q2	−0.27	−2.66	.008[a]	0.03	13.29 (12.39 to 14.19)	80.77 (79.72 to 81.83)
Q3	−0.20	−1.94	.053	0.02	NA	NA
Q4	−0.14	−1.26	.208	0.01	NA	NA
A05						
Q1	−0.23	−2.02	.046	0.03	13.31 (12.25 to 14.37)	69.70 (67.67 to 71.74)
Q2	−0.31	−2.67	.008[a]	0.07	11.93 (10.86 to 12.99)	56.48 (54.38 to 58.57)
Q3	−0.20	−1.67	.098	0.04	NA	NA
Q4	−0.02	−0.15	.884	0.02	NA	NA

Abbreviations: ADNI, Alzheimer's Disease Neuroimaging Initiative; NA, not applicable.

[a] Values derived from regressions fitted with the interaction effect of apolipoprotein E ε4 risk and centiloid on the rate of annual tau accumulation in respective Braak stages and connectivity stages in ADNI and Avid-A05. Lower and upper cut point means and CIs were estimated through selecting the point of no overlap and reoverlap of 95% confidence intervals derived from bootstrapped regressions. The regression models are controlled for age and sex. Additional regression models correcting for diagnosis are shown in eTable 4 in Supplement 1.

[b] Significance at false discovery rate–corrected $P < .05$.

in ApoE4 carriers. We computed required sample sizes to detect simulated intervention effects with 30% attenuation of tau PET change as an end point through global, temporal-meta, and Q1 ROIs in ADNI. When using a sliding window approach spanning 70 centiloids, we found that detecting tau attenuation as a treatment effect would require overall lower sample sizes in ApoE4 carriers compared to ApoE4 noncarriers (eFigure 2 in Supplement 1). For global and Q1 tau PET readouts, the sensitivity to detect treatment effects diverged particularly at approximately 10 centiloids, consistent with the previous analysis in which we showed ApoE4-related tau accumulation acceleration at this centiloid threshold (Figure 3). Congruent results were obtained when using a lower centiloid boundary approach (eFigure 2in Supplement 1), indicating that ApoE4 carrier inclusion in trials using tau PET as a surrogate end point can reduce sample sizes required to detect treatment effects, especially at lower Aβ levels. This exploratory analysis could not be reliably repeated in Avid-A05 owing to skewed sample sizes across the centiloid spectrum leading to biased power estimations.

Discussion

In this cohort study, we demonstrate an association between ApoE4 carriage and enhanced Aβ pathology that mediated faster tau accumulation across early Braak stage regions and an acceleration of cortical tau spreading in ApoE4 carriers at lower Aβ levels. This suggests a potential indirect and direct effect of ApoE4 on tau, first by driving Aβ accumulation (which triggers tau accumulation) and second by lowering the Aβ threshold at which tau spreading accelerates from local epicenters across connected regions. We found that Aβ-related tau trajectories diverged around 12 to 15 centiloids between ApoE4 carriers and noncarriers, at which neuritic plaque pathology is already observed postmortem,[44] but below the typical 26-centiloid cutoff for amyloid PET positivity.[45] This indicates that tau spreading may be triggered earlier in ApoE4 carriers and therefore may be beneficial to explore disease-modifying anti-Aβ treatments at lower Aβ levels. Supporting this, our simulated trials show that tau accumulation attenuation can be detected at lower Aβ levels in ApoE4 carriers, therefore encouraging earlier disease-modifying intervention in carriers of the strongest risk factor for developing sporadic AD.

Our first major finding that Aβ mediated faster tau-PET increase in ApoE4 carriers vs noncarriers provides evidence that accelerated tau progression in ApoE4 carriers may be partly driven by stronger Aβ deposition. Mediating effects of Aβ on the association between ApoE4 and accelerated tau accumulation were specifically found for cortical Braak stage regions but not for the entorhinal cortex (ie, Braak I), where age-related tau PET increase is also found in the absence of Aβ.[46]

Figure 1. Group Average Tau Positron Emission Tomography (PET) Standardized Uptake Value Ratios (SUVRs) at Baseline Stratified by Apolipoprotein E ε4 (ApoE4) Status and Diagnostic Group

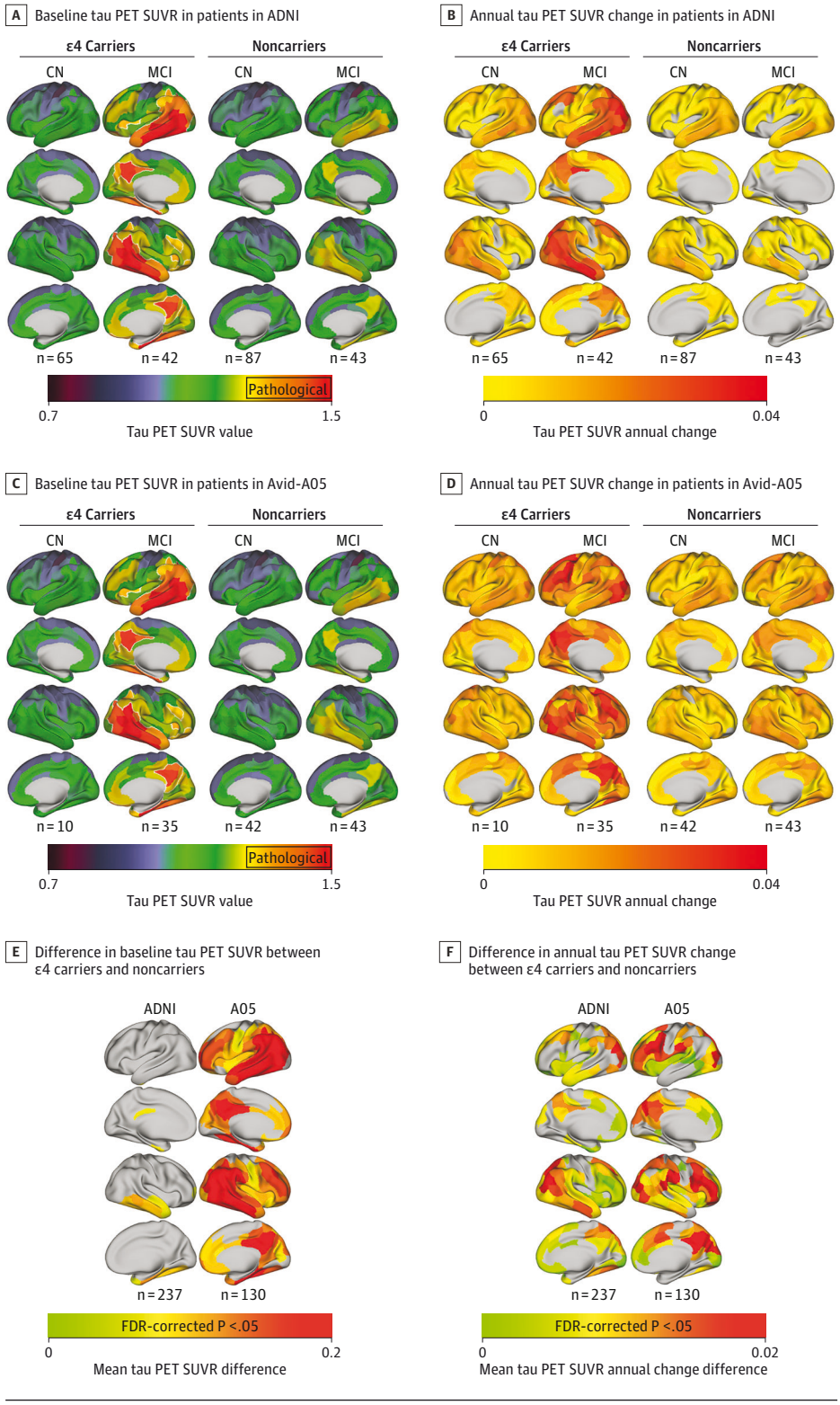

Tau PET SUVRs are shown as continuous values, white outlines define areas that surpass a preestablished pathological tau SUVR threshold of 1.3[44] in participants in the Alzheimer's Disease Neuroimaging Initiative (ADNI) (A) and in the Avid-A05 study (C). Number of patients displayed under each group rendering; group average tau SUVR annual change rates defined by linear mixed models, stratified by ApoE4 carriership and diagnostic group in patients in ADNI (B) and those in the Avid-A05 study (D). Tukey honestly significant difference (95% CI) post hoc tests on region of interest–wise analysis of covariance reveal mean differences between tau PET SUVR values of ApoE4 carriers minus those of noncarriers (E) and their annual tau PET SUVR change (F) stratified by sample. FDR indicates false discovery rate.

This is in line with past research demonstrating that tau accumulation in the entorhinal cortex is not mediated by Aβ in ApoE4 carriers,[47] suggesting that ApoE4 is specifically associated with Aβ-related cortical tau accumulation, but not to the initial entorhinal emergence of tau. This result pattern also provides an explanation for why ApoE4 carriers without Aβ pa-

Figure 2. Global Mediation Analyses

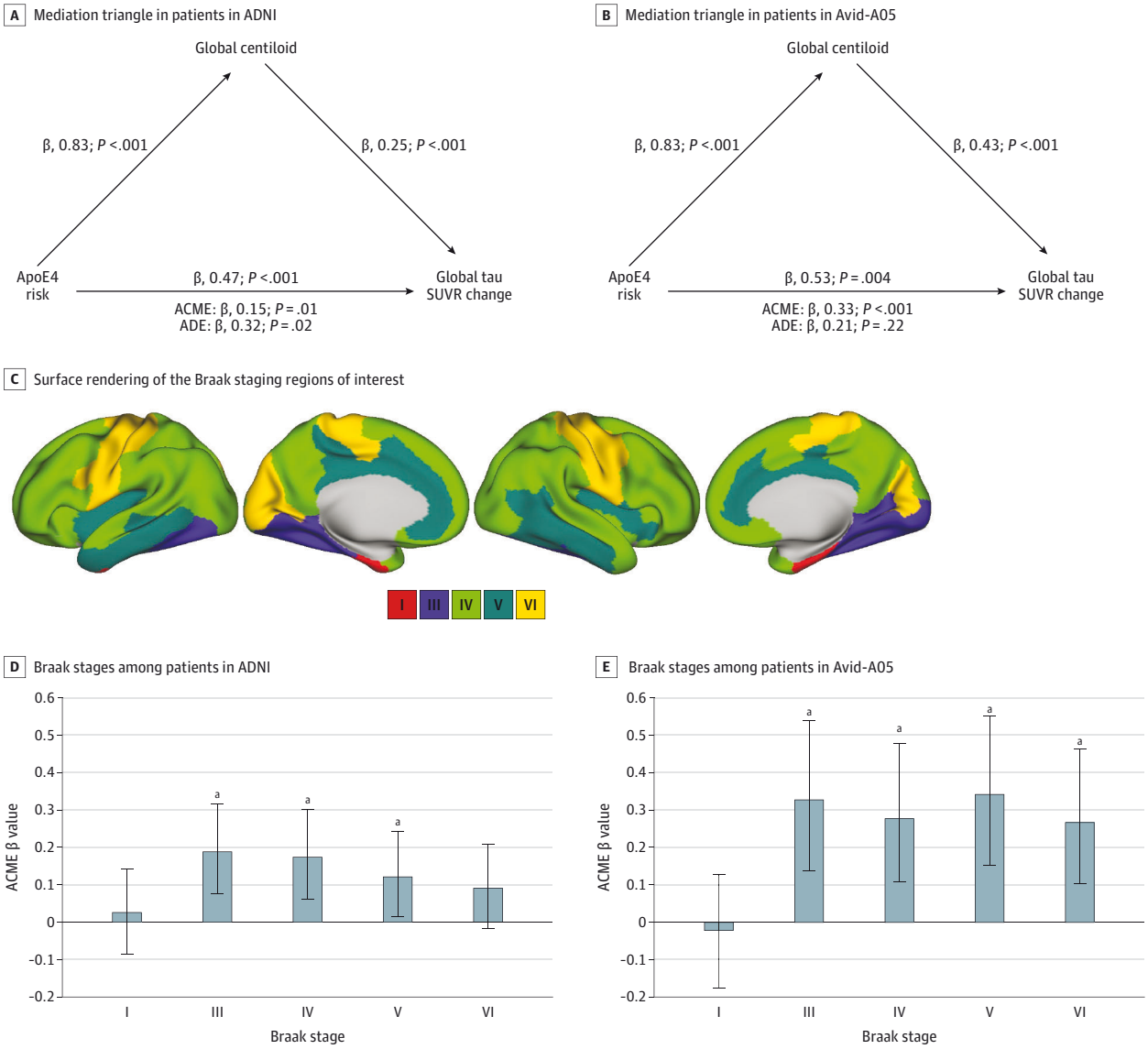

The average causal mediation effect (ACME) and the average direct effect (ADE) are displayed under each mediation triangle as estimated from bootstrapped mediation models. The models are controlled for age and sex and tested in the Alzheimer's Disease Neuroimaging Initiative (ADNI) (A) and Avid-A05 (B). Surface rendering of the Braak staging regions of interest by which longitudinal tau positron emission tomography changes were determined (C). Bar charts present ACME *b* values of mediation analyses (apolipoprotein E ε4 [ApoE4] risk as predictor, amyloid standardized uptake value ratio (SUVR) as mediator, and the annual tau SUVR rate of change across Braak stages as the dependent variable). Error bars represent 95% CIs of mediation bootstrapping in ADNI (D) and Avid-A05 (E).

thology exhibit tau in the medial temporal lobe but seldom beyond this region and do not develop pure tauopathies.[24,25]

Our second main finding revealed that ApoE4 was not only associated with accelerated tau accumulation through higher Aβ levels, but also had possible synergistic effects with Aβ on tau spreading, congruent with cross-sectional evidence of higher tau PET at given level of Aβ in ApoE4 carriers.[43] Specifically, we demonstrated that the rate of Aβ-related tau accumulation was moderated by ApoE4 across regions vulnerable to early-stage tau aggregation and spread (ie, in regions strongly connected to tau epicenters Q1-Q2).[3,16,29] These results are congruent with a biphasic AD pathophysiological framework, which proposes an Aβ-dependent then a later Aβ-independent tau accumulation phase,[30] supported by mouse model evidence demonstrating that Aβ-targeting antibodies reduced early but not later tau changes.[48] ApoE4-related tau trajectories diverged at relatively low levels of around 12 to 15 centiloids consistently across both samples, suggesting that ApoE4 may influence tau accumulation before patients are Aβ-PET positive using commonly applied thresholds.[44,45] This finding highlights the need for earlier centiloid-gauged therapeutic windows for ApoE4 carriers to effectively intervene in Aβ-related tau spreading.[27]

jamanetwork/2023/neu/11_06_2023/noi230081pap PAGE: right 7 SESS: 54 OUTPUT: Oct 21 12:16 2023

Figure 3. Interaction Effect Between Apolipoprotein E ε4 (ApoE4) Status and Centiloid on the Annual Rate of Tau Standardized Uptake Value Ratio (SUVR) Change Through Braak Stages III to VI

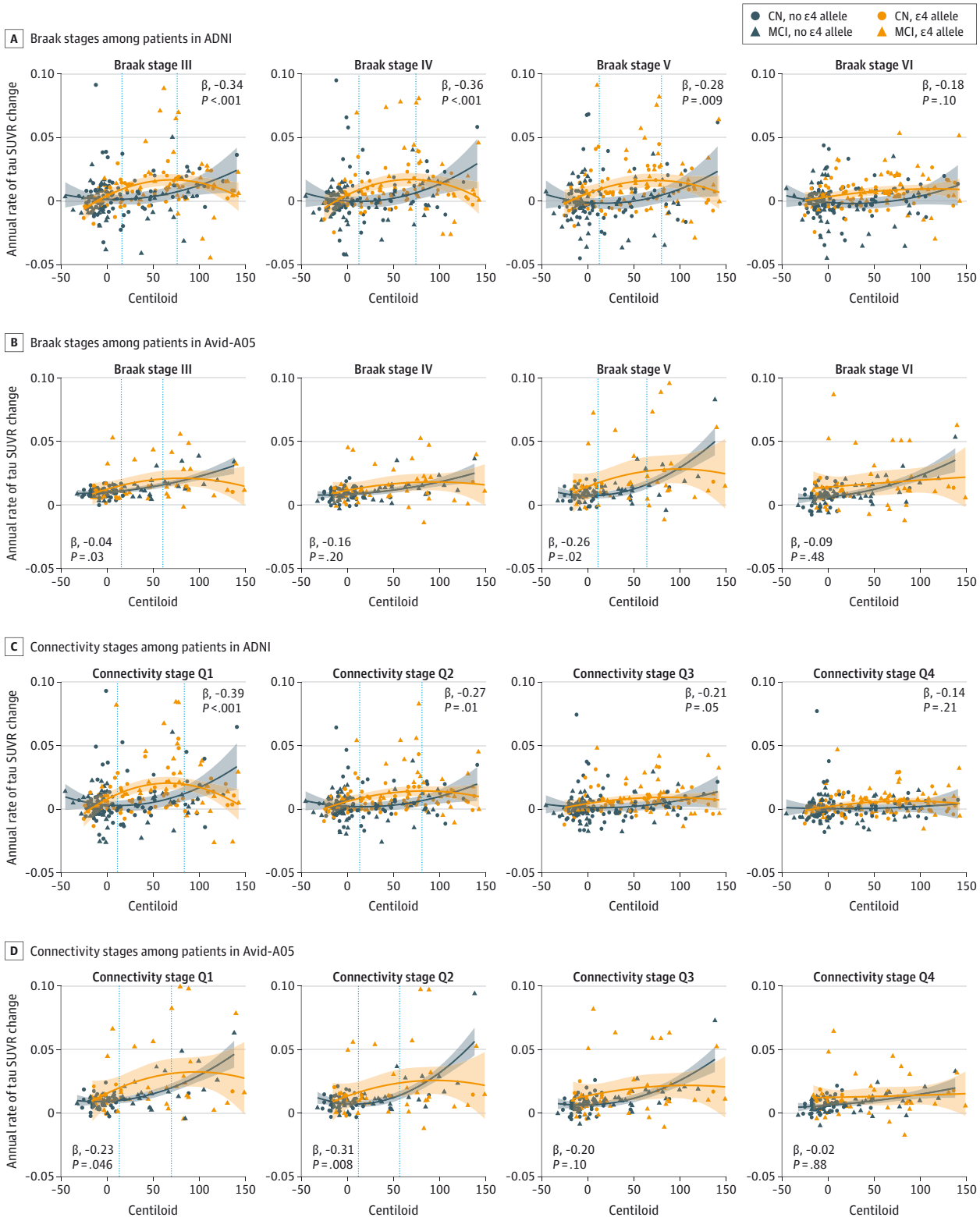

ApoE4 carriers show an amyloid-related increase in tau accumulation in early disease stages. Vertical dashed lines represent the centiloid threshold at which groups diverge and converge, estimated according to a nonparametric bootstrapping technique with 1000 iterations identifying the point at which confidence intervals around regression lines diverge and converge, presented with shaded 95% CI thresholds.

A key question is how Aβ facilitates tau spreading despite spatial incongruity and how ApoE4 modulates this process. Recent network connectivity research suggests that the onset of transneuronal tau spreading is subject to remote connectivity changes induced by the emergence of Aβ in regions connected to the entorhinal cortex[49] (where tau typically emerges first). This process may be accelerated in Apoe4 carriers who, according to electrophysiological[50] and functional magnetic resonance imaging (fMRI)[51] evidence, exhibit hyperconnectivity in primary Aβ-harboring regions compared to noncarriers. Remote Aβ-induced hyperconnectivity to tau epicenters may facilitate its spread to the rest of the cortex in ApoE4 carriers. It is unclear why ApoE4 carriers exhibit increased neuronal hyperconnectivity, but recent neuroinflammation research reveals that ApoE4-related Aβ plaques are structurally less compact[52] and trigger a greater inflammatory response,[53] which may amplify its pathological effects. Further, recent work in transgenic mouse models has found that ApoE4 is associated with earlier Aβ seeding and a stronger Aβ-induced astrogliosis,[54] and recent work in humans has shown that markers of astrocyte abnormality (ie, glial fibrillary acidic protein) are linked to a stronger association between Aβ and tau biomarkers.[55] Therefore, ApoE4 may be associated with an earlier Aβ-induced astrogliosis, triggering earlier-onset tau spreading; however, this remains to be specifically tested.

Our exploratory analysis, in which we used simulated interventions across several Aβ-defined therapeutic windows and boundaries, illustrated that, compared to noncarriers, fewer ApoE4 carriers were required to detect intervention-related tau attenuation at lower Aβ levels. This analysis translates this study's major findings into an interventional context by conveying how the rate and timing of Aβ-related tau accumulation and chosen readout region may impact clinical trial design and, consequently, meeting surrogate end points. Q1 exhibited the largest intergroup differences, possibly reflecting its sensitivity to capturing individualized tau PET accumulation.[3] Importantly, this analysis is calculated according to observed tau accumulation rates and not specific to anti-Aβ intervention and thus does not consider when anti-Aβ treatment can no longer attenuate tau accumulation, which we predict would occur in line with the centiloid thresholds established in the previous analysis.[3]

We argue, as others have, that the current rigid approach of dichotomizing participants according to preestablished Aβ PET thresholds without considering patient-specific risk factors begs reconsideration.[32] There are reports of Aβ-PET negative individuals with AD-like tau pathology[56,57] who may exemplify patients who enter the AD spectrum while formally defined as Aβ-negative owing to accelerated tau spreading at lower Aβ levels. This concept may clarify why empirical research has identified increased medial temporal lobe tau in Aβ-negative ApoE4 carriers compared to noncarriers[24,58] by proposing this increased tau to be Aβ related but at subthreshold levels. A novel aspect of the present study is including moderately cognitively impaired Aβ-negative patients, a group that inevitably includes patients without AD; however, this is statistically and conceptually necessary to detect the subthreshold Aβ-related tau spreading in individuals with AD.

Strengths and Limitations

A strength of the present study is the independent validation in the Avid-A05 sample, which conveyed overall congruent results. Nevertheless, cognitively normal ApoE4 carriers are underrepresented in Avid-A05, leading to slightly more advanced tau levels (Figure 1), which may explain why mediation and interaction effects tended to be skewed slightly toward later Braak stages. Furthermore, the use of individualized connectivity-based tau spreading stages can more sensitively capture spatial heterogeneity in tau accumulation, therefore better gauging the extent of tau spreading compared to Braak stage–specific readouts.[59] Nevertheless, several caveats should be considered when interpreting our results. First, unspecific flortaucipir off target is commonplace,[60] particularly in the hippocampus and basal ganglia—hence their exclusion from our analysis. However, we cannot confirm that confounding was not introduced from off-target binding elsewhere. Excluded regions, such as the hippocampus, may be particularly informative about early-stage tau spreading,[61,62] which unfortunately we cannot explore until larger data with second-generation tau PET tracers become available to us. Second, tau accumulation modeling across connected regions relies on the accurate mapping of tau PET to resting state functional magnetic resonance imaging-assessed functional connectivity, which, owing to distant multisynaptic connections,[63,64] cannot be structurally confirmed owing to current methodological shortcomings.[65] Third, this project's focus is purely pathophysiological and has exclusively drawn conclusions from a surrogate end point (ie, tau accumulation) but, as future clinical progression is associated with tau severity, we believe our findings are likely to translate into clinical outcomes. Accordingly, we demonstrate that longitudinal MMSE scores, converted to annual MMSE change rates, align with tau PET increases and predict tau PET changes (eTable 4 in Supplement 1). It should be mentioned that ADNI and Avid-A05 have slightly different clinical diagnostic criteria for mild cognitive impairment and cognitively normal designations; however, we believe this did not lead to incongruous clinical classifications between the 2 cohorts owing to the rigorous expert clinical judgment in both protocols. Moreover, we emphasize the exploratory nature of the sample size estimation analysis, which was not replicated in Avid-A05 due to insufficient data throughout the centiloid spectrum and overly dispersed tau PET SUVR change rates influencing power predictions. Additionally, this project has reported *P* values uncorrected for multiple comparisons to reduce type II error, which we believe to be statistically appropriate given the hypothesis-driven and cross-validation approach.[39,66] Additionally, this study would generally benefit from longer tau PET follow-up times, particularly at early and potentially slower tau spreading stages, and the inclusion of more diverse cohorts, since ApoE4 may have different effects across races.[67]

Conclusions

In conclusion, we demonstrate independently validated evidence that ApoE4 was associated with accelerated and earlier Aβ-related

tau spreading, which may drive faster clinical AD progression in ApoE4 carriers. Our findings have implications for trial design by illustrating that ApoE4 carriers may require earlier intervention to effectively attenuate tau spreading and associated clinical deterioration. Moreover, our results motivate further research into Aβ thresholds that determine clinical trial inclusion according to patient-specific characteristics, such as ApoE4, so that AD progression can be targeted in time to prevent tau spreading.

ARTICLE INFORMATION

Accepted for Publication: September 7, 2023.

Published Online: November 6, 2023. doi:10.1001/jamaneurol.2023.4038

Author Affiliations: Institute for Stroke and Dementia Research, University Hospital, Ludwig Maximilian University of Munich, Munich, Germany (Steward, Biel, Dewenter, Roemer, Wagner, Dehsarvi, Dichgans, Ewers, Franzmeier); Department of Neurology, University Hospital, Ludwig Maximilian University of Munich, Munich, Germany (Roemer); Eli Lilly and Company, Indianapolis, Indiana (Rathore, Otero Svaldi, Higgins, Shcherbinin); Department of Nuclear Medicine, University Hospital, Ludwig Maximilian University of Munich, Munich, Germany (Brendel); Munich Cluster for Systems Neurology, Munich, Germany (Brendel, Dichgans, Franzmeier); German Center for Neurodegenerative Diseases, Munich, Germany (Ewers); Department of Psychiatry and Neurochemistry, Institute of Neuroscience and Physiology, The Sahlgrenska Academy, University of Gothenburg, Sweden (Franzmeier).

Author Contributions: Ms Steward and Dr Franzmeier had full access to all of the data in the study and take responsibility for the integrity of the data and the accuracy of the data analysis.
Concept and design: Steward, Brendel, Dichgans, Franzmeier.
Acquisition, analysis, or interpretation of data: Steward, Biel, Dewenter, Roemer, Wagner, Dehsarvi, Rathore, Otero Svaldi, Higgins, Brendel, Dichgans, Shcherbinin, Ewers, Franzmeier.
Drafting of the manuscript: Steward, Brendel, Dichgans, Franzmeier.
Critical review of the manuscript for important intellectual content: Steward, Biel, Dewenter, Roemer, Wagner, Dehsarvi, Rathore, Otero Svaldi, Higgins, Brendel, Dichgans, Shcherbinin, Ewers, Franzmeier.
Statistical analysis: Steward, Roemer, Wagner, Dehsarvi, Rathore, Higgins, Franzmeier.
Obtained funding: Brendel.
Administrative, technical, or material support: Steward, Dehsarvi, Brendel.
Supervision: Brendel, Ewers, Franzmeier.

Conflict of Interest Disclosures: Drs Otero Svaldi and Shcherbinin report employment at stock options from Eli Lilly and Company during the conduct of the study and outside the submitted work, and have a patent pending at Eli Lilly related to this research. Dr Brendel reports personal fees from Roche, GE Healthcare, and Life Molecular Imaging as well as grants from Life Molecular Imaging and Roche outside the submitted work. Dr Ewers reports grants from ERA PerMed during the conduct of the study and grants from Eli Lilly outside the submitted work. Dr Franzmeier reports grants from Avid Radiopharmaceuticals and Hertie Network of Excellence in Clinical Neuroscience during the conduct of the study as well as grants from Bright Focus Foundation, the Alzheimer's Association, the Alzheimer Forschung Initiative, and the German Parkinson Society outside the submitted work. No other disclosures were reported.

Data Sharing Statement: See Supplement 2.

REFERENCES

1. Schöll M, Lockhart SN, Schonhaut DR, et al. PET imaging of tau deposition in the aging human brain. *Neuron*. 2016;89(5):971-982. doi:10.1016/j.neuron.2016.01.028

2. Vogel JW, Iturria-Medina Y, Strandberg OT, et al; Alzheimer's Disease Neuroimaging Initiative; Swedish BioFinder Study. Spread of pathological tau proteins through communicating neurons in human Alzheimer's disease. *Nat Commun*. 2020;11(1):2612. doi:10.1038/s41467-020-15701-2

3. Franzmeier N, Dewenter A, Frontzkowski L, et al. Patient-centered connectivity-based prediction of tau pathology spread in Alzheimer's disease. *Sci Adv*. 2020;6(48):eabd1327. doi:10.1126/sciadv.abd1327

4. Franzmeier N, Neitzel J, Rubinski A, et al; Alzheimer's Disease Neuroimaging Initiative (ADNI). Functional brain architecture is associated with the rate of tau accumulation in Alzheimer's disease. *Nat Commun*. 2020;11(1):347. doi:10.1038/s41467-019-14159-1

5. Cope TE, Rittman T, Borchert RJ, et al. Tau burden and the functional connectome in Alzheimer's disease and progressive supranuclear palsy. *Brain*. 2018;141(2):550-567. doi:10.1093/brain/awx347

6. Adams JN, Maass A, Harrison TM, Baker SL, Jagust WJ. Cortical tau deposition follows patterns of entorhinal functional connectivity in aging. *Elife*. 2019;8:e49132. doi:10.7554/eLife.49132

7. Jack CR Jr, Knopman DS, Jagust WJ, et al. Hypothetical model of dynamic biomarkers of the Alzheimer's pathological cascade. *Lancet Neurol*. 2010;9(1):119-128. doi:10.1016/S1474-4422(09)70299-6

8. Jack CR Jr, Bennett DA, Blennow K, et al. NIA-AA Research Framework: toward a biological definition of Alzheimer's disease. *Alzheimers Dement*. 2018;14(4):535-562. doi:10.1016/j.jalz.2018.02.018

9. Biel D, Brendel M, Rubinski A, et al; Alzheimer's Disease Neuroimaging Initiative (ADNI). Tau-PET and in vivo Braak-staging as prognostic markers of future cognitive decline in cognitively normal to demented individuals. *Alzheimers Res Ther*. 2021;13(1):137. doi:10.1186/s13195-021-00880-x

10. Ossenkoppele R, Smith R, Mattsson-Carlgren N, et al. Accuracy of tau positron emission tomography as a prognostic marker in preclinical and prodromal Alzheimer disease: a head-to-head comparison against amyloid positron emission tomography and magnetic resonance imaging. *JAMA Neurol*. 2021;78(8):961-971. doi:10.1001/jamaneurol.2021.1858

11. La Joie R, Visani AV, Baker SL, et al. Prospective longitudinal atrophy in Alzheimer's disease correlates with the intensity and topography of baseline tau-PET. *Sci Transl Med*. 2020;12(524):eaau5732. doi:10.1126/scitranslmed.aau5732

12. Biel D, Luan Y, Brendel M, et al; Alzheimer's Disease Neuroimaging Initiative. Combining tau-PET and fMRI meta-analyses for patient-centered prediction of cognitive decline in Alzheimer's disease. *Alzheimers Res Ther*. 2022;14(1):166. doi:10.1186/s13195-022-01105-5

13. Buckley RF, Mormino EC, Rabin JS, et al. Sex differences in the association of global amyloid and regional tau deposition measured by positron emission tomography in clinically normal older adults. *JAMA Neurol*. 2019;76(5):542-551. doi:10.1001/jamaneurol.2018.4693

14. Buckley RF, Scott MR, Jacobs HIL, et al. Sex mediates relationships between regional tau pathology and cognitive decline. *Ann Neurol*. 2020;88(5):921-932. doi:10.1002/ana.25878

15. Rabin JS, Yang HS, Schultz AP, et al. Vascular risk and β-amyloid are synergistically associated with cortical tau. *Ann Neurol*. 2019;85(2):272-279. doi:10.1002/ana.25399

16. Steward A, Biel D, Brendel M, et al. Functional network segregation is associated with attenuated tau spreading in Alzheimer's disease. *Alzheimers Dement*.2023;19(5):2034-2046. doi:10.1002/alz.061626

17. Franzmeier N, Ossenkoppele R, Brendel M, et al. The BIN1 rs744373 Alzheimer's disease risk SNP is associated with faster Abeta-associated tau accumulation and cognitive decline. *Alzheimers Dement*. 2022;18(1):103-115. doi:10.1002/alz.055113

18. Franzmeier N, Rubinski A, Neitzel J, Ewers M; Alzheimer's Disease Neuroimaging Initiative (ADNI). The BIN1 rs744373 SNP is associated with increased tau-PET levels and impaired memory. *Nat Commun*. 2019;10(1):1766. doi:10.1038/s41467-019-09564-5

19. Baek MS, Cho H, Lee HS, Lee JH, Ryu YH, Lyoo CH. Effect of APOE ε4 genotype on amyloid-β and tau accumulation in Alzheimer's disease. *Alzheimers Res Ther*. 2020;12(1):140. doi:10.1186/s13195-020-00710-6

20. Hersi M, Irvine B, Gupta P, Gomes J, Birkett N, Krewski D. Risk factors associated with the onset and progression of Alzheimer's disease: a systematic review of the evidence. *Neurotoxicology*. 2017;61:143-187. doi:10.1016/j.neuro.2017.03.006

21. Benson GS, Bauer C, Hausner L, et al. Don't forget about tau: the effects of ApoE4 genotype on Alzheimer's disease cerebrospinal fluid biomarkers in subjects with mild cognitive impairment-data from the Dementia Competence Network. *J Neural Transm (Vienna)*. 2022;129(5-6):477-486. doi:10.1007/s00702-022-02461-0

22. Hong YJ, Kim CM, Lee JH, Sepulcre J. Correlations between APOE4 allele and regional amyloid and tau burdens in cognitively normal older individuals. *Sci Rep*. 2022;12(1):14307. doi:10.1038/s41598-022-18325-2

23. Montal V, Diez I, Kim CM, et al. Network tau spreading is vulnerable to the expression gradients of *APOE* and glutamatergic-related genes. *Sci Transl Med*. 2022;14(655):eabn7273. doi:10.1126/scitranslmed.abn7273

24. Farfel JM, Yu L, De Jager PL, Schneider JA, Bennett DA. Association of APOE with tau-tangle pathology with and without β-amyloid. *Neurobiol Aging*. 2016;37:19-25. doi:10.1016/j.neurobiolaging.2015.09.011

25. Crary JF, Trojanowski JQ, Schneider JA, et al. Primary age-related tauopathy (PART): a common pathology associated with human aging. *Acta Neuropathol*. 2014;128(6):755-766. doi:10.1007/s00401-014-1349-0

26. Sando SB, Melquist S, Cannon A, et al. APOE epsilon 4 lowers age at onset and is a high risk factor for Alzheimer's disease; a case control study from central Norway. *BMC Neurol*. 2008;8:9. doi:10.1186/1471-2377-8-9

27. van Dyck CH, Swanson CJ, Aisen P, et al. Lecanemab in early Alzheimer's disease. *N Engl J Med*. 2023;388(1):9-21. doi:10.1056/NEJMoa2212948

28. Ward A, Crean S, Mercaldi CJ, et al. Prevalence of apolipoprotein E4 genotype and homozygotes (APOE e4/4) among patients diagnosed with Alzheimer's disease: a systematic review and meta-analysis. *Neuroepidemiology*. 2012;38(1):1-17. doi:10.1159/000334607

29. Pichet Binette A, Franzmeier N, Spotorno N, et al; Alzheimer's Disease Neuroimaging Initiative. Amyloid-associated increases in soluble tau relate to tau aggregation rates and cognitive decline in early Alzheimer's disease. *Nat Commun*. 2022;13(1):6635. doi:10.1038/s41467-022-34129-4

30. Hyman BT. Amyloid-dependent and amyloid-independent stages of Alzheimer disease. *Arch Neurol*. 2011;68(8):1062-1064. doi:10.1001/archneurol.2011.70

31. Meisl G, Hidari E, Allinson K, et al. In vivo rate-determining steps of tau seed accumulation in Alzheimer's disease. *Sci Adv*. 2021;7(44):eabh1448. doi:10.1126/sciadv.abh1448

32. Jack CR Jr, Wiste HJ, Weigand SD, et al. Defining imaging biomarker cut points for brain aging and Alzheimer's disease. *Alzheimers Dement*. 2017;13(3):205-216. doi:10.1016/j.jalz.2016.08.005

33. Corder EH, Saunders AM, Risch NJ, et al. Protective effect of apolipoprotein E type 2 allele for late onset Alzheimer disease. *Nat Genet*. 1994;7(2):180-184. doi:10.1038/ng0694-180

34. Navitsky M, Joshi AD, Kennedy I, et al. Standardization of amyloid quantitation with florbetapir standardized uptake value ratios to the Centiloid scale. *Alzheimers Dement*. 2018;14(12):1565-1571. doi:10.1016/j.jalz.2018.06.1353

35. Albert MS, DeKosky ST, Dickson D, et al. The diagnosis of mild cognitive impairment due to Alzheimer's disease: recommendations from the National Institute on Aging-Alzheimer's Association workgroups on diagnostic guidelines for Alzheimer's disease. *Alzheimers Dement*. 2011;7(3):270-279. doi:10.1016/j.jalz.2011.03.008

36. Schaefer A, Kong R, Gordon EM, et al. Local-global parcellation of the human cerebral cortex from intrinsic functional connectivity MRI. *Cereb Cortex*. 2018;28(9):3095-3114. doi:10.1093/cercor/bhx179

37. Ewers M, Luan Y, Frontzkowski L, et al; Alzheimer's Disease Neuroimaging Initiative and the Dominantly Inherited Alzheimer Network. Segregation of functional networks is associated with cognitive resilience in Alzheimer's disease. *Brain*. 2021;144(7):2176-2185. doi:10.1093/brain/awab112

38. de Leon MJ, Pirraglia E, Osorio RS, et al; Alzheimer's Disease Neuroimaging Initiative; National Alzheimer's Coordinating Center. The nonlinear relationship between cerebrospinal fluid Aβ42 and tau in preclinical Alzheimer's disease. *PLoS One*. 2018;13(2):e0191240. doi:10.1371/journal.pone.0191240

39. Armstrong RA. When to use the Bonferroni correction. *Ophthalmic Physiol Opt*. 2014;34(5):502-508. doi:10.1111/opo.12131

40. Fleisher AS, Chen K, Liu X, et al. Apolipoprotein E ε4 and age effects on florbetapir positron emission tomography in healthy aging and Alzheimer disease. *Neurobiol Aging*. 2013;34(1):1-12. doi:10.1016/j.neurobiolaging.2012.04.017

41. Maass A, Landau S, Baker SL, et al; Alzheimer's Disease Neuroimaging Initiative. Comparison of multiple tau-PET measures as biomarkers in aging and Alzheimer's disease. *Neuroimage*. 2017;157:448-463. doi:10.1016/j.neuroimage.2017.05.058

42. Young CB, Johns E, Kennedy G, et al; Alzheimer's Disease Neuroimaging Initiative; A4 Study Team. APOE effects on regional tau in preclinical Alzheimer's disease. *Mol Neurodegener*. 2023;18(1):1. doi:10.1186/s13024-022-00590-4

43. Therriault J, Benedet AL, Pascoal TA, et al; Alzheimer's Disease Neuroimaging Initiative. APOEε4 potentiates the relationship between amyloid-β and tau pathologies. *Mol Psychiatry*. 2021;26(10):5977-5988. doi:10.1038/s41380-020-0688-6

44. La Joie R, Ayakta N, Seeley WW, et al. Multisite study of the relationships between antemortem [^{11}C]PIB-PET centiloid values and postmortem measures of Alzheimer's disease neuropathology. *Alzheimers Dement*. 2019;15(2):205-216. doi:10.1016/j.jalz.2018.09.001

45. Amadoru S, Doré V, McLean CA, et al. Comparison of amyloid PET measured in centiloid units with neuropathological findings in Alzheimer's disease. *Alzheimers Res Ther*. 2020;12(1):22. doi:10.1186/s13195-020-00587-5

46. Weigand AJ, Bangen KJ, Thomas KR, et al; Alzheimer's Disease Neuroimaging Initiative. Is tau in the absence of amyloid on the Alzheimer's continuum? a study of discordant PET positivity. *Brain Commun*. 2020;2(1):fcz046. doi:10.1093/braincomms/fcz046

47. Salvadó G, Grothe MJ, Groot C, et al; Alzheimer's Disease Neuroimaging Initiative. Differential associations of APOE-ε2 and APOE-ε4 alleles with PET-measured amyloid-β and tau deposition in older individuals without dementia. *Eur J Nucl Med Mol Imaging*. 2021;48(7):2212-2224. doi:10.1007/s00259-021-05192-8

48. Oddo S, Billings L, Kesslak JP, Cribbs DH, LaFerla FM. Abeta immunotherapy leads to clearance of early, but not late, hyperphosphorylated tau aggregates via the proteasome. *Neuron*. 2004;43(3):321-332. doi:10.1016/j.neuron.2004.07.003

49. Lee WJ, Brown JA, Kim HR, et al. Regional Aβ-tau interactions promote onset and acceleration of Alzheimer's disease tau spreading. *Neuron*. 2022;110(12):1932-1943. e5. doi:10.1016/j.neuron.2022.03.034

50. Koelewijn L, Lancaster TM, Linden D, et al. Oscillatory hyperactivity and hyperconnectivity in young *APOE*-ε4 carriers and hypoconnectivity in Alzheimer's disease. *Elife*. 2019;8:e36011. doi:10.7554/eLife.36011

51. Pihlajamäki M, Sperling RA. Functional MRI assessment of task-induced deactivation of the default mode network in Alzheimer's disease and at-risk older individuals. *Behav Neurol*. 2009;21(1):77-91. doi:10.1155/2009/276384

52. Stephen TL, Cacciottolo M, Balu D, et al. APOE genotype and sex affect microglial interactions with plaques in Alzheimer's disease mice. *Acta Neuropathol Commun*. 2019;7(1):82. doi:10.1186/s40478-019-0729-z

53. Rodriguez GA, Tai LM, LaDu MJ, Rebeck GW. Human APOE4 increases microglia reactivity at Aβ plaques in a mouse model of Aβ deposition. *J Neuroinflammation*. 2014;11(1):111. doi:10.1186/1742-2094-11-111

54. Liu CC, Zhao N, Fu Y, et al. ApoE4 accelerates early seeding of amyloid pathology. *Neuron*. 2017;96(5):1024-1032.e3. doi:10.1016/j.neuron.2017.11.013

55. Bellaver B, Povala G, Ferreira PCL, et al. Astrocyte reactivity influences amyloid-β effects on tau pathology in preclinical Alzheimer's disease. *Nat Med*. 2023;29(7):1775-1781. doi:10.1038/s41591-023-02380-x

56. Weigand AJ, Edwards LE, Thomas KR, Bangen KJ, Bondi MW; Alzheimer's Disease Neuroimaging Initiative. Comprehensive characterization of elevated tau PET signal in the absence of amyloid-beta. *Brain Commun*. 2022;4(6):fcac272. doi:10.1093/braincomms/fcac272

57. Leal SL, Lockhart SN, Maass A, Bell RK, Jagust WJ. Subthreshold amyloid predicts tau deposition in aging. *J Neurosci*. 2018;38(19):4482-4489. doi:10.1523/JNEUROSCI.0485-18.2018

58. Therriault J, Benedet AL, Pascoal TA, et al. Association of apolipoprotein E ε4 with medial temporal tau independent of amyloid-β. *JAMA Neurol*. 2020;77(4):470-479. doi:10.1001/jamaneurol.2019.4421

59. Leuzy A, Binette AP, Vogel JW, et al; Alzheimer's Disease Neuroimaging Initiative. Comparison of group-level and individualized brain regions for measuring change in longitudinal tau positron emission tomography in Alzheimer disease. *JAMA Neurol*. 2023;80(6):614-623. doi:10.1001/jamaneurol.2023.1067

60. Lemoine L, Leuzy A, Chiotis K, Rodriguez-Vieitez E, Nordberg A. Tau positron emission tomography imaging in tauopathies: the added hurdle of off-target binding. *Alzheimers Dement (Amst)*. 2018;10:232-236. doi:10.1016/j.dadm.2018.01.007

61. Lace G, Savva GM, Forster G, et al; MRC-CFAS. Hippocampal tau pathology is related to neuroanatomical connections: an ageing population-based study. *Brain*. 2009;132(Pt 5):1324-1334. doi:10.1093/brain/awp059

62. Mu Y, Gage FH. Adult hippocampal neurogenesis and its role in Alzheimer's disease. *Mol Neurodegener*. 2011;6(1):85. doi:10.1186/1750-1326-6-85

63. Honey CJ, Sporns O, Cammoun L, et al. Predicting human resting-state functional connectivity from structural connectivity. *Proc Natl Acad Sci U S A*. 2009;106(6):2035-2040. doi:10.1073/pnas.0811168106

64. Grandjean J, Zerbi V, Balsters JH, Wenderoth N, Rudin M. Structural basis of large-scale functional

connectivity in the mouse. *J Neurosci*. 2017;37(34):8092-8101. doi:10.1523/JNEUROSCI.0438-17.2017

65. Abhinav K, Yeh F-C, Pathak S, et al. Advanced diffusion MRI fiber tracking in neurosurgical and neurodegenerative disorders and neuroanatomical studies: a review. *Biochim Biophys Acta*. 2014;1842(11):2286-2297. doi:10.1016/j.bbadis.2014.08.002

66. Rothman KJ. No adjustments are needed for multiple comparisons. *Epidemiology*. 1990;1(1):43-46. doi:10.1097/00001648-199001000-00010

67. Naslavsky MS, Suemoto CK, Brito LA, et al. Global and local ancestry modulate APOE association with Alzheimer's neuropathology and cognitive outcomes in an admixed sample. *Mol Psychiatry*. 2022;27(11):4800-4808. doi:10.1038/s41380-022-01729-x

68. Weiner MW, Veitch DP, Aisen PS, et al; Alzheimer's Disease Neuroimaging Initiative. The Alzheimer's Disease Neuroimaging Initiative 3: continued innovation for clinical trial improvement. *Alzheimers Dement*. 2017;13(5):561-571. doi:10.1016/j.jalz.2016.10.006

69. Analysis of 18F-AV-1451 PET imaging in cognitively healthy, MCI, and AD subjects (MCI). ClinicalTrials.gov identifier: NCT02116010. Updated September 22, 2020. Accessed October 4, 2023. https://academic.oup.com/amamanualofstyle/book/27941/chapter/207563234

70. Pontecorvo MJ, Devous Sr MD, Navitsky M, et al; 18F-AV-1451-A05 investigators. Relationships between flortaucipir PET tau binding and amyloid burden, clinical diagnosis, age and cognition. *Brain*. 2017;140(3):748-763. doi:10.1016/j.jalz.2016.10.006

Supplementary Material

MRI and PET Acquisition

For ADNI, structural MRI was acquired on 3T Siemens (SIEMENS Healthineers, Erlangen, Germany) and 3T GE scanners. T1-weighted structural scans were collected using an MPRAGE sequence (TR=2300ms; Voxel size=1x1x1mm; for parameter details see: https://adni.loni.usc.edu/wp-content/uploads/2017/07/ADNI3-MRI-protocols.pdf). PET data was assessed post intravenous injection of ^{18}F-labeled tracers (Flortaucipir: 6x5min time-frames, 75-105min post-injection; Florbetapir: 4x5min time-frames, 50-70min post-injection; Florbetaben: 4x5min time-frames, 90-110min post-injection; for more information see http://adni.loni.usc.edu/methods/pet-analysis-method/pet-analysis/).

In A05, PET data was assessed post intravenous injection of ^{18}F-labeled tracers (^{18}F-flortaucipir: 4x5min time-frames, approx. 80min post-injection; ^{18}F-florbetapir: 2x5min time-frames, approx. 50min post-injection)

PET preprocessing

For ADNI, dynamically acquired tau-PET images were realigned and averaged to obtain single Flortaucipir images. Using brain extracted T1-weighted images and ANTs-derived non-linear spatial normalization parameters (Avants et al., 2011), tau-PET images were affine registered to T1-weighted images, spatially normalized to MNI space and intensity normalized using an inferior cerebellar grey reference (Baker et al., 2017). For A05, Tau-PET images were preprocessed by Avid investigators. Specifically, native-space tau-PET images were rigidly co-registered to T1-weighted structural MRI and spatially normalized to MNI standard MNI space using FSL 'fnirt' (https://fsl.fmrib.ox.ac.uk/fsl/fslwiki/FNIRT). SUVRs were obtained by intensity normalization to the inferior cerebellum.

All tau-PET images were then parcelled into 200 Schaefer atlas cortical regions of interest (ROIs) by averaging voxels falling within a given ROI (Schaefer et al., 2018). We specifically chose this atlas because of its exclusion of areas susceptible to Flortaucipir tracer off-target binding (Leuzy et al., 2019; Marquié et al., 2015). The atlas was masked using a group-specific grey matter mask binarized at 0.3 probability.

Resting-state fMRI acquisition and preprocessing

rs-fMRI was obtained using a 3D echo-planar imaging (EPI) sequence with a total of 200 fMRI volumes per subject (TR=3000ms; TE=30ms; flip angle=90°; Voxel size=3.4mm isotropic).

To determine a connectivity template for modelling connectivity-based tau spreading, ten minutes of 3T resting-state fMRI data recorded on Siemens scanners (TR=3s) of 42 CN subjects (age: 72±7.24 years; 26 females) without evidence of AD pathology (i.e. global ^{18}F-Florbetapir SUVR<1.11) were included. The images were slice-time and motion corrected and co-registered to native T1-weighted images. To denoise EPI images, we regressed out nuisance covariates of eroded white matter and cerebrospinal fluid segments plus six motion parameters and their time and dispersion derivatives, followed by detrending and band-pass filtering (0.01-0.08Hz). To further reduce movement artifacts which may compromise connectivity assessment (Power et al., 2014) we performed motion scrubbing, removing volumes exceeding a 0.3mm frame-wise displacement threshold, plus one prior and two subsequent volumes. Pre-processed fMRI images were subsequently normalized to MNI space using ANTs.

Supplementary Table 1. Demographic and Clinical data stratified by group

	ε4–	ε4+	p-value
	ADNI		
N	130	107	
Sex (F/M)	64/66	61/46	0.29
Age	74.8 (7.03)	72.8 (7.61)	0.04
Clinical Diagnosis (CN/MCI)	87/43	65/42	0.39
Aβ Positivity (-/+)	90[b,c]/40[a,d]	37[a,d]/70[b,c]	<0.001
Education (years)	16.6 (2.52)	16.3 (2.44)	0.37
Mean tau-PET follow-up (years)	2.07 (1.09)	1.78 (0.738)	0.02
Mean BL Aβ & tau-PET difference (years)	-0.05 (0.20)	-0.01 (0.25)	0.145
MMSE	29.0 (1.39)	28.1 (1.83)	0.002
	A05		
N	85	45	
Sex	35/50	25/20	0.17
Age	71.6 (9.89)	67.6(9.02)	0.03
Clinical Diagnosis (CN/MCI)	42[c,b]/43[a]	10[a]/35	0.004
Aβ Positivity (-/+)	63[c]/22	21[a,d] /24 [c]	0.003
Education	15.4 (2.45)	15.8 (2.02)	0.32
Mean tau-PET follow-up (years)	1.45(0.193)	1.37 (0.290)	0.06
MMSE	28.8 (1.46)	28.0 (1.83)	0.01

M male, F female, CN cognitively normal, MCI mildly cognitively impaired, MMSE Mini Mental State Examination, BL Baseline
different from— a CN ε4–, b MCI ε4–, c CN ε4+
different from— a Aβ- ε4–, c Aβ- ε4+, d Aβ- ε4+
Mean BL amyloid & tau-PET difference (years) not included for A05. All BL amyloid scans within 30 days of BL tau-PET scans. Values are presented as mean (SD), Amyloid positivity according to threshold of 1.1 amyloid-PET SUVR. p-values were derived from ANOVA for continuous measures and from Chi squared tests for categorical measures. A05 Follow up times were not assessed as all scans were carried out at 9 months (+/-2) and 18 months (+/-2) after the initial scan. 12 A05 subjects did not have available education data.

Supplementary Table 2. Regression model ANOVA & Akaike information criterion

	F	p-value	AIC	
			Quadratic	Linear
Braak Stages				
ADNI				
Braak III	6.83	0.001	-1270.3	-1260.5
Braak IV	6.58	0.002	-1223.2	-1213.9
Braak V	3.43	0.034	-1157.6	-1154.6
Braak VI	1.43	0.242	-1301.7	-1302.74
A05				
Braak III	2.58	0.080	-847.1	-845.7
Braak IV	0.86	0.427	-839.3	-841.5
Braak V	2.44	0.091	-710.1	-708.9
Braak VI	0.37	0.690	-743.7	-746.9
Connectivity Stages				
ADNI				
Q1	8.14	0.000	-1200.7	-1188.3
Q2	3.37	0.036	-1381.1	-1378.1
Q3	3.37	0.036	-1454.4	-1454.8
Q4	0.96	0.383	-1505.5	-1507.5
A05				
Q1	1.95	0.147	-703.8	-703.7
Q2	3.74	0.027	-719.9	-716.1
Q3	1.49	0.229	-738.5	-739.3
Q4	0.02	0.981	-819.7	-823.6

AIC Akaike information criterion

The table displays F, and p-values derived from ANOVAs fitted quadratic and linear regression models fitted with interaction effect of ApoE4 risk and Centiloid or Centiloid^2 on the rate of annual tau accumulation in respective Braak stages and connectivity stages in ADNI and A05. The table also displays AICs for the respective quadratic and linear models.

Supplementary Table 3. Mediation Results controlled for clinical diagnosis

	B	CI L	CI U	p-value
		ADNI		
Global	0.14	0.03	0.27	0.006
Braak I	0.05	0.17	-0.06	0.38
Braak III	0.19	0.31	0.06	<0.001
Braak IV	0.169	0.29	0.06	0.002
Braak V	0.119	0.24	0.01	0.04
Braak VI	0.10	0.21	-0.02	0.10
		A05		
Global	0.25	0.1	0.44	<0.001
Braak I	-0.01	-0.14	0.12	0.918
Braak III	0.24	0.09	0.43	<0.001
Braak IV	0.20	0.07	0.38	<0.001
Braak V	0.26	0.11	0.45	<0.001
Braak VI	0.21	0. 07	0.39	<0.001

CI L 95% Confidence interval lower, CI U 95% Confidence interval upper. Values are ACME values derived from mediation analyses with ApoE4 risk as predictor, centiloid as mediator, and the annual tau SUVR rate of change (ROC) in the respective Braak stage as the dependent variable. The table displays beta-estimates and p-values. The mediation models are controlled for age, sex and clinical diagnosis.

Supplementary table 4. Interaction effects estimated by linear regression controlled for clinical diagnosis

	b	t-value	p-value	Par. R^2	Lower cut-point			Upper cut-point		
					mean	CI L	CI U	mean	CI L	CI U
Braak Stages										
ADNI										
Braak III	-0.34	-3.34	<0.001	0.05	16.10	15.43	16.76	75.90	75.05	76.75
Braak IV	-0.36	-3.45	<0.001	0.05	12.44	11.74	13.15	74.20	73.33	75.06
Braak V	-0.27	-2.58	0.010	0.03	12.43	11.43	13.42	79.80	78.76	80.84
Braak VI	-0.18	-1.63	0.105	0.014	–	–	–	–	–	–
A05										
Braak III	-0.26	-2.14	0.035	0.04	15.42	14.14	16.70	60.47	58.32	62.61
Braak IV	-0.15	-1.24	0.219	0.02	–	–	–	–	–	–
Braak V	-0.26	-2.19	0.030	0.04	11.03	9.89	12.17	63.96	61.82	66.0
Braak VI	-0.09	-0.71	0.482	0.03	–	–	–	–	–	–
Connectivity Stages										
ADNI										
Q1	-0.38	-3.72	<0.001	0.06	11.20	10.61	11.80	83.60	82.74	84.45
Q2	-0.26	-2.56	0.011	0.03	13.29	12.39	14.19	80.77	79.72	81.83
Q3	-0.20	-1.86	0.064	0.02	–	–	–	–	–	–
Q4	-0.13	-1.19	0.234	0.01	–	–	–	–	–	–
A05										
Q1	-0.23	-1.95	0.053	0.03	13.31	12.25	14.37	69.70	67.67	71.74
Q2	-0.31	-2.62	0.010	0.07	11.93	10.86	13	56.48	54.38	58.57
Q3	-0.20	-1.65	0.102	0.04	–	–	–	–	–	–
Q4	-0.02	-0.19	0.846	0.02	–	–	–	–	–	–

CI L 95% Confidence interval lower, CI U 95% Confidence interval upper

Values derived from regressions fitted with the interaction effect of ApoE4 risk and Centiloid[2] on the rate of annual tau accumulation in respective Braak stages and connectivity stages in ADNI and A05. Lower and upper cut-points means and CI values estimated through selecting the point of no overlap of 95% and re-overlap of confidence intervals of bootstrapped regressions. The table displays standardized b-estimates, T-values, and p-values. The regression models are controlled for age, sex and clinical diagnosis.

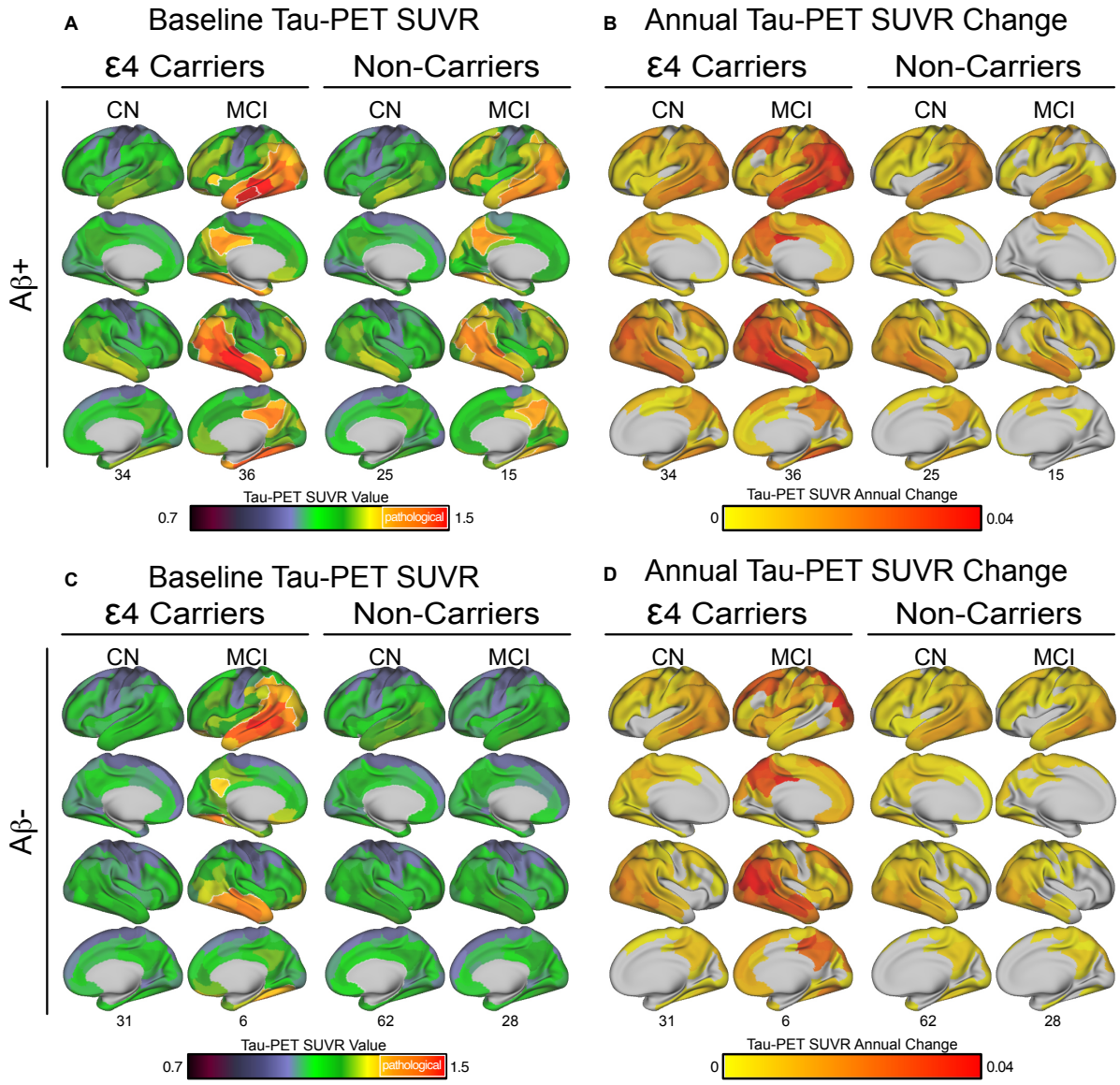

Supplementary Figure 1. Group-average tau-PET SUVRs in ADNI at baseline stratified by ApoE4 carriership, diagnostic group and Aβ positivity. Tau-PET SUVRs are showed as continuous values, white outlines define areas which surpass a pre-established pathological tau-PET SUVR threshold of 1.3 (Maass et al., 2017) in Aβ+ subjects (A) and Aβ– subjects (C). Number of subjects displayed under each group rendering, Group average tau-SUVR annual change rates defined by linear mixed models, stratified by ApoE4 carriership and diagnostic group in Aβ+ subjects (B) and Aβ– subjects (D).

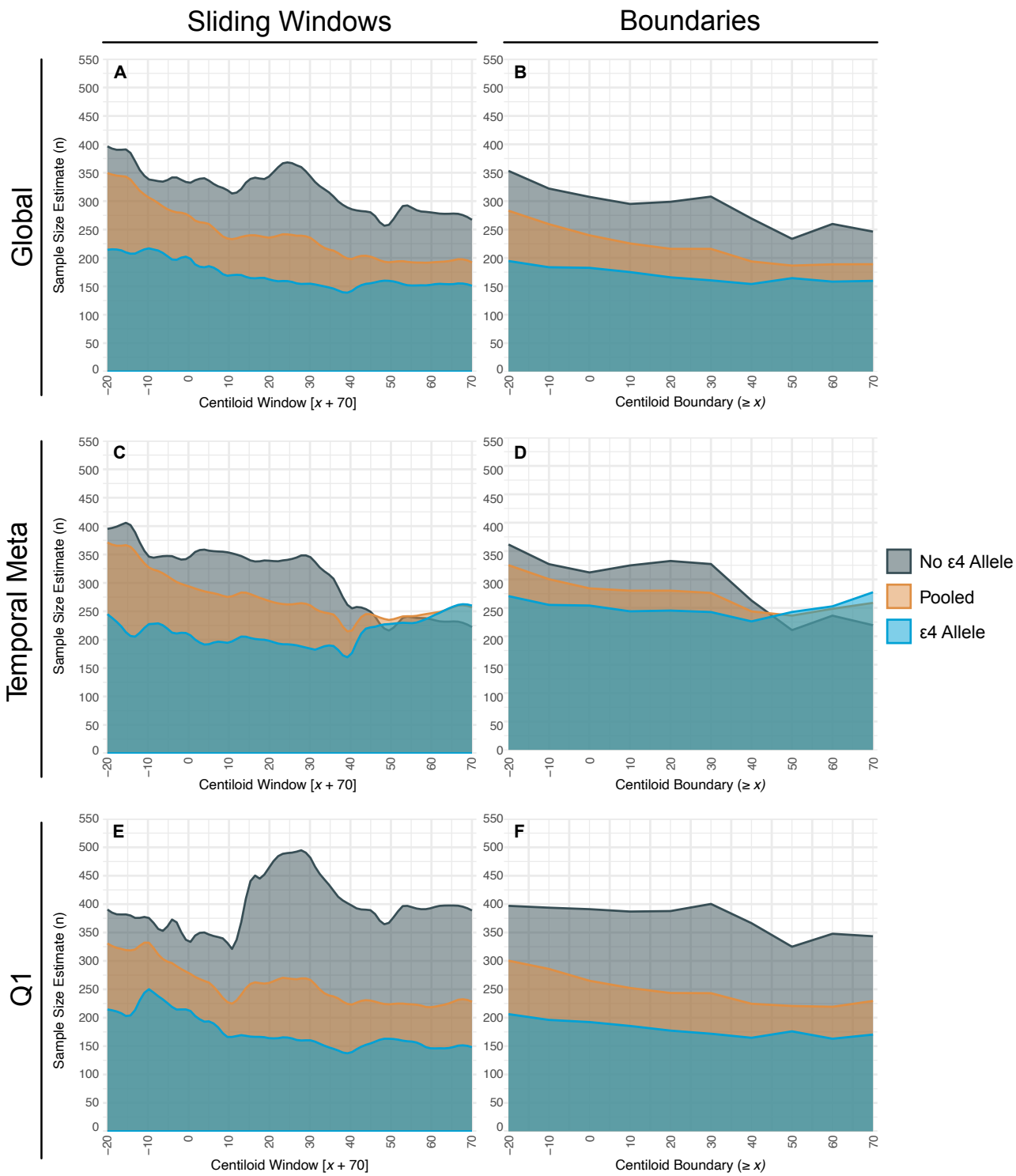

Supplementary Figure 2. Required sample sizes to detect simulated intervention effects with tau change as an endpoint estimated through sliding windows of centiloid starting at [-20;50] moving up in steps of 1 to [100;140] estimated at 30 (A, C, E) and through centiloid boundaries capturing all subjects with a centiloid the same or higher as the boundary starting at -20 increasing in steps of 10 (B, D, F). Sample sizes were estimated according to 3 different tau-PET readout regions: Global (A, B) i.e. average across all 200 cortical Schaefer ROIs, Temporal Meta (C, D) and Q1 (E, F). Results demonstrate that non-e4 carriers may require higher sample sizes to detect intervention effects throughout the centiloid scale, but particularly at earlier centiloid levels.

5 GENERAL DISCUSSION

5.1 Modulators of tau spreading in AD

The major findings of this thesis suggest that the rate of tau spreading in AD can be modulated by two major factors, functional network organisation and the genetic risk factor ApoE4. The first study of this thesis demonstrates that stronger brain network segregation i.e. stronger within than between-network connectivity, is associated with slower subsequent tau progression particularly in early tau susceptible regions. Furthermore, it suggests that the global connectivity of the tau epicentre, the supposed region which tau emerges, plays an important role in future tau dynamics, whereby higher epicentre segregation predicts slower subsequent tau progression in the rest of the brain. Overall, this study indicates that sparser inter-network connections attenuate connectivity-driven trans-neuronal tau spreading and emphasises the functional connectome as a route for tau spreading. The second study of this thesis focused on the impact of a major genetic risk factor, ApoE4, on the rate of tau spreading in relation to Aβ levels. This research reveals that ApoE4 carriers not only had increased tau pathology owing to stronger Aβ deposition but also increased tau spreading at lower Aβ levels in early tau susceptible regions compared to non-carriers. These results indicate that ApoE4 drives increased and earlier tau spreading directly and indirectly through Ab, indicating the need to reconsider anti-amyloid therapeutic windows for ApoE4 carriers for the timely interception of Aβ triggered tau.

5.2 Functional architecture and Tau spreading heterogeneity

Numerous preclinical and clinical studies propose that connectivity plays a pivotal role in shaping the dynamics of tau spreading through the cortex (Cope et al., 2018; Franzmeier et al., 2020b; Ossenkoppele et al., 2019; Wu et al., 2016) thus placing connectivity as a major mediator in the process of tau propagation. The findings of the first study in this thesis elaborate on this concept and illustrate how connectivity patterns, at the level of large-scale brain organization, influence the rate at which tau spreads across the brain. Here it is demonstrated that individuals exhibiting stronger between-network connectivity compared to within-network connectivity experience faster tau accumulation across the cortex. This specifically posits that more diffuse inter-network connections support the inter-regional

spreading of tau, while more constrained inter-network connections slow its widespread propagation through the rest of the brain. These findings consolidate the growing body of research that identifies the functional connectome as a major route for trans-neuronal tau spreading (Cope et al., 2018; Franzmeier et al., 2020b; Lee et al., 2022; Vogel et al., 2021) and highlights the significance of individual variability in connectivity patterns for AD prognosis. Individualised connectome characteristics thus become crucial for tailoring therapeutic interventions, offering valuable insights into patient-specific rates of subsequent tau progression.

This study significantly advances our understanding of connectivity and tau spreading at the individual level through its highly subject-specific methodology, marking the first instance of mapping longitudinal tau progression rates to individual rs-fMRI-derived functional connectome dynamics. Recent prior investigations have elucidated how connectivity characteristics contribute to the pace of tau propagation by merging group-averaged connectivity patterns and longitudinal tau-PET, specifically identifying that hub regions accelerate tau spreading (Frontzkowski et al., 2022; Lee et al., 2022). This previous research utilises connectivity data averaged across individuals which provides a robust overview of global connectivity patterns, thereby offering general insight into the influence of global functional connectivity on tau progression. However, despite overall similarity in functional connectome patterns across individuals, notable inter-individual differences exist, particularly in regions like the parietal and frontal cortices (Finn et al., 2015; Horien et al., 2019; Li et al., 2017) which are commonly affected by tau in early disease stages (Braak et al., 1991) and therefore potentially highly influential to tau dynamics. Hence, the personalised mapping of tau to connectivity undertaken in this study enhances the comprehension of the intricate relationship between individualised functional connectome features and their role in shaping distinct inter-individual tau dynamics in AD.

Exploring factors that influence network segregation become especially important considering its association with the rate of tau spreading identified in this thesis. Understanding these factors could offer insights into preserving segregation in older age, potentially mitigating cognitive decline and neurodegenerative processes. The extent of brain network segregation varies among individuals resulting in variations in cognition, for example stronger segregation is linked to enhanced cognitive functions such as intelligence and memory (Chan et al., 2014; Wang et al., 2021), as well as cognitive resilience in AD

(Ewers et al., 2021). However, what shapes network segregation is unclear, but environmental factors seemingly impact the level of brain network segregation, such as education and socioeconomic status. University educated older adults exhibited slower brain network degradation, a process that inevitably happens with aging (Betzel et al., 2014; Chan et al., 2014), compared to non-university educated older adults, irrespective of underlying pathology (Chan et al., 2021). Additionally, middle-aged adults with lower socioeconomic status exhibited less segregated networks compared to those with higher socioeconomic status (Chan et al., 2018). These findings underscore the importance of considering external influences in understanding brain network segregation which may provide valuable insights into the adaptability of segregation potentially having implications for cognitive aging and vulnerability to tau spreading in AD.

The longitudinal modelling of tau spreading conducted in both studies of this thesis suggests that connectivity-based modelling outperforms Braak staging in capturing the progression of tau accumulation. Both studies uncovered a clear hierarchical tau spreading pattern, concordant with previous literature, wherein tau initially propagates to regions most closely connected to its site of onset, with less functionally connected regions being affected later in its progression (Cope et al., 2018; Franzmeier et al., 2020b; Vogel et al., 2020). Through connectivity stages, tau's hierarchical progression aligned with the overall advancement of AD, as gauged by tau burden in the epicentre (first study), or global Aβ burden (second study). This hierarchical pattern was also evident in conventional Braak staging, validating the reliability of connectivity-ranked staging. However, Braak staging showed less distinct differences between the initial and final tau deposition stages. This discrepancy suggests that connectivity stages may offer a more precise understanding of tau deposition patterns by accommodating any variations in tau distribution. While Braak staging remains reliable for predicting AD progression at a population level, this study indicates that it may overlook individual differences in tau deposition which are increasingly recognized in tau-PET research (Biel et al., 2022; Ossenkoppele et al., 2016; Singleton et al., 2021; Vogel et al., 2021) and has implications for the accurate staging of tau, which is vital for the prognosis and management of individual patients.

5.3 Implications of ApoE4 on targeting tau pathology

The second study of this thesis presents novel evidence, from two independent cohorts, indicating that ApoE4 carriers exhibit tau spreading at lower Aβ levels. This suggests that special consideration may be necessary regarding the timing of therapeutic interventions targeting Aβ in these individuals. This study is the first to define centiloid thresholds at which ApoE4 carrier tau accumulation trajectories accelerate significantly compared to that of non-carriers, which were consistently estimated at 12 to 15 centiloids in early connectivity and Braak stages. At these defined centiloid levels ApoE4 carriers exhibit a sharp increase in tau accumulation in early tau susceptible regions, conveying a rapid increase in Aβ-related tau spreading at a considerably lower centiloid level than that used to distinguish inclusion in clinical trials, i.e. the Aβ positivity threshold (Amadoru et al., 2020; Fleisher et al., 2011; Klein et al., 2019). These findings are particularly relevant for anti-Aβ trial design as it conveys the need for earlier centiloid-gauged therapeutic windows for ApoE4 carriers to effectively intervene Aβ-accelerated downstream tau spreading. These findings align with the Lecanemab phase III trial results, an anti-Aβ monoclonal antibody therapy, which although reached its primary endpoint, showed less efficacy in ApoE4 carriers, with homozygotes seeing no attenuation in MMSE decline (van Dyck et al., 2022).

Inter-individual variations in the progression of Aβ-related tau spreading, as implicated by this thesis, oppose determining trial inclusion based on a rigid global Aβ-threshold. This threshold is pivotal for categorizing individuals into AD spectrum or non-AD groups based on Aβ-PET uptake levels, aiding the precise selection of AD spectrum participants for clinical trials, typically set at around 24 centiloids (Clark et al., 2011; La Joie et al., 2019; Navitsky et al., 2018). The findings of this study suggest two critical implications of using a rigid Aβ-threshold. Firstly, there's a risk of overlooking potential AD spectrum subjects who fall below the Aβ threshold, despite having Aβ pathology and facing imminent progression. Secondly, subjects who already exhibit extensive Aβ-related tau spreading are likely to be included. These scenarios could result in trials missing out on a potentially promising target group and being enriched with individuals who are too advanced, reducing the chance of intercepting amyloid-triggered tau early enough. This idea aligns with the generally underwhelming outcomes so far observed in the numerous anti-Aβ therapy trials conducted in the last decade (Perneczky et al., 2023) all of which exclude subjects below the Aβ threshold [e.g. (Klein et al., 2019; van Dyck et al., 2022)]. Hence, a strong rationale emerges

for trials to intervene at an earlier disease stage which could be facilitated by adapting the Aβ threshold to encompass heterogeneity in Aβ's capacity to trigger tau spreading, which certainly extends beyond ApoE4 to other common factors. This highlights the necessity to identify modifying factors which is crucial for tailoring trial inclusion criteria to each individual's optimal Aβ level, aiming to enrich trials with subjects whose emerging tau pathology can be effectively impeded by anti-Aβ therapies.

A pertinent question is the underlying biological mechanism to how ApoE4 facilitates Aβ's capacity to trigger tau spreading. The tau accumulation trajectory of ApoE4 carriers increased at a considerably lower centiloid level than that of non-carriers indicating that Aβ has an amplified ability to trigger tau spreading in ApoE4 carriers. To approach this question, it's important to first address the longstanding problem of how Aβ triggers tau spreading despite the spatial incongruity between the deposition patterns of these two hallmark proteinopathies. A possible explanation is that Aβ impacts tau spreading distally by provoking hyperconnectivity in tau-affected regions. Aβ provoked neuronal hyperexcitability has been indicated by both preclinical and clinical research (Ben-Nejma et al., 2019; Palmqvist et al., 2017; Shah et al., 2016) which when accumulated in regions connected to entorhinal tau harbouring regions, is demonstrated to accelerate tau spreading (Lee et al., 2022). Nevertheless, the question remains as to why this process would be exacerbated in ApoE4 carriers. It has been reported that ApoE4 carriers have increased neuronal activity in regions which typically hold initial Aβ plaque pathology i.e., prefrontal, temporal and parietal cortices, compared to non-carriers (Koelewijn et al., 2019; Pihlajamäki & Sperling, 2009; Wishart et al., 2006) which may exacerbate the remote effects on tau spreading. However, the mechanistic basis of Aβ-induced hyperexcitability in ApoE4 carriers remains poorly understood, yet insights from neuroinflammation research may offer some explanation. Preclinical evidence suggests that ApoE4 is linked to supressed beneficial microglial actions on Aβ plaques, resulting in less compact plaques compared to that in ApoE3 carrying mice (Rodriguez et al., 2014; Stephen et al., 2019) thus leading to an exacerbated pathological effect. However, human studies focusing on the interplay between ApoE4 related inflammatory responses and AD pathology are limited (Parhizkar & Holtzman, 2022) but necessary to shed more light into AD physiology in ApoE4 carriers.

5.4 Clinical relevance and implications for therapy

The studies in this thesis collectively advocate the use of personalised tau staging measurements derived from tau epicentre connectivity. This aligns with the need for a transition towards precision medicine in AD, addressing the variability in tau trajectories observed at the individual level, which can diverge from group-average patterns. The exploratory analysis of the first study reveals the significance of precisely defining the epicentre as ROIs housing pathological levels of tau. This analysis determined the optimal SUVR threshold for delineating the epicentre to achieve better insights into future tau progression. It was observed that defining the epicentre as a region with a notably high baseline tau load in which all ROIs exhibit an SUVR greater than 1.3 [i.e. an established pathological threshold (Maass et al., 2017)], offers the most robust prediction of a patient's future tau progression rate based on epicentre segregation. Conversely, as the epicentre definition becomes less stringent, there is a notable decrease in predictive accuracy. This implies that including ROIs without a pathological level of tau at baseline does not enhance the prediction of the rate of connectivity-driven tau spreading, rather, it worsens it. Overall, these results favour the use of personalised tau-spreading models over conventional staging methods so that epicentres can be defined according to patient-specific tau deposition thus permitting the inclusion of any potential atypical epicentre regions, thus restricting the epicentre to regions which hold pathological tau early in disease pathophysiological progression. Furthermore, increasing the accuracy of the epicentre further improves the identification of connectivity regions which are formulated on ranked connectivity to the epicentre, basing this on non-epicentre ROIs would lead to misguided connectivity based-tau spreading model.

Furthermore, the exploratory analysis of the second study, which focuses on sensitivity to detecting tau attenuation in ApoE4 carriers vs. non-carriers in a simulated intervention, indicated that use of a personalised connectivity derived tau readout region, i.e. Q1, is more sensitive to detecting tau dynamics than stereotypical readout regions. This investigation estimated the sample sizes needed to detect a 30% reduction in tau accumulation due to simulated intervention effects (see section 3 supplementary). This was conducted through different centiloid levels through three different tau readout regions: Global, temporal-meta and Q1. Out of the three readout regions, Q1 demonstrated the largest inter-group differences, i.e., between ApoE4 carriers and non-carriers, indicating its increased sensitivity for detecting

tau reduction in subjects with normal cognition and MCI. Sample sizes derived from the Q1 readout region followed a similar pattern across centiloid levels as observed in the Global readout region, but with amplified results, indicating its accuracy to detecting tau accumulation levels with heightened sensitivity. In contrast, the temporal-meta region did not exhibit the same pattern as the global readout, suggesting an inaccurate reflection of tau accumulation. This has important implications for therapeutic intervention as it suggests that the sensitivity to detecting treatment effects can be altered by the tau readout region. Using stereotypical readout regions, such as the commonly used temporal-meta region which encompasses initial Braak stages (Jack Jr et al., 2017), may less accurately capture the initial dynamics of tau pathology. These results support the use of patient-specific connectivity derived tau readout regions in clinical trials to increase the accuracy and sensitivity of gauging tau accumulation attenuation in response to therapeutic intervention.

Furthermore, the results of the second study's exploratory analysis indicate potential benefit of considering ApoE4 carriers separately in clinical trials. The large differences in estimated sample sizes between ApoE4 carriers and non-carriers to detect intervention effects illustrates the advantage of tailoring trials based on genetic background. Specifically, fewer ApoE4 carriers were needed to detect a significant reduction in tau accumulation which, as discussed above, was particularly evident in the Q1 tau readout region. Given that 40 to 60% of AD patients carry an ApoE4 allele (Ward et al., 2012), treating ApoE4 carriers separately could lead to more targeted and efficient interventions for this large population of AD patients. Accordingly, stratifying these genetic populations in trials could enable the optimization of therapy timing, by treating at the centiloid window linked to highest sensitivity for detecting treatments effects as depicted in this analysis, thereby streamlining sample sizes. Besides improving sensitivity, there are further potential benefits associated with stratifying by ApoE4 carriage in trials such as optimising the biological target and preventing dangerous side effects. Firstly, the differing efficacy of past anti-amyloid therapies in ApoE4 carriers indicate potential variations in ideal Aβ aggregation state targets. For example, Lecanemab (Van Dyck et al., 2022), primarily targeting Aβ protofibrils, showed minimal to no efficacy in ApoE4 carriers who saw better efficacy in response to Aducanumab (Budd Haeberlein et al., 2022), which predominantly targeted Aβ-plaques, thus ApoE4 carriers may benefit from a different biological target to non-carriers. Additionally, ApoE4 carriers experienced a higher prevalence of side effects, specifically amyloid-related imaging abnormalities with oedema (ARIA-E) and/or haemorrhage (ARIA-H) (Honig et al., 2023; Mintun et al., 2021; Salloway

et al., 2022) indicating that a more focused selection criteria is needed for ApoE4 carriers that may differ to that of non-carriers. Overall, considering ApoE4 carriers separately could potentially improve the overall effectiveness of clinical trials and accelerate the development of treatments for Alzheimer's disease.

5.5 Limitations

The graph theoretical measure of brain network segregation, utilised to gauge the balance of connectivity within and between networks in the first study of this thesis, relies on a standard seven-network parcellation (Schaefer et al., 2018). However, defining how the functional brain should be parcellated lacks a definitive solution. While this method is stable at the group level, it may not fully capture individual variability. Brain organization varies notably among individuals, especially in association networks, with fronto-parietal regions showing particular inter-individual heterogeneity in older age (Li et al., 2017) and generally disrupted activity in association networks but heightened activity in primary networks (Andrews-Hanna et al., 2007; Li et al., 2015; Tomasi & Volkow, 2012). These differences may challenge the applicability of standard parcellations derived from young adults to the subjects of this study. Relying on such a parcellation may overlook critical nuances in network organization, compromising segregation accuracy. It would be invaluable to evaluate this parcellation in an older adult cohort, which remains unexplored. Nonetheless, despite these limitations, this study's core finding identifying the role of dispersed connections versus segregated connections in facilitating tau spreading, remain robust to parcellation limitations.

In both studies within this thesis, tau spreading is modelled on functional connections, which hinges on the assumption that functional connectivity aligns with structural connectivity. Functional connectivity, which assesses correlations in spontaneous neural activity across different brain regions assumes that regions exhibiting synchronized activity are functionally connected. It is important to recognise that, although there is a large overlap between functional and structural connectivity (Jacobs et al., 2018), structural connectivity does not wholly account for all the functional connections within the brain. Comparisons between diffusion weighted MRI (DWI) and rs-fMRI derived connectivity indicate that strong functional connections can exist between non-structurally connected regions (Honey et al., 2009) which raises some doubt for trans-neuronal tau spreading mapped by functional connectivity. However, mapping the structural connectome, which is so far exclusively

addressed with DWI, presents methodological limitations (Figley et al., 2022) and although a large proportion of white matter tracts are consistently identified, there exists large incongruences between studies (Maier-Hein et al., 2017). Importantly, DWI cannot detect indirect multi-synaptic connections (Abhinav et al., 2014) which explains a large part of the variance between structural and functional connectomes (Honey et al., 2009).

One conceptual limitation worth considering is the potential for error in estimating tau propagation trajectories, stemming from the degeneration of connections. Both studies model tau spreading according to patient specific tau-epicentre connectivity, whereby the regions to which subsequent tau will accumulate are estimated according to baseline connectivity (first study) or template connectivity (second study). However, a conceptual challenge arises from the fact that neural connections both shape and are shaped by tau progression. Tau leads to the collapse of neural connections, thus potentially disrupting the accuracy of tau propagation trajectories estimated from earlier or template connectivity patterns. A specific problem that emerges is the possible reconfiguration of the functional connectome due to the disrupted connections. It is well documented that focal lesions can induce considerable widespread perturbations in functional connectivity (Carrera & Tononi, 2014), a phenomenon that may parallel the consequences of tau-related axonal degeneration. Damage to a long-range connection or a hub region, which connects otherwise disconnected regions (Harriger et al., 2012), could exert widespread changes on functional connectivity, resulting in the rerouting of tau spreading. Connectome changes could occur at early stages of tau spreading, before the onset of cognitive decline. A potential approach to address connectome rerouting could involve reformulating tau routing with updated connectivity patterns as tau progresses. However, this necessitates access to large datasets containing coinciding longitudinal tau-PET and rsfMRI scans, which are not available to us. This would also enable investigations into how tau pathology impacts connectivity dynamics throughout its progression, thus possibly providing strategies to control for prominent rerouting characteristics when calculating connectivity derived tau stages.

Another conceptual limitation to consider is the overgeneralisation of brain network dynamics construed by network segregation. Graph theory has significantly advanced the understanding of the functional connectome by dissecting spontaneous distributed brain activity into an organized large-scale network consisting of various specialized systems (Bullmore & Sporns, 2009). Network segregation defines the delicate equilibrium of inter-

and intra-network communication, a crucial aspect for efficient information transfer between specialised regions, in one simple measure. It necessitates that regions within a network, contributing to a common function, exhibit robust connections, while connections between network regions, contributing to disparate functions, are minimized (Power et al., 2011; Sporns & Betzel, 2016). While network segregation acts a highly valuable tool leveraged in functional brain research to quantify and explore differences in the functional organization of the brain, it may oversimplify the intricate relationship between networks. Research suggests the functional connectome comprises of a complex balance of segregation and integration influencing cognitive outcomes differentially (Cohen & D'Esposito, 2016; Wang et al., 2021). However, when examining the facilitation of tau spreading, network segregation serves effectively for identifying the balance of dispersed or constrained connections, aiding in identifying individuals at risk of accelerated tau propagation. While it offers a practical means to estimate the rate of connectivity-mediated tau spreading, careful consideration should be taken when extrapolating these findings to cognitive outcomes, as there may be complex interplay of factors to consider.

A methodological limitation to consider when interpreting the results of both studies is the impact of AD pathology on the hemodynamic response function, which is critical for neurovascular coupling in fMRI. Cerebral blood flow has been found to be affected in AD, with literature reporting hypoperfusion and disrupted vascular regulation even in the early stage of the disease before neurodegeneration (Iturria-Medina et al., 2016; Mattsson et al., 2014; Rabin et al., 2019; Ruitenberg et al., 2005; Yew et al., 2017). Particularly strong vascular dysregulation has been found in ApoE4 carriers (Trachtenberg et al., 2012b). Such dysregulation may lead to impaired coordination between neurons and the vascular system leading to inadequate or delayed blood supply to active brain regions and thus a lack of or delayed BOLD signal to be picked up by fMRI. Although many fMRI abnormalities have been reported in AD, it is unclear whether these are due to neuronal changes or vascular uncoupling (Trachtenberg et al., 2012a), thus more mechanistic investigation is needed to judge the extent that vascular dysregulation impacts the interpretability of fMRI findings in AD cohorts.

5.6 Conclusion

The findings of this thesis shed light on the dynamic nature of tau propagation within the brain and reinforce the notion that the rate of tau's progression from its, typically, temporal lobe starting location to the rest of the cortex can be modulated by specific factors. By adopting a highly individualised approach, this research introduces novel evidence to the existing literature, delineating nuanced differences in tau spreading attributable to common characteristics. These findings have significant implications for understanding AD progression, implying a complex interplay of various factors that influence the timing of tau's onset and speed of progression from its epicentre to other cortical regions. Recognising the effect of these factors is crucial for developing targeted interventions and personalised treatment strategies tailored to the unique needs of each AD patient. Such insights may pave the way for more effective management and intervention approaches aimed at slowing pathological tau accumulation in the brain.

6 REFERENCES OF INTRODUCTION AND GENERAL DISCUSSION

Abhinav, K., Yeh, F.-C., Pathak, S., Suski, V., Lacomis, D., Friedlander, R. M., & Fernandez-Miranda, J. C. (2014). Advanced diffusion MRI fiber tracking in neurosurgical and neurodegenerative disorders and neuroanatomical studies: a review. *Biochimica et Biophysica Acta (BBA)-Molecular Basis of Disease, 1842*(11), 2286-2297.

Adams, J. N., Maass, A., Harrison, T. M., Baker, S. L., & Jagust, W. J. (2019). Cortical tau deposition follows patterns of entorhinal functional connectivity in aging. *Elife, 8*, e49132.

Ahmed, Z., Cooper, J., Murray, T. K., Garn, K., McNaughton, E., Clarke, H., . . . O'Neill, M. J. (2014). A novel in vivo model of tau propagation with rapid and progressive neurofibrillary tangle pathology: the pattern of spread is determined by connectivity, not proximity. *Acta neuropathologica, 127*(5), 667-683. doi:10.1007/s00401-014-1254-6

Albert, M. S., DeKosky, S. T., Dickson, D., Dubois, B., Feldman, H. H., Fox, N. C., . . . Petersen, R. C. (2013). The diagnosis of mild cognitive impairment due to Alzheimer's disease: recommendations from the National Institute on Aging-Alzheimer's Association workgroups on diagnostic guidelines for Alzheimer's disease. *Focus, 11*(1), 96-106.

Amadoru, S., Doré, V., McLean, C. A., Hinton, F., Shepherd, C. E., Halliday, G. M., . . . Masters, C. L. (2020). Comparison of amyloid PET measured in Centiloid units with neuropathological findings in Alzheimer's disease. *Alzheimer's Research & Therapy, 12*(1), 22.

Andrews-Hanna, J. R., Snyder, A. Z., Vincent, J. L., Lustig, C., Head, D., Raichle, M. E., & Buckner, R. L. (2007). Disruption of large-scale brain systems in advanced aging. *Neuron, 56*(5), 924-935.

Bature, F., Guinn, B.-a., Pang, D., & Pappas, Y. (2017). Signs and symptoms preceding the diagnosis of Alzheimer's disease: a systematic scoping review of literature from 1937 to 2016. *BMJ Open, 7*(8), e015746. doi:10.1136/bmjopen-2016-015746

Bejanin, A., Schonhaut, D. R., La Joie, R., Kramer, J. H., Baker, S. L., Sosa, N., . . . Rabinovici, G. D. (2017). Tau pathology and neurodegeneration contribute to

cognitive impairment in Alzheimer's disease. *Brain, 140*(12), 3286-3300. doi:10.1093/brain/awx243

Bellenguez, C., Küçükali, F., Jansen, I. E., Kleineidam, L., Moreno-Grau, S., Amin, N., . . . Andrade, V. (2022). New insights into the genetic etiology of Alzheimer's disease and related dementias. *Nature genetics, 54*(4), 412-436.

Ben-Nejma, I. R., Keliris, A. J., Daans, J., Ponsaerts, P., Verhoye, M., Van der Linden, A., & Keliris, G. A. (2019). Increased soluble amyloid-beta causes early aberrant brain network hypersynchronisation in a mature-onset mouse model of amyloidosis. *Acta neuropathologica communications, 7*, 1-15.

Benson, G. S., Bauer, C., Hausner, L., Couturier, S., Lewczuk, P., Peters, O., . . . Pantel, J. (2022). Don't forget about tau: the effects of ApoE4 genotype on Alzheimer's disease cerebrospinal fluid biomarkers in subjects with mild cognitive impairment—data from the Dementia Competence Network. *Journal of Neural Transmission, 129*(5-6), 477-486.

Betzel, R. F., Byrge, L., He, Y., Goñi, J., Zuo, X.-N., & Sporns, O. (2014). Changes in structural and functional connectivity among resting-state networks across the human lifespan. *Neuroimage, 102*, 345-357.

Biel, D., Brendel, M., Rubinski, A., Buerger, K., Janowitz, D., Dichgans, M., . . . for the Alzheimer's Disease Neuroimaging, I. (2021). Tau-PET and in vivo Braak-staging as prognostic markers of future cognitive decline in cognitively normal to demented individuals. *Alzheimer's Research & Therapy, 13*(1), 137. doi:10.1186/s13195-021-00880-x

Biel, D., Luan, Y., Brendel, M., Hager, P., Dewenter, A., Moscoso, A., . . . the Alzheimer's Disease Neuroimaging, I. (2022). Combining tau-PET and fMRI meta-analyses for patient-centered prediction of cognitive decline in Alzheimer's disease. *Alzheimer's Research & Therapy, 14*(1), 166. doi:10.1186/s13195-022-01105-5

Blacker, D., Haines, J., Rodes, L., Terwedow, H., Go, R., Harrell, L., . . . Meyers, D. (1997). ApoE-4 and age at onset of Alzheimer's disease: the NIMH genetics initiative. *Neurology, 48*(1), 139-147.

Braak, H., & Braak, E. (1991). Neuropathological stageing of Alzheimer-related changes. *Acta neuropathologica, 82*(4), 239-259.

Braak, H., & Braak, E. (1997). Diagnostic criteria for neuropathologic assessment of Alzheimer's disease. *Neurobiology of aging, 18*(4), S85-S88.

Brooker, D., Fontaine, J. L., Evans, S., Bray, J., & Saad, K. (2014). Public health guidance to facilitate timely diagnosis of dementia: ALzheimer's COoperative Valuation in Europe recommendations. *International journal of geriatric psychiatry, 29*(7), 682-693.

Brown, B. M., Rainey-Smith, S. R., Dore, V., Peiffer, J. J., Burnham, S. C., Laws, S. M., . . . Rowe, C. C. (2018). Self-reported physical activity is associated with tau burden measured by positron emission tomography. *Journal of Alzheimer's Disease, 63*(4), 1299-1305.

Buckley, R. F., Mormino, E. C., Rabin, J. S., Hohman, T. J., Landau, S., Hanseeuw, B. J., . . . Properzi, M. J. (2019). Sex differences in the association of global amyloid and regional tau deposition measured by positron emission tomography in clinically normal older adults. *JAMA Neurology, 76*(5), 542-551.

Buckley, R. F., O'Donnell, A., McGrath, E. R., Jacobs, H. I., Lois, C., Satizabal, C. L., . . . Sperling, R. A. (2022). Menopause status moderates sex differences in tau burden: a Framingham PET study. *Annals of neurology, 92*(1), 11-22.

Budd Haeberlein, S., Aisen, P., Barkhof, F., Chalkias, S., Chen, T., Cohen, S., . . . Von Hehn, C. (2022). Two randomized phase 3 studies of aducanumab in early Alzheimer's disease. *The journal of prevention of Alzheimer's disease, 9*(2), 197-210.

Bullmore, E., & Sporns, O. (2009). Complex brain networks: graph theoretical analysis of structural and functional systems. *Nature reviews neuroscience, 10*(3), 186-198.

Calafate, S., Buist, A., Miskiewicz, K., Vijayan, V., Daneels, G., De Strooper, B., . . . Moechars, D. (2015). Synaptic contacts enhance cell-to-cell tau pathology propagation. *Cell reports, 11*(8), 1176-1183.

Carrera, E., & Tononi, G. (2014). Diaschisis: past, present, future. *Brain, 137*(9), 2408-2422.

Chan, M. Y., Han, L., Carreno, C. A., Zhang, Z., Rodriguez, R. M., LaRose, M., . . . Wig, G. S. (2021). Long-term prognosis and educational determinants of brain network decline in older adult individuals. *Nature Aging, 1*(11), 1053-1067. doi:10.1038/s43587-021-00125-4

Chan, M. Y., Na, J., Agres, P. F., Savalia, N. K., Park, D. C., & Wig, G. S. (2018). Socioeconomic status moderates age-related differences in the brain's functional

network organization and anatomy across the adult lifespan. *Proceedings of the National Academy of Sciences, 115*(22), E5144-E5153.

Chan, M. Y., Park, D. C., Savalia, N. K., Petersen, S. E., & Wig, G. S. (2014). Decreased segregation of brain systems across the healthy adult lifespan. *Proceedings of the National Academy of Sciences, 111*(46), E4997-E5006.

Clark, C. M., Schneider, J. A., Bedell, B. J., Beach, T. G., Bilker, W. B., Mintun, M. A., . . . Flitter, M. L. (2011). Use of florbetapir-PET for imaging β-amyloid pathology. *JAMA, 305*(3), 275-283.

Clavaguera, F., Bolmont, T., Crowther, R. A., Abramowski, D., Frank, S., Probst, A., . . . Staufenbiel, M. (2009). Transmission and spreading of tauopathy in transgenic mouse brain. *Nature cell biology, 11*(7), 909-913.

Cohen, J. R., & D'Esposito, M. (2016). The segregation and integration of distinct brain networks and their relationship to cognition. *Journal of neuroscience, 36*(48), 12083-12094.

Cope, T. E., Rittman, T., Borchert, R. J., Jones, P. S., Vatansever, D., Allinson, K., . . . O'Brien, J. T. (2018). Tau burden and the functional connectome in Alzheimer's disease and progressive supranuclear palsy. *Brain, 141*(2), 550-567.

Crary, J. F., Trojanowski, J. Q., Schneider, J. A., Abisambra, J. F., Abner, E. L., Alafuzoff, I., . . . Bigio, E. H. (2014). Primary age-related tauopathy (PART): a common pathology associated with human aging. *Acta neuropathologica, 128*, 755-766.

Damoiseaux, J. S., Rombouts, S. A., Barkhof, F., Scheltens, P., Stam, C. J., Smith, S. M., & Beckmann, C. F. (2006). Consistent resting-state networks across healthy subjects. *Proceedings of the National Academy of Sciences, 103*(37), 13848-13853.

De Calignon, A., Polydoro, M., Suárez-Calvet, M., William, C., Adamowicz, D. H., Kopeikina, K. J., . . . Carlson, G. A. (2012). Propagation of tau pathology in a model of early Alzheimer's disease. *Neuron, 73*(4), 685-697.

Duara, R., & Barker, W. (2023). Heterogeneity in Alzheimer's disease diagnosis and progression rates: implications for therapeutic trials. *Neurotherapeutics, 19*(1), 8-25.

Dumurgier, J., & Sabia, S. (2021). Life expectancy in dementia subtypes: exploring a leading cause of mortality. *Lancet Healthy Longev, 2*(8), e449-e450. doi:10.1016/S2666-7568(21)00166-5

Ewers, M., Luan, Y., Frontzkowski, L., Neitzel, J., Rubinski, A., Dichgans, M., . . . Levin, J. (2021). Segregation of functional networks is associated with cognitive resilience in Alzheimer's disease. *Brain, 144*(7), 2176-2185.

Figley, C. R., Uddin, M. N., Wong, K., Kornelsen, J., Puig, J., & Figley, T. D. (2022). Potential pitfalls of using fractional anisotropy, axial diffusivity, and radial diffusivity as biomarkers of cerebral white matter microstructure. *Frontiers in Neuroscience, 15*, 799576.

Finn, E. S., Shen, X., Scheinost, D., Rosenberg, M. D., Huang, J., Chun, M. M., . . . Constable, R. T. (2015). Functional connectome fingerprinting: identifying individuals using patterns of brain connectivity. *Nature neuroscience, 18*(11), 1664-1671.

Fleisher, A. S., Chen, K., Liu, X., Roontiva, A., Thiyyagura, P., Ayutyanont, N., . . . Reiman, E. M. (2011). Using Positron Emission Tomography and Florbetapir F 18 to Image Cortical Amyloid in Patients With Mild Cognitive Impairment or Dementia Due to Alzheimer Disease. *Archives of Neurology, 68*(11), 1404-1411. doi:10.1001/archneurol.2011.150

Franzmeier, N., Dewenter, A., Frontzkowski, L., Dichgans, M., Rubinski, A., Neitzel, J., . . . Buerger, K. (2020a). Patient-centered connectivity-based prediction of tau pathology spread in Alzheimer's disease. *Science advances, 6*(48), eabd1327.

Franzmeier, N., Neitzel, J., Rubinski, A., Smith, R., Strandberg, O., Ossenkoppele, R., . . . Ewers, M. (2020b). Functional brain architecture is associated with the rate of tau accumulation in Alzheimer's disease. *Nature Communications, 11*(1), 347.

Franzmeier, N., Rubinski, A., Neitzel, J., Kim, Y., Damm, A., Na, D. L., . . . Ewers, M. (2019). Functional connectivity associated with tau levels in ageing, Alzheimer's, and small vessel disease. *Brain, 142*(4), 1093-1107. doi:10.1093/brain/awz026

Frisoni, G. B., Boccardi, M., Barkhof, F., Blennow, K., Cappa, S., Chiotis, K., . . . Gietl, A. (2017). Strategic roadmap for an early diagnosis of Alzheimer's disease based on biomarkers. *The Lancet Neurology, 16*(8), 661-676.

Frontzkowski, L., Ewers, M., Brendel, M., Biel, D., Ossenkoppele, R., Hager, P., . . . Franzmeier, N. (2022). Earlier Alzheimer's disease onset is associated with tau

pathology in brain hub regions and facilitated tau spreading. *Nature Communications, 13*(1), 4899. doi:10.1038/s41467-022-32592-7

Gatz, M., Reynolds, C. A., Fratiglioni, L., Johansson, B., Mortimer, J. A., Berg, S., . . . Pedersen, N. L. (2006). Role of Genes and Environments for Explaining Alzheimer Disease. *Archives of General Psychiatry, 63*(2), 168-174. doi:10.1001/archpsyc.63.2.168

Gauthier, C. J., & Fan, A. P. (2019). BOLD signal physiology: models and applications. *Neuroimage, 187*, 116-127.

Gratuze, M., Leyns, C. E., & Holtzman, D. M. (2018). New insights into the role of TREM2 in Alzheimer's disease. *Molecular neurodegeneration, 13*, 1-16.

Grothe, M. J., Barthel, H., Sepulcre, J., Dyrba, M., Sabri, O., Teipel, S. J., . . . Initiative, A. s. D. N. (2017). In vivo staging of regional amyloid deposition. *Neurology, 89*(20), 2031-2038.

Harriger, L., Van Den Heuvel, M. P., & Sporns, O. (2012). Rich club organization of macaque cerebral cortex and its role in network communication.

Holland, D., Frei, O., Desikan, R., Fan, C. C., Shadrin, A. A., Smeland, O. B., . . . Dale, A. M. (2021). The genetic architecture of human complex phenotypes is modulated by linkage disequilibrium and heterozygosity. *Genetics, 217*(3). doi:10.1093/genetics/iyaa046

Honey, C. J., Sporns, O., Cammoun, L., Gigandet, X., Thiran, J.-P., Meuli, R., & Hagmann, P. (2009). Predicting human resting-state functional connectivity from structural connectivity. *Proceedings of the National Academy of Sciences, 106*(6), 2035-2040.

Honig, L. S., Barakos, J., Dhadda, S., Kanekiyo, M., Reyderman, L., Irizarry, M., . . . Sabbagh, M. (2023). ARIA in patients treated with lecanemab (BAN2401) in a phase 2 study in early Alzheimer's disease. *Alzheimer's & Dementia: Translational Research & Clinical Interventions, 9*(1), e12377.

Horien, C., Shen, X., Scheinost, D., & Constable, R. T. (2019). The individual functional connectome is unique and stable over months to years. *Neuroimage, 189*, 676-687.

Iturria-Medina, Y., Sotero, R. C., Toussaint, P. J., Mateos-Pérez, J. M., & Evans, A. C. (2016). Early role of vascular dysregulation on late-onset Alzheimer's disease based on multifactorial data-driven analysis. *Nature Communications, 7*(1), 11934.

Jack, C. R., Knopman, D. S., Jagust, W. J., Petersen, R. C., Weiner, M. W., Aisen, P. S., . . . Weigand, S. D. (2013). Tracking pathophysiological processes in Alzheimer's disease: an updated hypothetical model of dynamic biomarkers. *The Lancet Neurology, 12*(2), 207-216.

Jack Jr, C. R., Wiste, H. J., Weigand, S. D., Therneau, T. M., Lowe, V. J., Knopman, D. S., . . . Kantarci, K. (2017). Defining imaging biomarker cut points for brain aging and Alzheimer's disease. *Alzheimer's & Dementia, 13*(3), 205-216.

Jacobs, H. I. L., Hedden, T., Schultz, A. P., Sepulcre, J., Perea, R. D., Amariglio, R. E., . . . Johnson, K. A. (2018). Structural tract alterations predict downstream tau accumulation in amyloid-positive older individuals. *Nat Neurosci, 21*(3), 424-431. doi:10.1038/s41593-018-0070-z

Jansen, W. J., Ossenkoppele, R., Knol, D. L., Tijms, B. M., Scheltens, P., Verhey, F. R. J., . . . Group, a. t. A. B. S. (2015). Prevalence of Cerebral Amyloid Pathology in Persons Without Dementia: A Meta-analysis. *JAMA, 313*(19), 1924-1938. doi:10.1001/jama.2015.4668

Karlsson, I. K., Escott-Price, V., Gatz, M., Hardy, J., Pedersen, N. L., Shoai, M., & Reynolds, C. A. (2022). Measuring heritable contributions to Alzheimer's disease: polygenic risk score analysis with twins. *Brain Communications, 4*(1). doi:10.1093/braincomms/fcab308

Khalil, M., Teunissen, C. E., Otto, M., Piehl, F., Sormani, M. P., Gattringer, T., . . . Fazekas, F. (2018). Neurofilaments as biomarkers in neurological disorders. *Nature Reviews Neurology, 14*(10), 577-589.

Klein, G., Delmar, P., Voyle, N., Rehal, S., Hofmann, C., Abi-Saab, D., . . . Bateman, R. (2019). Gantenerumab reduces amyloid-β plaques in patients with prodromal to moderate Alzheimer's disease: a PET substudy interim analysis. *Alzheimer's Research & Therapy, 11*, 1-12.

Koelewijn, L., Lancaster, T. M., Linden, D., Dima, D. C., Routley, B. C., Magazzini, L., . . . Tansey, K. E. (2019). Oscillatory hyperactivity and hyperconnectivity in young APOE-ε4 carriers and hypoconnectivity in Alzheimer's disease. *Elife, 8*, e36011.

La Joie, R., Ayakta, N., Seeley, W. W., Borys, E., Boxer, A. L., DeCarli, C., . . . Hwang, J.-H. (2019). Multisite study of the relationships between antemortem [11C] PIB-PET

Centiloid values and postmortem measures of Alzheimer's disease neuropathology. *Alzheimer's & Dementia, 15*(2), 205-216.

La Joie, R., Visani, A. V., Baker, S. L., Brown, J. A., Bourakova, V., Cha, J., . . . Rabinovici, G. D. (2020). Prospective longitudinal atrophy in Alzheimer's disease correlates with the intensity and topography of baseline tau-PET. *Science Translational Medicine, 12*(524), eaau5732. doi:doi:10.1126/scitranslmed.aau5732

Lee, W. J., Brown, J. A., Kim, H. R., La Joie, R., Cho, H., Lyoo, C. H., . . . Seeley, W. W. (2022). Regional Aβ-tau interactions promote onset and acceleration of Alzheimer's disease tau spreading. *Neuron, 110*(12), 1932-1943. e1935.

Leuzy, A., Chiotis, K., Lemoine, L., Gillberg, P.-G., Almkvist, O., Rodriguez-Vieitez, E., & Nordberg, A. (2019). Tau PET imaging in neurodegenerative tauopathies—still a challenge. *Molecular psychiatry, 24*(8), 1112-1134. doi:10.1038/s41380-018-0342-8

Li, H.-J., Hou, X.-H., Liu, H.-H., Yue, C.-L., Lu, G.-M., & Zuo, X.-N. (2015). Putting age-related task activation into large-scale brain networks: a meta-analysis of 114 fMRI studies on healthy aging. *Neuroscience & Biobehavioral Reviews, 57*, 156-174.

Li, R., Yin, S., Zhu, X., Ren, W., Yu, J., Wang, P., . . . Li, J. (2017). Linking inter-individual variability in functional brain connectivity to cognitive ability in elderly individuals. *Frontiers in aging neuroscience, 9*, 385.

Liu, C.-C., Zhao, N., Fu, Y., Wang, N., Linares, C., Tsai, C.-W., & Bu, G. (2017). ApoE4 accelerates early seeding of amyloid pathology. *Neuron, 96*(5), 1024-1032. e1023.

Maass, A., Landau, S., Baker, S. L., Horng, A., Lockhart, S. N., La Joie, R., . . . Jagust, W. J. (2017). Comparison of multiple tau-PET measures as biomarkers in aging and Alzheimer's disease. *Neuroimage, 157*, 448-463. doi:10.1016/j.neuroimage.2017.05.058

Mahley, R. W. (2016). Central nervous system lipoproteins: ApoE and regulation of cholesterol metabolism. *Arteriosclerosis, thrombosis, and vascular biology, 36*(7), 1305-1315.

Maier-Hein, K. H., Neher, P. F., Houde, J.-C., Côté, M.-A., Garyfallidis, E., Zhong, J., . . . Descoteaux, M. (2017). The challenge of mapping the human connectome based on diffusion tractography. *Nature Communications, 8*(1), 1349. doi:10.1038/s41467-017-01285-x

Mattsson, N., Tosun, D., Insel, P. S., Simonson, A., Jack Jr, C. R., Beckett, L. A., . . . Weiner, M. W. (2014). Association of brain amyloid-β with cerebral perfusion and structure in Alzheimer's disease and mild cognitive impairment. *Brain, 137*(5), 1550-1561.

Medeiros, R., Baglietto-Vargas, D., & LaFerla, F. M. (2011). The role of tau in Alzheimer's disease and related disorders. *CNS neuroscience & therapeutics, 17*(5), 514-524.

Mintun, M. A., Lo, A. C., Duggan Evans, C., Wessels, A. M., Ardayfio, P. A., Andersen, S. W., . . . Brys, M. (2021). Donanemab in early Alzheimer's disease. *New England Journal of Medicine, 384*(18), 1691-1704.

Molinuevo, J. L., Ayton, S., Batrla, R., Bednar, M. M., Bittner, T., Cummings, J., . . . Blennow, K. (2018). Current state of Alzheimer's fluid biomarkers. *Acta neuropathologica, 136*(6), 821-853. doi:10.1007/s00401-018-1932-x

Navitsky, M., Joshi, A. D., Kennedy, I., Klunk, W. E., Rowe, C. C., Wong, D. F., . . . Devous Sr, M. D. (2018). Standardization of amyloid quantitation with florbetapir standardized uptake value ratios to the Centiloid scale. *Alzheimer's & Dementia, 14*(12), 1565-1571.

Ossenkoppele, R., Iaccarino, L., Schonhaut, D. R., Brown, J. A., La Joie, R., O'Neil, J. P., . . . Gorno-Tempini, M.-L. (2019). Tau covariance patterns in Alzheimer's disease patients match intrinsic connectivity networks in the healthy brain. *NeuroImage: Clinical, 23*, 101848.

Ossenkoppele, R., Schonhaut, D. R., Schöll, M., Lockhart, S. N., Ayakta, N., Baker, S. L., . . . Rabinovici, G. D. (2016). Tau PET patterns mirror clinical and neuroanatomical variability in Alzheimer's disease. *Brain, 139*(5), 1551-1567. doi:10.1093/brain/aww027

Ossenkoppele, R., Smith, R., Mattsson-Carlgren, N., Groot, C., Leuzy, A., Strandberg, O., . . . Hansson, O. (2021). Accuracy of Tau Positron Emission Tomography as a Prognostic Marker in Preclinical and Prodromal Alzheimer Disease: A Head-to-Head Comparison Against Amyloid Positron Emission Tomography and Magnetic Resonance Imaging. *JAMA Neurology, 78*(8), 961-971. doi:10.1001/jamaneurol.2021.1858

Palmqvist, S., Insel, P. S., Stomrud, E., Janelidze, S., Zetterberg, H., Brix, B., . . . Blennow, K. (2019). Cerebrospinal fluid and plasma biomarker trajectories with increasing

amyloid deposition in Alzheimer's disease. *EMBO molecular medicine, 11*(12), e11170.

Palmqvist, S., Schöll, M., Strandberg, O., Mattsson, N., Stomrud, E., Zetterberg, H., . . . Hansson, O. (2017). Earliest accumulation of β-amyloid occurs within the default-mode network and concurrently affects brain connectivity. *Nature Communications, 8*(1), 1214.

Parhizkar, S., & Holtzman, D. M. (2022). *APOE mediated neuroinflammation and neurodegeneration in Alzheimer's disease.* Paper presented at the Seminars in immunology.

Perneczky, R., Jessen, F., Grimmer, T., Levin, J., Flöel, A., Peters, O., & Froelich, L. (2023). Anti-amyloid antibody therapies in Alzheimer's disease. *Brain, 146*(3), 842-849.

Pihlajamäki, M., & Sperling, R. A. (2009). Functional MRI assessment of task-induced deactivation of the default mode network in Alzheimer's disease and at-risk older individuals. *Behavioural neurology, 21*(1-2), 77-91.

Pontecorvo, M. J., Devous, M. D., Kennedy, I., Navitsky, M., Lu, M., Galante, N., . . . investigators, f. t. F.-A.-.-A. (2019). A multicentre longitudinal study of flortaucipir (18F) in normal ageing, mild cognitive impairment and Alzheimer's disease dementia. *Brain, 142*(6), 1723-1735. doi:10.1093/brain/awz090

Porsteinsson, A., Isaacson, R., Knox, S., Sabbagh, M., & Rubino, I. (2021). Diagnosis of early Alzheimer's disease: clinical practice in 2021. *The journal of prevention of Alzheimer's disease, 8*, 371-386.

Power, J. D., Cohen, A. L., Nelson, S. M., Wig, G. S., Barnes, K. A., Church, J. A., . . . Schlaggar, B. L. (2011). Functional network organization of the human brain. *Neuron, 72*(4), 665-678.

Power, J. D., Mitra, A., Laumann, T. O., Snyder, A. Z., Schlaggar, B. L., & Petersen, S. E. (2014). Methods to detect, characterize, and remove motion artifact in resting state fMRI. *Neuroimage, 84*, 320-341. doi:10.1016/j.neuroimage.2013.08.048

Prokic, I., Cowling, B. S., & Laporte, J. (2014). Amphiphysin 2 (BIN1) in physiology and diseases. *Journal of molecular medicine, 92*, 453-463.

Rabin, J. S., Yang, H. S., Schultz, A. P., Hanseeuw, B. J., Hedden, T., Viswanathan, A., . . . Klein, H. (2019). Vascular risk and β-amyloid are synergistically associated with cortical tau. *Annals of neurology, 85*(2), 272-279.

Reitz, C., Jun, G., Naj, A., Rajbhandary, R., Vardarajan, B. N., Wang, L.-S., . . . Graff-Radford, N. R. (2013). Variants in the ATP-binding cassette transporter (ABCA7), apolipoprotein E ϵ4, and the risk of late-onset Alzheimer disease in African Americans. *JAMA, 309*(14), 1483-1492.

Risacher, S. L., Anderson, W. H., Charil, A., Castelluccio, P. F., Shcherbinin, S., Saykin, A. J., . . . Initiative, A. s. D. N. (2017). Alzheimer disease brain atrophy subtypes are associated with cognition and rate of decline. *Neurology, 89*(21), 2176-2186.

Rodriguez, G. A., Tai, L. M., LaDu, M. J., & Rebeck, G. W. (2014). Human APOE4 increases microglia reactivity at Aβ plaques in a mouse model of Aβ deposition. *Journal of neuroinflammation, 11*, 1-14.

Rogaeva, E., Meng, Y., Lee, J. H., Gu, Y., Kawarai, T., Zou, F., . . . Hasegawa, H. (2007). The neuronal sortilin-related receptor SORL1 is genetically associated with Alzheimer disease. *Nature genetics, 39*(2), 168-177.

Ruitenberg, A., Den Heijer, T., Bakker, S. L., Van Swieten, J. C., Koudstaal, P. J., Hofman, A., & Breteler, M. M. (2005). Cerebral hypoperfusion and clinical onset of dementia: the Rotterdam Study. *Annals of Neurology: Official Journal of the American Neurological Association and the Child Neurology Society, 57*(6), 789-794.

Salloway, S., Chalkias, S., Barkhof, F., Burkett, P., Barakos, J., Purcell, D., . . . Umans, K. (2022). Amyloid-related imaging abnormalities in 2 phase 3 studies evaluating aducanumab in patients with early Alzheimer disease. *JAMA Neurology, 79*(1), 13-21.

Schaefer, A., Kong, R., Gordon, E. M., Laumann, T. O., Zuo, X.-N., Holmes, A. J., . . . Yeo, B. T. (2018a). Local-global parcellation of the human cerebral cortex from intrinsic functional connectivity MRI. *Cerebral cortex, 28*(9), 3095-3114.

Shah, D., Praet, J., Hernandez, A. L., Höfling, C., Anckaerts, C., Bard, F., . . . Villa, A. (2016). Early pathologic amyloid induces hypersynchrony of BOLD resting-state networks in transgenic mice and provides an early therapeutic window before amyloid plaque deposition. *Alzheimer's & Dementia, 12*(9), 964-976.

Singleton, E., Hansson, O., Pijnenburg, Y. A., La Joie, R., Mantyh, W. G., Tideman, P., . . . Strandberg, O. (2021). Heterogeneous distribution of tau pathology in the behavioural variant of Alzheimer's disease. *Journal of Neurology, Neurosurgery & Psychiatry, 92*(8), 872-880.

Sporns, O., & Betzel, R. F. (2016). Modular brain networks. *Annual review of psychology, 67*, 613-640.

Stephen, T. L., Cacciottolo, M., Balu, D., Morgan, T. E., LaDu, M. J., Finch, C. E., & Pike, C. J. (2019). APOE genotype and sex affect microglial interactions with plaques in Alzheimer's disease mice. *Acta Neuropathologica Communications, 7*(1), 82. doi:10.1186/s40478-019-0729-z

Steward, A., Biel, D., Brendel, M., Dewenter, A., Roemer, S., Rubinski, A., . . . Franzmeier, N. (2022). Functional network segregation is associated with attenuated tau spreading in Alzheimer's disease. *Alzheimer's & Dementia, 19*(5), 2034-2046.

Steward, A., Biel, D., Dewenter, A., Roemer, S., Wagner, F., Dehsarvi, A., . . . Franzmeier, N. (2023). ApoE4 and Connectivity-Mediated Spreading of Tau Pathology at Lower Amyloid Levels. *JAMA Neurology, 80*(12), 1295-1306. doi:10.1001/jamaneurol.2023.4038

Takizawa C, Thompson PL, van Walsem A, et al. Epidemiological and economic burden of Alzheimer's disease: a systematic literature review of data across Europe and the United States of America. J Alzheimers Dis 2015;43:1271–84

Teipel, S., Drzezga, A., Grothe, M. J., Barthel, H., Chételat, G., Schuff, N., . . . Hoffmann, W. (2015). Multimodal imaging in Alzheimer's disease: validity and usefulness for early detection. *The Lancet Neurology, 14*(10), 1037-1053.

Thal, D. R., Rüb, U., Orantes, M., & Braak, H. (2002). Phases of A beta-deposition in the human brain and its relevance for the development of AD. *Neurology, 58*(12), 1791-1800. doi:10.1212/wnl.58.12.1791

Therriault, J., Benedet, A. L., Pascoal, T. A., Mathotaarachchi, S., Chamoun, M., Savard, M., . . . Tissot, C. (2020). Association of apolipoprotein E ε4 with medial temporal tau independent of amyloid-β. *JAMA Neurology, 77*(4), 470-479.

Tomasi, D., & Volkow, N. D. (2012). Aging and functional brain networks. *Molecular psychiatry, 17*(5), 549-558.

Trachtenberg, A. J., Filippini, N., Cheeseman, J., Duff, E. P., Neville, M. J., Ebmeier, K. P., . . . Mackay, C. E. (2012a). The effects of APOE on brain activity do not simply reflect the risk of Alzheimer's disease. *Neurobiology of aging, 33*(3), 618. e611-618. e613.

Trachtenberg, A. J., Filippini, N., & Mackay, C. E. (2012b). The effects of APOE-ε4 on the BOLD response. *Neurobiology of aging, 33*(2), 323-334.

Van den Heuvel, M. P., & Sporns, O. (2013). Network hubs in the human brain. *Trends in cognitive sciences, 17*(12), 683-696.

van der Flier, W. M., Pijnenburg, Y. A., Fox, N. C., & Scheltens, P. (2011). Early-onset versus late-onset Alzheimer's disease: the case of the missing APOE ε4 allele. *The Lancet Neurology, 10*(3), 280-288.

van Dyck, C. H., Swanson, C. J., Aisen, P., Bateman, R. J., Chen, C., Gee, M., . . . Cohen, S. (2022). Lecanemab in early Alzheimer's disease. *New England Journal of Medicine*.

Vogel, J. W., Iturria-Medina, Y., Strandberg, O. T., Smith, R., Levitis, E., Evans, A. C., . . . the Swedish BioFinder, S. (2020). Spread of pathological tau proteins through communicating neurons in human Alzheimer's disease. *Nature Communications, 11*(1), 2612. doi:10.1038/s41467-020-15701-2

Vogel, J. W., Young, A. L., Oxtoby, N. P., Smith, R., Ossenkoppele, R., Strandberg, O. T., . . . Hansson, O. (2021). Four distinct trajectories of tau deposition identified in Alzheimer's disease. *Nat Med, 27*(5), 871-881. doi:10.1038/s41591-021-01309-6

Vogels, T., Leuzy, A., Cicognola, C., Ashton, N. J., Smolek, T., Novak, M., . . . Zilka, N. (2020). Propagation of tau pathology: integrating insights from postmortem and in vivo studies. *Biological psychiatry, 87*(9), 808-818.

Wang, L., Benzinger, T. L., Su, Y., Christensen, J., Friedrichsen, K., Aldea, P., . . . Ances, B. M. (2016). Evaluation of Tau Imaging in Staging Alzheimer Disease and Revealing Interactions Between β-Amyloid and Tauopathy. *JAMA Neurol, 73*(9), 1070-1077. doi:10.1001/jamaneurol.2016.2078

Wang, R., Liu, M., Cheng, X., Wu, Y., Hildebrandt, A., & Zhou, C. (2021). Segregation, integration, and balance of large-scale resting brain networks configure different cognitive abilities. *Proceedings of the National Academy of Sciences, 118*(23), e2022288118.

Ward, A., Crean, S., Mercaldi, C. J., Collins, J. M., Boyd, D., Cook, M. N., & Arrighi, H. M. (2012). Prevalence of apolipoprotein E4 genotype and homozygotes (APOE e4/4) among patients diagnosed with Alzheimer's disease: a systematic review and meta-analysis. *Neuroepidemiology, 38*(1), 1-17.

Wightman, D. P., Jansen, I. E., Savage, J. E., Shadrin, A. A., Bahrami, S., Holland, D., . . . Drange, O. K. (2021). A genome-wide association study with 1,126,563 individuals identifies new risk loci for Alzheimer's disease. *Nature genetics, 53*(9), 1276-1282.

Winblad, B., Amouyel, P., Andrieu, S., Ballard, C., Brayne, C., Brodaty, H., . . . Feldman, H. (2016). Defeating Alzheimer's disease and other dementias: a priority for European science and society. *The Lancet Neurology, 15*(5), 455-532.

Wishart, H. A., Saykin, A. J., Rabin, L. A., Santulli, R. B., Flashman, L. A., Guerin, S. J., . . . McAllister, T. W. (2006). Increased brain activation during working memory in cognitively intact adults with the APOE ε4 allele. *American Journal of Psychiatry, 163*(9), 1603-1610.

Wu, J. W., Hussaini, S. A., Bastille, I. M., Rodriguez, G. A., Mrejeru, A., Rilett, K., . . . Boonen, R. A. (2016). Neuronal activity enhances tau propagation and tau pathology in vivo. *Nature neuroscience, 19*(8), 1085-1092.

Ye, B. S., Kim, H. J., Kim, Y. J., Jung, N.-Y., Lee, J. S., Lee, J., . . . Vogel, J. W. (2018). Longitudinal outcomes of amyloid positive versus negative amnestic mild cognitive impairments: a three-year longitudinal study. *Scientific reports, 8*(1), 5557.

Yeo, B. T., Krienen, F. M., Sepulcre, J., Sabuncu, M. R., Lashkari, D., Hollinshead, M., . . . Polimeni, J. R. (2011). The organization of the human cerebral cortex estimated by intrinsic functional connectivity. *Journal of neurophysiology*.

Yew, B., Nation, D. A., & Initiative, A. s. D. N. (2017). Cerebrovascular resistance: effects on cognitive decline, cortical atrophy, and progression to dementia. *Brain, 140*(7), 1987-2001.

Young, C. B., Johns, E., Kennedy, G., Belloy, M. E., Insel, P. S., Greicius, M. D., . . . Mormino, E. C. (2023). APOE effects on regional tau in preclinical Alzheimer's disease. *Molecular neurodegeneration, 18*(1), 1.

Zetterberg, H., & Bendlin, B. B. (2021). Biomarkers for Alzheimer's disease—preparing for a new era of disease-modifying therapies. *Molecular psychiatry, 26*(1), 296-308.

7 ACKNOWLEDGEMENTS

Firstly, I would like to express my gratitude to my supervisor Nico for his endless support, guidance and continuous encouragement throughout my PhD. I am truly honoured to be part of his research group at the ISD, and couldn't have had a more enjoyable and educational PhD experience.

Secondly, I would like to thank my wonderful lab co-members and extended lab members: Anna Dewenter, Davina Biel, Sebastian Roemer, Fabian Wanger, Amir Dehsarvi, Zeyu Zhu, Jule Filler, Rong Fang, Jannis Denecke, Lukai Zheng and Anna Rubinski. Who have made daily life more enjoyable and provided plenty of entertainment over numerous conferences and retreats.

Finally, I would like to thank my parents for their unwavering encouragement and support, which has been crucial in helping me reach this point in my life. I am also deeply thankful to my best friend Carrie for her enduring friendship, invaluable advice and constant support through my entire educational journey.

8 LIST OF PUBLICATIONS

Roemer S, Brendel M, Gnörich J, Malpetti M, Zaganjori M, Quattrone A, Gross M, **Steward A**, Dewenter A, Wagner F, Dehsarvi A, Ferschmann C, Wall S, Palleis C, Rauchmann B S, Katzdobler S, Jäck A, Stockbauer A, Fietzek U, Weidinger E, Zwergal A, Stöcklein S, Perneczky R, Barthel H, Sabri O, Levin J, Höglinger G U, Franzmeier N, for the Munich Integrative NeuroDegeneration (MIND) Cohort. Subcortical tau is associated with diaschisis-like hypoperfusion in connected cortical regions in patients with 4R tauopathies, *Brain* (Accepted)

Franzmeier N, Dehsarvi A, **Steward A**, Biel D, Dewenter A, Roemer S, Wagner F, Groß M, Brendel M, Moscoso A, Arunachalam P, Blennow K, Zetterberg H, Ewers M, Schöll M, Alzheimer's Disease Neuroimaging Initiative (ADNI). Elevated CSF GAP-43 is associated with accelerated tau accumulation and spread in Alzheimer's disease. Nature Communications (2024). doi.org/10.1038/s41467-023-44374-w

Steward A, Biel D, Dewenter A, Roemer S, Wagner F, Dehsarvi A, Saima Rathore S, Otero Svaldi D, Higgins I, Brendel M, Dichgans M, Shcherbinin S,Ewers M, Franzmeier N. Apoe4 and Connectivity-Mediated Spreading of Tau Pathology at Lower Amyloid Levels. JAMA Neurology (2023). doi:10.1001/jamaneurol.2023.4038

Biel D, Suárez-Calvet M, Hager P, Rubinski A, Dewenter A, **Steward A**, Roemer S, Ewers M, Haass C, Brendel M, Franzmeier N, Alzheimer's Disease Neuroimaging Initiative (ADNI). sTREM2 is associated with amyloid-related p-tau increases and glucose hypermetabolism in Alzheimer's disease. Molecular Medicine (2023): e16987. doi:10.15252/emmm.202216987

Steward A, Biel D, Brendel M, Dewenter A, Roemer S, Rubinski A, Ewers M, Franzmeier N & the Alzheimer's Disease Neuroimaging Initiative. Functional network segregation is associated with attenuated tau spreading in Alzheimer's disease." Alzheimer's & Dementia (2022). doi:10.1002/alz.12867

Biel D, Luan Y, Brendel M, Hager P, Dewenter A, Moscoso A, Otero Svaldi D, A. Higgins X, Pontecorvo M, Roemer S, **Steward A**, Rubinski A, Zheng L, Schoell M, Shcherbinin S, Ewers M, Franzmeier N & the Alzheimer's Disease Neuroimaging Initiative. Combining tau-PET and fMRI meta-analyses for patient-centered prediction of cognitive decline in Alzheimer's disease. Alz Res Therapy14, 166 (2022). doi:10.1186/s13195-022-01105-5

Krieger-Redwood K, **Steward A**, Gao Z, Wang X, Halai A, Smallwood J, Jefferies E. Creativity in verbal associations is linked to semantic control, *Cerebral Cortex*, bhac405(2022). doi:10.1093/cercor/bhac405

Frontzkowski L, Ewers M, Brendel M, Biel D, Ossenkoppele R, Hager P, **Steward A,** Dewenter A, Roemer S, Rubinski A, Buerger K, Janowitz D, Pichet Binette A, Smith R, Strandberg O, Mattsson Carlgren N, Dichgans M, Hansson O, Franzmeier, N. Earlier Alzheimer's disease onset is associated with tau pathology in brain hub regions and facilitated tau spreading. Nat Commun 13, 4899 (2022). doi:10.1038/s41467-022-32592-7

9 AFFIDAVIT

I hereby confirm that the dissertation “Exploring Modulators of Tau Spreading in Alzheimer’s Disease Through Multi-Modal Neuroimaging Biomarkers” is the result of my own work and that I have only used sources or materials listed and specified in the dissertation.

Hiermit versichere ich an Eides statt, dass ich die vorliegende Dissertation “Exploring Modulators of Tau Spreading in Alzheimer’s Disease Through Multi-Modal Neuroimaging Biomarkers” selbstständig angefertigt habe, mich außer der angegebenen keiner weiteren Hilfsmittel bedient und alle Erkenntnisse, die aus dem Schrifttum ganz oder annähernd übernommen sind, als solche kenntlich gemacht und nach ihrer Herkunft unter Bezeichnung der Fundstelle einzeln nachgewiesen habe.

Munich, 22nd May 2024 Anna Steward

10 DECLARATION OF AUTHOR CONTRIBUTIONS

Study I: (Steward et al., 2022, Alzheimer's & Dementia) "Functional network segregation is associated with attenuated tau spreading in AD"

Authors: Anna Steward, Davina Biel, Matthias Brendel, Anna Dewenter, Sebastian Roemer, Anna Rubinski, Ying Luan, Martin Dichgans, Michael Ewers and Nicolai Franzmeier

Contribution of co-authors: AS, NF contributed to the concept and design of the study. AS, DB, SR, AR, AD, YL, MB, MD, NF contributed to the acquisition and analysis, or interpretation of the data. AS, MB, MD, NF contributed to the drafting of the manuscript. AS, SR, AR, AD, YL, NF contributed to the statistical analysis. AS, AD, MB provided administrative, technical, or material support. AS, DB, AD, SR, AR, AD, YL, MB, MD, ME, NF provided a critical review of the manuscript for important intellectual content. MB and NF obtained funding and ME, NF provided supervision.

My contribution to this publication: Together with NF, I contributed to the design of the study. I handled and analysed the preprocessed rs-fMRI, tau-PET and amyloid-PET data and performed all statistical analyses. I interpreted results, drafted and revised the manuscript.

Study II: (Steward et al., 2023, JAMA Neurology) “ApoE4 and Connectivity-Mediated Spreading of Tau Pathology at Lower Amyloid Levels

Authors: Anna Steward, Davina Biel, Anna Dewenter, Sebastian Roemer, Fabian Wagner, Amir Dehsarvi, Saima Rathore, Diana Otero Svaldi, Ixavier Higgins, Matthias Brendel, Martin Dichgans, Sergey Shcherbinin, Michael Ewers and Nicolai Franzmeier

Contribution of co-authors: AS, NF contributed to the concept and design of the study. AS, DB, ADew, SRoe, FW, ADeh, DOS, SRat, IH, MB, MD, NF contributed to the acquisition and analysis, or interpretation of the data. AS, MB, MD, NF contributed to the drafting of the manuscript. AS, SRoe, FW, ADeh, SRat, IH, NF contributed to the statistical analysis. AS, ADeh, MB provided administrative, technical, or material support. AS, DB, ADew, SRoe, FW, ADeh, SRat, DOS, IH, MB, MD, SS, ME, NF provided a critical review of the manuscript for important intellectual content. MB obtained funding and MB, ME, NF provided supervision.

My contribution to this publication: Together with NF, I designed the study. I handled and analysed the preprocessed rs-fMRI, tau-PET and amyloid-PET data and performed all statistical analyses. I interpreted results, drafted and revised the manuscript.